The Hong Kong Polytechnic University

Institute of Textiles & Clothing

Novel Hyperbranched Macromolecules as Modifiers in Biodegradable Nanocomposites

BY

Wang Yanming

A Thesis Submitted in Partial Fulfillment of the Requirements

for the Degree of Master of Philosophy

August 2010

Certificate of Originality

I hereby declare that this thesis is my own work and that, to the best of my knowledge and belief, it reproduces no material previously published or written, nor material that has been accepted for the award of any other degree or diploma, except where due acknowledgement has been made in the text.

_____

Wang Yanming

(August 2010)

Abstract

Dendritic macromolecules represent a novel class of structurally controlled macromolecules with highly branched structures and densely populated surface groups. Hyperbranched polymers are a subclass member, which can be made by a one-pot, single-step polymerization approach in large quantities and thus present economically great promising products for large-scale industrial applications. In this research, two types of novel biodegradable hyperbranched polymers containing a domination of either carboxylic acid groups (HBP-COOH) or hydroxyl groups (HBP-OH) at the peripheral surface were synthesized and characterized. Combining these organic nanostuffs to improve performances of bulk polymers has been undertaken. Via a solvent casting method, the nano-agents have successfully been integrated into aliphatic polyesters such as poly(L-lactic acid) (PLA) and poly(ε-caprolactone) (PCL) to achieve desired biodegradable composite materials. The incorporated modifiers have been comprehensively investigated with respect to their effects on physical, mechanical, thermal, and morphological properties of the end products. Herein, it can be seen that both of the hyperbranched products induce a positive effect on intrinsic ductility and toughness of the bulk polymers. An optimal content of the fillers added (~3 or 6% by weight) can give rise to improved mechanical properties of the materials significantly. In contrast to HBP-OH, HBP-COOH generally exhibits better effectiveness, which accounts for the end group effect in the composite systems. As revealed by the microscopic morphological

study, the filler molecules can agglomerate to form well-defined spherical nanoclusters in the polymer matrixes. A debonding-initiated shear yielding mechanism is probably involved in the toughening of the composite materials. Besides, it is confirmed that all the specimens under study are fully biodegradable. The incorporation of the organic fillers does affect the bio-stability nature of PLA and PCL, but the degree is subjected to factors such as concentration, type and molecular weight of the fillers, and degradation conditions. In general, higher molecular weight filler or higher filler content would likely induce an increase in biodegradable rate for the end materials. The degradation is faster in an alkaline medium than in a neutral environment.

Acknowledgements

Foremost, with a deep sense of gratitude, I wish to express my sincere thanks to my supervisor, Dr. Kevin Cheuk, for his immense help in planning and valuable advice. The many improvements in my knowledge about polymer science and in my writing and presentation skills can be attributed to his guidance. I would like to thank my co-supervisor Prof. John Xin and Dr. Chi Hung Yeung, respectively for their scientific support in my research.

I would also like to thank Prof. Marcus Yuen, Prof. Robert K Y Li and Prof. Yang Leng for serving on my committee and providing me with valuable comments that have greatly enhanced the quality of my dissertation.

I am grateful to my colleagues who have enriched my graduate experiences: Dr. Yong Zhu, Dr. Jing Li, Dr. Shaojun Chen. I would like to thank them for their many insightful discussions of my research project. All people at the Department (past and present) are thanked for building up the greatest environment to work in.

During my MPhil study, I would like to thank Dr. Szeto, Mr. Ho, Ms. Sun, Dr. Law and Mr. Frankie for their assistance in my experiments. Mr. Lo at Department of Applied Physics for valuable advices in my SEM characterizations, Mr. Kwan and Dr. Yan at Department of Applied Biology and Chemical Technology (ABCT) for valuable advices in my NMR characterizations, Mr. Jeremy Man Nin Yeung at

Materials Research Center, The Hong Kong Polytechnic University for assistance in DMA and XRD experiments and Dr. Cheng Hao Lee and Mr. Tsz Kin Cheung from Hong Kong University of Science and Technology for assistance in TEM characterizations.

The work described in this paper was partially supported by the Research Grants Council of Hong Kong (Project Nos.: PolyU 5140/06E and 5136/07E). This project also benefited from the financial support of the University Grants Committee of Hong Kong (Grant No.: A-PH60, A-PD1N, A-PH94, A-SA45, and J-BB6N).

Finally, I would like to express my deepest appreciation to my family. Without their unconditional love, support, and sacrifice, I could not have come this far and completed my Mphil study.

TABLE OF CONTENTS

CERTIFICATE OF ORIGINALITY ii

ABSTRACTS iii

ACKNOWLEDGEMENTS v

TABLE OF CONTENTS vii

LIST OF FIGURES xv

LIST OF TABLES xxiii

LIST OF ABBREVIATIONS xxv

LIST OF SYMBOL NOMENCLATURE xxvii

Chapter 1: Introduction

1.1 Introduction 1

1.2 Objectives of the research 3

1.3 Project Significance and Value 4

1.4 Originality of present work 5

1.5 Research Methodology

1.5.1 Synthesis of novel hyperbranched macromolecules 5

1.5.2 Preparation of composites 5

1.5.3 Major analytical techniques to characterize hyperbranched polymer (HBP) and their modified composite 6

Chapter 2 Literature Review

2.1 Hyperbranched polymer

2.1.1 Introduction 7

2.1.2 Synthetic methods of hyperbranched polymers 8

2.1.3 Properties of hyperbranched polymers

2.1.3.1 Thermal properties 11

2.1.3.2 Mechanical and rheological properties 13

2.1.3.3 Solution properties 15

2.1.4 Modification of hyperbrached polymers 16

2.1.5 Potential applications of hyperbranched polymers

2.1.5.1 Applications in Coatings 17

2.1.5.2 Modifiers and additives 17

2.1.5.3 Applications in polymer electrolytes 18

2.1.5.4 Fabrication of novel nanomaterials 18

2.1.5.5 Biomedical applications (biomaterials) 20

2.1.5.6 Patterning of hyperbranched polymer films 20

2.1.6 Hyperbranched polyester

2.1.6.1 Introduction 21

2.1.6.2 Preparation of hyperbranched polyester 21

2.1.6.3 Chemical structure of hyperbranched polyester 22

2.1.6.4 Properties of hyperbranched polyester 23

2.1.6.5 Applications of hyperbranched polyester 24

2.2 Biodegradable polymer

2.2.1 Introduction 25

2.2.2 Biodegradable Polymers Classifications 30

2.2.3 Methods of biodegradation 31

2.2.4 Applications for biodegradable polymers 35

2.2.5 Poly(ε-caprolactone)

2.2.5.1 Structure of PCL 41

2.2.5.2 Properties of PCL 41

2.2.5.3 Degradability of PCL 42

2.2.5.4 Applications of PCL 42

2.2.6 Poly(lactic acid)

2.2.6.1 Structure of PLA 44

2.2.6.2 Properties of PLA 44

2.2.6.3 Degradability of PLA 46

2.2.6.4 Applications of PLA 49

2.3 Biodegradable Polymer Blends

2.3.1 Introduction 52

2.3.2 Blends and compatibilization of Poly(ε-caprolactone) 54

2.3.3 Blends and compatibilization of Poly(lactic acid) 59

2.3.4 Modification of biodegradable polymer (PCL and PLA) by hyperbranched polymer-based nanostructures 64

Chapter 3 Hyperbranched Polymer Synthesis and Characterization

3.1 Introduction 66

3.2 Experimental

3.2.1 Materials 68

3.2.2 Synthesis of HBP with acid end-groups 68

3.2.3 Synthesis of HBP with hydroxyl end-groups 69

3.2.4 Control of hyperbranched polymerisation 69

3.2.5 Structural identification by Nuclear Magnetic Resonance Spectroscopy 69

3.2.6 Fourier-Transform Infra-red spectroscopy (FT-IR) 70

3.2.7 Gel Permeation Chromatography 70

3.3 Results and discussion

3.3.1 Synthesis of HBP with acid end-groups 70

3.3.2 Synthesis of HBP with hydroxyl end-groups 71

3.3.3 Control of hyperbranched polymerisation 71

3.3.4 Chemical structure of HBP(COOH) 72

3.3.5 Chemical structure of HBP(OH) 73

3.3.6 Chemical structure of allylamine-capped HBP(OH) 73

3.3.7 Structural identification by NMR 74

3.3.8 Fourier-Transform Infra-red spectroscopy (FT-IR) 82

3.4 Conclusion 84

Chapter 4: Fabrication and Characterization of HBP-reinforced PCL composites

4.1 Introduction 85

4.2 Experimental

4.2.1 Materials 86

4.2.2 Fabrication of PCL composites 86

4.2.3 Tensile tests 87

4.2.4 Differential Scanning Calorimetry (DSC) 88

4.2.5 Dynamic Mechanical Analysis (DMA) 89

4.2.6 Scanning Electron Microscopy (SEM) 90

4.2.7 Transmission electron microscopy (TEM) 91

4.2.8 Degradation 91

4.3 Results and discussion

4.3.1 Fabrication of PCL composite specimens 93

4.3.2 Mechanical properties

4.3.2.1 Tensile test of HBP(COOH)-reinforced PCL nanocomposites 93

4.3.2.2 Tensile test of HBP(OH)-reinforced PCL nanocomposites 99

4.3.3 Thermal and thermomechanical studies

4.3.3.1 Differential Scanning Calorimetry (DSC) 103

4.3.3.1.1 DSC of HBP(COOH) modified PCL nanocomposites 103

4.3.3.1.2 DSC of HBP(OH) modified PCL nanocomposites 109

4.3.3.2 Dynamic Mechanical Analysis (DMA)

4.3.3.2.1 DMA of HBP(CA) modified PCL nanocomposites 111

4.3.3.2.2 DMA of HBP(OH) modified PCL nanocomposites 116

4.3.4 Scanning Electron Microscopy (SEM)

4.3.4.1 SEM of HBP(COOH) modified PCL nanocomposites 120

4.3.4.2 SEM of HBP(OH) modified PCL nanocomposites 124

4.3.5 Transmission electron microscopy (TEM) 126

4.3.5.1 TEM of HBP(COOH) modified PCL nanocomposites 126

4.3.5.2 TEM of HBP(OH) modified PCL nanocomposites 129

4.3.6 Degradation study

4.3.6.1 Biodegradability of HBP(COOH) 130

4.3.6.2 Biodegradability of HBP(COOH)/PCL composites 130

4.3.6.3 Biodegradability of HBP(OH) 135

4.3.6.4 Biodegradability of HBP(OH)-1/PCL composites 136

4.4 Conclusion 137

Chapter 5: Fabrication and characterization of HBP-reinforced PLA composites

5.1 Introduction 140

5.2 Experimental

5.2.1 Materials 142

5.2.2 Fabrication of PLA composites 142

5.2.3 Tensile tests 143

5.2.4 Differential Scanning Calorimetry (DSC) 143

5.2.5 Dynamic Mechanical Analysis (DMA) 144

5.2.6 Scanning Electron Microscopy (SEM) 145

5.2.7 Transmission electron microscopy (TEM) 145

5.2.8 Degradation 145

5.3 Results and discussion

5.3.1 Fabrication of PLA composite specimens 145

5.3.2 Mechanical properties

5.3.2.1 Tensile test of HBP(COOH)-reinforced PLA nanocomposites 146

5.3.2.2 Tensile test of HBP(OH) modified PLA nanocomposites 151

5.3.3 Thermal and thermomechanical studies

5.3.3.1 Differential Scanning Calorimetry (DSC) 152

5.3.3.2 Dynamic Mechanical Analysis (DMA) 156

5.3.4 Scanning Electron Microscopy (SEM) 161

5.3.5 Transmission electron microscopy (TEM) 164

5.3.6 Degradation study

5.3.6.1 Biodegradability of HBP(COOH) 165

5.3.6.2 Biodegradability of HBP(COOH)/PLA composites 166

5.4 Conclusion 171

Chapter 6: Conclusion and Future outlook

6.1 Summary of the major achievements 174

6.1.1 Synthesis of desired HBPs and fabrication of composite materials 174

6.1.2 Characterization of HBPs 174

6.1.3 Effects of HBPs in PCL and PLA composite materials 175

6.1.4 Biodegradability study 175

6.2 Concluding remarks 176

6.3 Future outlook

6.3.1 Applications of HBP(COOH) and HBP(OH) to other polymeric systems 178

6.3.2 Novel hyperbranched polymers with other types of end groups 178

6.3.3 Further study on biodegradability of the nanocomposites 179

References 180

List of figures

Chapter 2

Figure 2.1 Schematic representation of a hyperbranched polymer constructed by the polymerization of AB_2 type monomers 10

Figure 2.2 Melt viscosity vs. molar mass of linear and hyperbranched polymers (a.m.u.: atomic mass unit.) 15

Figure 2.3 the typical molecular structure of hyperbrached polyester 22

Figure 2.4 Classification of the biodegradable polymers 31

Figure 2.5 Polymer degradation process by hydrolysis 34

Figure 2.6 Schematic diagram of poly(ε-caprolactone) 41

Figure 2.7 Schematic diagram of poly(L-lactic acid). 44

Figure 2.8 A biotic and biotic degradations during composting stage. 47

Chapter 3

Figure 3.1 Schematic diagram of HBP(COOH) 72

Figure 3.2 Schematic diagram of HBP(OH) 73

Figure 3.3 Schematic diagram of allylamine-capped HBP(OH) 74

Figure 3.4 ^{1}H-NMR spectrum of HBP(COOH)-2 75

Figure 3.5 ^{13}C-NMR spectrum of HBP(COOH)-2 75

Figure 3.6 ^{1}H-NMR spectrum of HBP(COOH)-3 76

Figure 3.7 ^{13}C-NMR spectrum of HBP(COOH)-3 77

Figure 3.8 ^{1}H-NMR spectrum of HBP(COOH)-4 78

Figure 3.9 ^{13}C-NMR spectrum of HBP(COOH)-4 78

Figure 3.10 ^{1}H-NMR spectrum of HBP(COOH)-5 79

Figure 3.11 ^{1}H-NMR spectrum of HBP(OH)-1 80

Figure 3.12 ^{13}C-NMR spectrum of HBP(OH)-1 81

Figure 3.13 ^{1}H-NMR spectrum of allylamine-capped HBP(OH) 82

Figure 3.14 FTIR spectra of HBP(COOH)-3 83

Figure 3.15 FTIR spectra of HBP(OH)-1 84

Chapter 4

Figure 4.1 A sample of a HBP(COOH)/PCL composite 93

Figure 4.2 Tensile stress-strain curves of the PCL composite with different HBP(COOH)-2 contents 94

Figure 4.3 Tensile stress-strain curves of the PCL composite with various HBP(COOH)-3 contents 95

Figure 4.4 Mechanical properties of PCL with various HBP(COOH)-3 concentrations 96

Figure 4.5 Tensile stress-strain curves of the PCL composite with different HBP(COOH)-4 contents 97

Figure 4.6 Mechanical properties of PCL with various HBP(COOH)-4 concentrations 97

Figure 4.7 Tensile stress-strain curves of the PCL composite with various HBP(OH)-1 contents 100

Figure 4.8 Mechanical properties of PCL with various HBP(OH)-1 weight percentages 100

Figure 4.9 Tensile stress-strain curves of the PCL composite with various HBP(OH)-2 contents 101

Figure 4.10 Mechanical properties of PCL with various HBP(OH)-2 concentrations 102

Figure 4.11 DSC thermograms for pure PCL and HBP(COOH)-2 modified composites 104

Figure 4.12 DSC thermograms for pure PCL and HBP(COOH)-3 modified composites 106

Figure 4.13 DSC thermograms for pure PCL and HBP(COOH)-4 modified composites 107

Figure 4.14 DSC thermograms for pure PCL and HBP(OH)-1 modified composites 109

Figure 4.15 DSC thermograms for pure PCL and HBP(OH)-2 modified composites 110

Figure 4.16 Tan δ vs. temperature curves of pure PCL and HBP(COOH)-3 modified PCL composites 113

Figure 4.17 Storage modulus G' vs. temperature curves of pure PCL and HBP(COOH)-3 modified PCL composites 113

Figure 4.18 Tan δ vs. temperature curves of pure PCL and HBP(COOH)-4 modified PCL composites 115

Figure 4.19 Storage modulus G' vs temperature curves of pure PCL and HBP(COOH)-4 modified PCL composites 115

Figure 4.20 Tanδ vs. temperature curves of pure PCL and HBP(OH)-1 modified composites 118

Figure 4.21 Storage modulus G' vs temperature curves of pure PCL and HBP(OH)-1 modified PCL composites 118

Figure 4.22 Tan δ vs. temperature curves of pure PCL and HBP(OH)-2 modified PCL composites

119

Figure 4.23 Storage modulus G' vs temperature curves of pure PCL and HBP(OH)-2 modified PCL composites 120

Figure 4.24 FE-SEM images of the fracture surface of PCL composite samples with different weight ratios of HBP(COOH)-3 and PCL: (a) 100/0; (b) 97/3; (c) 90/10; (d) 80/20 (The magnifications are ×5000) 122

Figure 4.25 FE-SEM images of the fracture surface of PCL composites with different weight ratios of HBP(COOH)-4 and PCL: (a) 100/0; (b) 94/6; (c) 90/10; (d) 80/20 (The magnifications are ×5000) 123

Figure 4.26 FE-SEM image of the fracture surface of PCL composites with different ratios of HBP(OH)-1 and PCL: (a) 100/0; (b) 97/3; (c) 94/6, and (d) 90/10 (The magnifications are ×5000) 125

Figure 4.27 TEM micrographs of (a) 3 wt. % HBP(COOH)-3/PCL composite, (b) 6 wt. % HBP(COOH)-4/PCL composite 127

Figure 4.28 TEM micrographs of 6 wt % HBP(OH)-1 modified PCL sample 129

Figure 4.29 Photographs of a HBP/PCL composite sheet (a) before and (b) after the degradation test 131

Figure 4.30 Weight loss and molecular weight of the blend vs. wt. % of HBP(COOH)-3 in PCL treated with PBS solution after the test 133

Figure 4.31 Weight loss and molecular weight of the blend vs. wt. % of HBP(COOH)-3 in PCL treated with 0.01M NaOH after the test 133

Figure 4.32 Weight loss and molecular weight of the blend vs. wt. % of HBP(COOH)-4 in PCL treated with PBS solution after the test 134

Figure 4.33 Weight loss and molecular weight of the blend vs. wt. % of HBP(COOH)-4 in PCL treated with 0.01M NaOH after the test. 135

Figure 4.34 Weight loss and molecular weight of the blend vs. wt. % of HBP(OH)-1 in PCL treated with PBS solution after the test 136

Figure 4.35 Weight loss and molecular weight of the blend vs. wt. % of HBP(OH)-1 in PCL treated with 0.01M NaOH solution after the test 137

Chapter 5

Figure 5.1 A sample of a HBP(COOH)/PLA composite 146

Figure 5.2 Tensile stress-strain curves of the PLA composite with different HBP(COOH)-1 contents 147

Figure 5.3 Tensile stress-strain curves of the PLA composite with various HBP(COOH)-3 contents 148

Figure 5.4 Mechanical properties of PLA with various HBP(COOH)-3 concentrations 148

Figure 5.5 Tensile stress-strain curves of the PLA composite with different HBP(COOH)-4 contents 149

Figure 5.6 Mechanical properties of PLA with various HBP(COOH)-4 concentrations

150

Figure 5.7 Tensile stress-strain curves of the PLA composite with different HBP(OH)-1 contents 151

Figure 5.8 Tensile stress-strain curves of the PLA composite with different HBP(OH)-2 contents 152

Figure 5.9 DSC thermograms for pure PLA and HBP(COOH)-3 modified composites 153

Figure 5.10 DSC thermograms for pure PLA and HBP(COOH)-4 modified composites 155

Figure 5.11 Log(tan δ vs. temperature curves of pure PLA and HBP(COOH)-3 modified PLA composites 157

Figure 5.12 Storage modulus G' vs. temperature curves of pure PLA and HBP(COOH)-3 modified PLA composite 158

Figure 5.13 Log(tan δ vs. temperature curves of pure PLA and HBP(COOH)-4 modified PLA composites 159

Figure 5.14 Storage modulus G' vs. temperature curves of pure PLA and HBP(COOH)-4 modified PLA composites 160

Figure 5.15 FE-SEM images of the fracture surface of PLA composite samples with different weight ratios of HBP(COOH)-3 and PLA: (a) 100/0 ;(b) 94/6 ;(c) 90/10; (d) 80/20 (All magnifications are ×5000) 162

Figure 5.16 FE-SEM images of the fracture surface of PLA composite samples with different weight ratios of HBP(COOH)-4 and PLA: (a) 100/0 ;(b) 94/6 ;(c) 90/10; (d) 80/20; (The magnifications are ×5000) 163

Figure 5.17 TEM micrographs of (a) 6 wt. % HBP(COOH)-3/PLA composite, (b) 3 wt. % HBP(COOH)-4/PLA composite 165

Figure 5.18 Photographs of a HBP/PLA composite sheet (a) before and (b) after the degradation test 166

Figure 5.19 Weight loss and molecular weight of the blend vs. wt. % of HBP(COOH)-3 in PLA treated with PBS solution after the test 169

Figure 5.20 Weight loss and molecular weight of the blend vs. wt. % of HBP(COOH)-3 in PLA treated with 0.01M NaOH solution after the test 169

Figure 5.21 Weight loss and molecular weight of the blend vs. wt. % of HBP(COOH)-4 in PLA treated with PBS solution after the test 170

Figure 5.22 Weight loss and molecular weight of the blend vs. wt. % of HBP(COOH)-4 in PLA treated with 0.01M NaOH solution after the test 171

List of tables

Table 1 The analytical techniques used to characterize the HBP modified bio-composites 6

Table 2 Factors affecting the hydrolytic degradation behaviour of biodegradable polymers. 24

Table 3: Biodegradable Polymers and Potential Applications 29

Table 4. Gel Permeation Chromatography data of the HBPs 71

Table 5 DSC data of HBP(COOH)-2/PCL blends 104

Table 6 DSC data of HBP(COOH)-3/PCL blends 106

Table 7 DSC data of HBP(COOH)-4/PCL blends 108

Table 8 DSC data of HBP(OH)-1/PCL blends 110

Table 9 DSC data of HBP(OH)-2/PCL blends 111

Table 10 The degradation data of HBP(COOH)-3 and HBP(COOH)-4 130

Table 11 The degradation data of HBP(COOH)-3/PCL and HBP(COOH)-4/PCL composites 134

Table 12 The degradation data of HBP(OH)-1 135

Table 13 DSC data of HBP(COOH)-3/PLA blend 154

Table 14 DSC data of HBP(COOH)-4/PLA blends 155

Table 15 The degradation data of HBP(COOH)-3/PLA and HBP(COOH)-4/PLA composites 170

List of Abbreviations

ASTM	American society for testing and materials
CA	citric acid
^{13}C NMR	carbon magnetic resonance spectroscopy
DMSO-d_6	dimethyl-d6 sulfoxide
DSC	differential scanning calorimetry
DB	degree of branching
DMA	dynamic mechanical analysis
EG	ethylene glycol
EVOH	ethylene vinyl alcohol
EDS	energy dispersive X-ray spectroscopy
FTIR	fourier-transform infra-red spectroscopy
GPC	gel permeation chromatography
HBP	hyberbranched polymers
HB	hyberbranched
HPLC	high-performance liquid chromatography
ISO	International Organization for Standardization
MPA	2,2-Bis(hydroxymethyl) propionic acid
MCP	micro-contact printing
^{1}H NMR	proton magnetic resonance spectroscopy

NMR	nuclear magnetic resonance spectroscopy
PCL	poly(ε-caprolactone)
PLA	poly(lactic acid)
PLLA	poly(L-lactic acid)
PHA	phytohemagglutinin
PBHB	poly-beta-hydroxybutyrate
PMMA	poly(methyl methacrylate)
PET	Polyethylene terephthalate
PBT	polybutylene terephthalate
PBS	phosphate-buffered saline
PVOH	poly(vinyl alcohol)
SCVP	self-condensing vinyl polymerization
SEM	scanning electron microscope
TEM	transmission electron microscopy
THF	tetrahydrofuran
TEFLON	Polytetrafluoroethylene, PTFE
XRD	X-ray diffraction

List of Symbol Nomenclature

G’	storage modulus of rheological properties
ΔH_c	the cool of crystallization of the sample
$\Delta H_{100,c}$	the cool of crystallization for a 100%crystalline PCL,
ΔH_m	the heat of fusion of the sample
$\Delta H_{100,m}$	the heat of fusion for a 100%crystalline PLA
M_w	molecular weights
M_n	number-average molecular weight
Tg	glass transition temperature
Tm	melting temperature
tan δ	loss tangent
Tp	the peak temperature
w_t	the dry weight remaining at a given degradation time
w_0	the initial weight.
X_c	the degree of crystallinity

Chapter 1: Introduction

1.1 Introduction

Nanocomposites are novel materials with drastically improved properties due to the incorporation of small amounts (usually, less than 10 wt%) of nano-sized fillers into a polymer matrix. Nanofillers can be classified according to their morphology, such as particles that are (i) layered (e.g., clays), (ii) spherical (e.g., silica) or (iii) acicular (e.g., whiskers, carbon nanotubes). Their specific geometrical dimensions, and thus aspect ratios, partially affect the final materials properties. Layered silicate clays offer high surface area, more than 700 m^2/g, i.e., a huge interface with the polymer (matrix), which governs the material properties.

The final behavior can be considerably improved by the strong and extensive polymer-nanofiller interactions, as well as, good particle dispersion. Nano-biocomposites are obtained by adding nanofillers to biopolymers such as poly(L-lactic acid) (PLA) and poly(ε-caprolactone) (PCL), resulting in very promising materials since they exhibit improved properties with preservation of the material biodegradability, without eco-toxicity. Such materials can be destined to biomedical applications and different short-term applications, e.g., packaging, agriculture or hygiene

devices. They thus represent a strong and emerging answer for improvement of eco-friendly materials.

Hyberbranched polymers (HBP)s have attracted great attention recently in application as additives in various fields, for example, toughening modifiers for thermosets (epoxy resins) in place of commercial tougheners such as rubbers, thermoplastics, or glass particles.[1]

HBPs are highly branched macromolecules described as having a globular structure with a multiplicity of reactive end groups. They are synthesized via a one-step polycondensation reaction, generating molecules with a high degree of branching and significantly lower viscosity compared to linear polymers of the same molecular weight[2]. In this project, a group of newly developed biodegradable HBPs are considered as candidates for composite application with biopolymers to achieve desired biodegradable composite materials. Polymer composites can benefit from such HBPs, for instance, their highly branched structures and densely populated surface groups allow for enhanced interaction with the bulk material, which in turn strengthen the matrix and could aid in improving various properties such as physical and mechanical properties. It is believed that the innovative architecture would open up a new direction and hence has high

potential for building up a new generation of renewable/biodegradable materials for applications not limited to the area of textile.

1.2 Objectives of the research

(a) To synthesize two types of tailored HBPscontaining either carboxyl acid (-COOH) or hydroxyl (-OH) surface endgroups with different molecular weights.

(b) To characterize the synthesized macromolecules by standard spectrophotometric techniques.

(c) To study the effects of the nanofillers on mechanical and thermal behaviors of two types of biodegradable polymer matrixes (PCL and PLA).

(d) To analyze structure and fracture morphology of the nanocomposites by microscopic techniques.

(e) To access in-vitro biodegradability of the end products.

1.3 Project Significance and Value

Whilst there is much excitement over the potential of nanotechnologies, concerns have been raised on their unpredicted environmental risks associated. Biodegradable polymer nanocomposites, owning to their readily degradable polymer matrix, have an even acuter problem in terms of uncontrolled release of nanomaterials to the environment. To address the problem, hence, the composite systems presented in this study are designed to be fully biodegradable, where the desired HBPs are used as the filler are biodegradable too. In sum, the new approach has several distinct advantages: 1) a wide range of functionalization on hyperbranched polymer structure for better control of material properties (e.g. fracture toughness, optical transparencies, etc.); 2) simple processing steps; 3) a commercially viable route for making novel green nanocomposites.

Although a number of scientific papers have been published in the field of biodegradable composites in the past decade, information about using hyperbranched macromolecules as fillers/modifiers is still very limited. The research project is no doubt of scientific and technological significances because the work would not only lead to new knowledge in HBP science, but also bring out a new possibility to combine unique HBPs into biodegradable composite systems, which would have great potential in a wide array of industrial applications.

1.4 Originality of present work

As mentioned, this is a new trial to combine special HBPs with a biodegradable composite system, where no similar studies have been reported previously. This is also the first time based on a novel method to synthesize the required HBPs, and later to study their effects associated with different properties of the composite materials. The outcomes of the work will open up a new area of biodegradable materials. The new findings and knowledge will also contribute to both polymer science and material science.

1.5 Research Methodology

1.5.1 Synthesis of novel hyperbranched macromolecules

Novel HBPs bearing acid and hydroxyl end-groups, respectively, are synthesized based on a novel method using only a small amount of solvent. (Detail procedure refer to **Chapter 3.2.2, 3.2.3 and 3.2.4**)

1.5.2 Preparation of composites

Blends of the synthesized HBPs and biopolymers were solution mixed and formed homogeneous thin composite films through controlled solvent evaporation. (Detail procedure refer to **Chapter 4.2.2 and 5.2.2**)

1.5.3 Major analytical techniques to characterize hyperbranched polymer (HBP) and their modified composite

A variety of advanced analytical techniques (listed in the **Table1** below) will be utilized to characterize the HBP modified bio-composites and evaluate their physical and chemical properties:

Table 1 The analytical techniques used to characterize the HBP modified bio-composites

Property	*Characterization method*
Chemical composition and functionalities (end-group) of modified hyperbranched polymers and HBP-modified composite	FTIR H and ^{13}C NMR
Molecular weight distribution of HBP	Gel Permeation Chromatography (GPC) and viscosity measurement
Mechanical properties	• Tensile test
Thermal and thermomechanical properties of HBP-modified composite	Differential Scanning Calorimetry(DSC) Dynamic Mechanical Analysis (DMA)
Crystallinity change (crack and brittle matrix determination)	• X-ray diffraction and optical microscopy
Morphology of HBP-modified composite and dispersion of HBP particles in polymer matrix	• Scanning electron microscope (SEM) • Transmission electron microscopy (TEM)
Degradability of composites	• Enzymatic and non-enzymatic methods

Chapter 2 Literature Review

2.1 Hyperbranched polymer

2.1.1 Introduction

Macromolecules with highly branched structure so called dendritic polymers have attracted considerable interest in the field of polymeric materials. As a family of three-dimensional macromolecules, dendritic polymers basically consisted of hyperbranched polymers, dendrimers, and hybrid structures. In fact, hyperbranched polymers and dendrimers have several features in common: Both types of polymer are synthesized based on AB_x-monomers, with multiple endgroups distributed at the surface and essentially nonentangled. However, while dendrimers are constructed in a step-wise fashion, are monodisperse, and symmetrically branched, the hyperbranched polymers are typically synthesized by one-pot process, are branched with irregular pattern, highly asymmetric and excellent polydispersity.[3]

Flory predicted that the hyperbranched polymers obtained should have an infinitely wide molecular weight distribution and that the highly branched chains would be nonentangled and amorphous in nature. Owing to the low degree of entanglements, Flory concluded that the materials would have poor mechanical strength. Unfortunately, no experiments were carried out until 30 years later that Kim and Webster published the first paper on the

synthesis and properties of highly branched polymers and so-called hyperbranched [5].

2.1.2 Synthetic methods of hyperbranched polymers

The hyperbranched polymers can be synthesized in a more facile way compared to that of dendrimers as it does not require the use of protection/deprotection steps. This is due to the fact that hyperbranched polymers are allowed to contain some linearly incorporated AB_x monomers. The most common synthetic route is a one-pot synthesis via polycondensation of AB_x monomers in the presence of a catalyst. Another strategy is using a core molecule and an AB_x monomer.

The lower cost of hyperbranched polymers synthetic processis is favorable for industrial scale production. Giving them an advantage over dendrimers in applications involving large amounts of reagents, although the properties of hyperbranched polymers are intermediate between those of dendrimers and linear polymers [6].

The synthesis of hyperbranched macromolecules were first proposed by Flory who theorized that polymers could be prepared by poly condensation of AB_x-functional monomers, where $x \geq 2$. The functional group A reacts only with functional group B of another molecule, the polymerization of AB_x monomer subsequently results in highly

branched polymers[4]. Apart from polycondensation, addition polymerization of monomers that consists of both initiating and propagating function within the same molecule[7], ring-opening polymerization[8], and self-condensing vinyl polymerization (SCVP)[9] can be used to synthesize hyperbranched macromolecules. Until now, a number of reviews on the synthetic approaches for hyperbranched polymers have been published[10-16] in terms of methodologies and reaction mechanisms.

The one-pot process in the preparation of hyperbranched polymers normally leads to uncontrollable growth. Consequently, the resulting structures are imperfect and polydisperse. Hyperbranched polymers, unlike dendrimers, the controllability of generations and molecular weight distribution are deteriorated. Due to the statistical aspect of coupling steps, steric hindrance effect of growing chains, reactivity of surface end groups and the propagation occurs at only two connecting sites among branching units, generates various polymer segment length.[17]

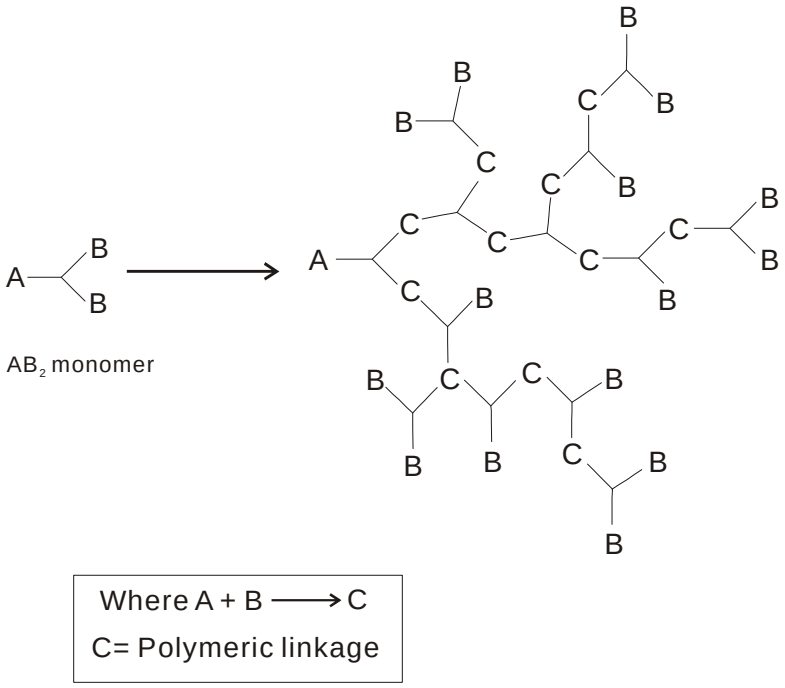

Figure 2.1 Schematic representation of a hyperbranched polymer constructed by the polymerization of AB_2 type monomers

Based on AB_2-type monomers, as demonstrated in **Figure2.1**, linear segments, known as defects, show one functional group B unreacted, whereas the terminal segments have two unreacted functional groups. The most prominent feature of hyperbranched polymers is "degree of branching" (DB) or "branching factor", which defined the number ratio of branched, terminal, and linear units in the structure of hyperbranched polymer. [10]

The degree of branching is defined as the ratio of the sum of the dendritic and the terminal repeating units to the sum of all repeating units within the structure as shown in Equation (1.1)[18].

$$DB(\%) = \frac{D+T}{D+T+L} \times 100 \qquad \text{Eq. (1.1)}$$

Where D, T and L represent the number of dendritic, terminal and linear units per molecule. The fractions of D-, L- and T-repeating units are usually determined by NMR spectroscopy. Equation1.2) has been further suggested for the estimation of the molar mass of a hyperbranched polymer by using the relative fraction of the repeating unit, respectively. [19]

$$DP_n = \frac{D+L+T}{T-D} \qquad \text{Eq. (1.2)}$$

2.1.3 Properties of hyperbranched polymers

2.1.3.1 Thermal properties

Owing to their highly branched structure, hyperbranched polymers are almost exclusively amorphous materials. Therefore, the glass transition temperature (T_g) is one of the most important thermal properties for hyperbranched polymer in certain potential applications such as powder coatings or rheology modifiers. During heating process, amorphous components convert at T_g from a glassy state to a fluid state, i.e., into a melt for low molar mass substances or a rubbery state for high molar mass components. In the melt state, thermal energy is sufficiently high for long segments of each polymer chain to move in random motions. In the amorphous state, polymer chains assume their unperturbed dimensions as they do in solution under theta-conditions. Below T_g, all

long-range segmental motion of polymer chain segments disappears. Rotations around single bonds become very difficult and the only molecular motions occurred are short-range motions of several contiguous chain segments and motions of substituent groups[20].

The situation is more complicated in the case of hyperbranched polymer, since the branching points and the presence of numerous functional end groups strongly influence segmental motions. The glass transition temperature of a hyperbranched polymer is not only affected by the chain-end structure, but also by the molecular weight and the overall macromolecular composition[51,21]. According to Schmal Johann et al. the properties of hyperbranched polymer can be considered as a combination of inter- and intramolecular effects. Different T_g values of hyperbranched polymers with various repeating units with the same end groups exhibit the intramolecular effect of segmental motion, whereas the change of T_g through modification of the end groups (in terms of hydrophilicity or hydrophobicity) can be assigned to translational motion and an intermolecular effect[22].

For dendritic polymer systems T_g increases with generation number to a limit, above which it remains nearly constant[53,23]. This increase in T_g with generation number is an indication of a decrease in chain mobility due to branching effect.

A number of studies shown that the chemical nature of end groups strongly affect the glass transition temperature. Sunder et al. used Differential Scanning Calorimetry (DSC) measurements to show that the flexibility of a modified highly polar hyperbranched polymer with large number of hydroxyl end groups is mainly controlled by two factors: (i) hydrogen bonding strength of the end groups, increasing the rigidity of the molecules and (ii) tendencies of the substituent to form higher ordered phases (mesophases, crystallization) [24]. It is noticeable that the degree of alkyl substitution has only weak effect on T_m, and there is a pronounced effect on T_g.[24]

2.1.3.2 Mechanical and rheological properties

Novel applications of a polymer are often closely related to its material and processing properties. Thus, the mechanical and rheological properties of hyperbranched polymers are of great importance.

Due to the highly branched, globular structure, the configuration of hyperbranched polymers is characterized by poor chain entanglements. The non-entangled state imposes poor mechanical properties, resulting in brittle dendritic-type polymers with limited use as thermoplastics[25]. The stress–strain behavior of hyperbranched polymers can be described as the ductility of metals as observed by Rogunova et al. for

hyperbranched polyesters. Similar to ductile metals, hyperbranched polyesters do not strain harden[26]. This is due to their globular structure, which prevents chain extension and orientation (the typical mechanisms of strain hardening). However, intermolecular associations, such as hydrogen bonding and possibly intermolecular crystallization of a few linear segments, provide linkages between the hyperbranched macromolecules[26].

Besides the mechanical properties, the viscosity behavior of linear and branched polymers shows remarkable differences. This was already noted by several scientists at the end of the 1960s[27-32]. **Figure2.2** illustrates the melt viscosity of linear and dendritic polyethers as a function of the molar mass (given in atomic mass units). For linear polymers, a drastic increase in melt viscosity is observed beyond a critical molecular weight. However, the line for hyperbranched polymers shows a continuous slope of 1.1 up to 100,000 a.m.u. with no observable critical weight limit. This behavior can be explained by the different physical structure of linear and hyperbranched macromolecules. At low molar mass, linear polymers consist of random coil chains. As the molecular weight increases, entanglement would be occurred at a critical molecular size, leading to a sharp increase in melt viscosity. Unlike linear polymers, the globular, highly branched architecture of hyperbranched polymers prevents chain entanglements, resulting in considerably smaller melt viscosities and a continuous slope of the η-function (see **Figure2.2**).

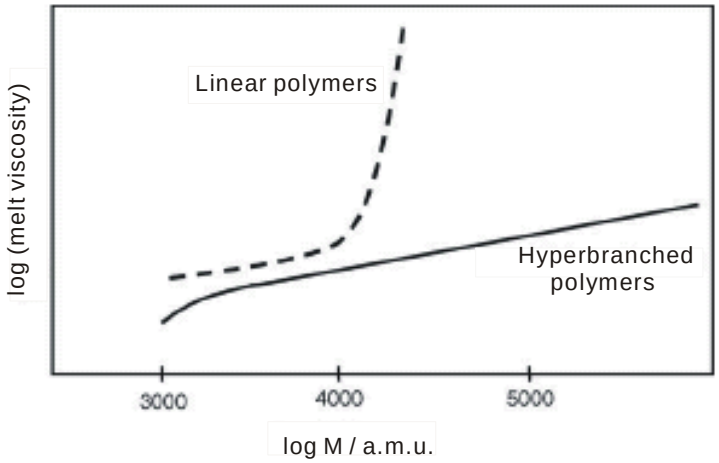

Figure 2.2 Melt viscosity vs. molar mass of linear and hyperbranched polymers (a.m.u.: atomic mass unit.)

2.1.3.3 Solution properties

A number of excellent research studies have been published focusing on dilute and semi-dilute properties of branched polymer systems[33-47].

Hyperbranched polymers have a significantly lower intrinsic viscosity, Mark–Houwink exponent, hydrodynamic volume, and ratio of radius of gyration to hydrodynamic radius in comparison to their linear analogues of the same molar mass. Also the osmotic second virial coefficient A_2 was used to characterize the effect of branching. The degree of branching decreases the second virial coefficient in 'good' solvents. Therefore, for a branched polymer, A_2 is always lower than that for the homologous linear polymer.[43-44]

For applications of hyperbranched polymers in the field of chemical engineering the phase behavior of concentrated hyperbranched polymer solutions is of great interest.

2.1.4 Modification of hyperbranched polymers

The properties of hyperbranched polymers are often affected by the nature of the polymer chain backbone, the end functional groups of polymer chain, degree of branching, chain segment length between branching points, and the molecular weight distribution. Hyperbranched polymers are often modified to tailor their properties for a special reason. Based on the highly branched architecture and the large number of end functional groups of hyperbranched macromolecules, five modification strategies have been developed:

(1)End capping with short chains or small organic molecules; [48-49]

(2) Terminal grafting via living polymerization;

(3) Growing hyperbranched polymers on the surface, or grafting from/onto the functionalized surface; [50]

(4) Hypergrafting to obtain hyperbranched polymers with a linear macromolecular core structure;[51-54]

(5) Blending or crosslinking approach

2.1.5 Potential applications of hyperbranched polymers

2.1.5.1 Applications in Coatings

Hyperbranched polymers have been used for various coating resins, such as powder coatings,[55-56] solid coatings[57], flame retardant coatings[58] and barrier coatings for flexible packaging[59], depending on their excellent solubility, low viscosity and abundant functional groups. The most widely studied hyperbranched polymers in the field of coatings are two commercially available products as follows: Boltorne (hyperbranched aliphatic polyesters)[55,57,58-63] and hyperbranched polyester- amides)[56,64]. In UV-curing process, the hyperbranched polymers are generally end-capped with methacrylate or acrylate groups[57-63,65]. Resins based on hyperbranched polymers have lower viscosities and improved curing condition than those of linear unsaturated polymers.

2.1.5.2 Modifiers and additives

Hyperbranched polymers can be applied as toughеners for thermosets[66-74], curing, cross-linking or adhesive agents[75-77], dye-receptive additives for polyolefins[78-79], compatilizers[80], dispersers[81,] processing aids, and rheology modifiers or blend components.[82-88]

2.1.5.3 Applications in polymer electrolytes

A solid polymeric electrolyte should meet the requirements of (1) being amorphous, (2) having a high solvating power for appropriate ions, (3) good ion transport, and (4) electrochemical stability. It is well known that oligo(ethylene glycol) segments satisfy the last three requirements, and hyperbranched polymers are usually amorphous. Thus, hyperbranched macromolecules bearing ethylene glycol (EG) chains have been designed, fabricated and applied as novel polymeric electrolytes or ion-conducting elastomers.

Hawker and coworkers[89] first prepared hyperbranched poly(ether ester)s containing linear EG units of various lengths in good yields with high molecular weights (M_w = 50,000–80,000) via polymerization of AB_2 monomers[90-92] with EG segments.

2.1.5.4 Fabrication of novel nanomaterials

Hyperbranched polymers and their substitutes can be used as nanomaterials for host–guest encapsulation and the fabrication of organic–inorganic hybrid materials, and even directly used as nanoreactors for some catalytic reactions.

The hyperbranched polyesters were observed to be suitable materials for templating nanostructures in organosilicates, and a porous organosilicate film derived from a hybrid

containing 30 wt.% polyester with an average pore size of 20 nm had been prepared[93]. Hyperbranched polyesters showed several merits used as template materials, such as higher solid content, higher polymer compositions in solution and excellent film quality than obtained with linear and star-shaped polyesters.

Hyperbranched polymers can also be utilized in nanoimprint lithography. A fascinating application of the nanoimprint lithography technique is the fabrication of magnetic quantum structures, comprising single magnetic domain bits surrounded by a nonmagnetic material. Lebib *et al.*[94-95] employed the commercially available hyperbranched poly(amide ester) Hybrane, prepared by polycondensation of cyclic anhydrides with diisopropanolamine as the top imaging resist to control the critical dimension in trilayer nanoimprint lithography. Dot arrays of 100 nm with critical dimension control with a resolution better than 10 nm were fabricated. Magnetic Co dot arrays with various diameters and thickness were made with the same mold. Compared with the traditional resist materials such as PMMA, the hyperbranched polymer showed higher chemical etch resistance. Recently, the technique has been applicable at room temperature and low-pressure, using Hybrane HS2550, a semi-crystalline hyperbranched resist polymer, and a high-density pattern with graftings of 75 nm line spacing has been realized[95].

2.1.5.5 Biomedical applications (biomaterials)

Well-defined hyperbranched polymers with multifunctional terminal groups and narrow polydispersity are available by improving synthesis procedures, hyperbranched polymers are receiving more attention in biomaterials application [126,96]. In this field, hyperbranched polymers can play two major roles: biocarriers and biodegradable materials. As biocarriers, hyperbranched macromolecules can offer their interior or peripheral functional groups to covalently immobilize biomolecules, or depending on their core–shell architecture, to sequester guest molecules.

2.1.5.6 Patterning of hyperbranched polymer films

Patterning of polymer films at micron or submicron resolution is technologically important in the field of microelectronics [97]. Because hyperbranched polymers have many functional groups, moieties with interesting optical, electrochemical, biological, and mechanical properties. Hyperbranched polymers can be easily processed into film structure. Thus, patterning of hyperbranched polymer films on the substrates is receiving considerable interest. Relevant techniques including template-based approach and photolithography have been developed by Crooks and coworkers. The templates consist of self-assembled monolayers fabricated by micro-contact printing (MCP)[101-102] and photolithographic patterning relies on a photomask alignment.

2.1.6 Hyperbranched polyester

2.1.6.1 Introduction

The hyperbranched polyester has been well developed in various types and broad application. It is one of the key structures in hyperbranched polymer family. Currently, hyperbranched polyesters have been the research focus by several groups studying hyperbranched polymer as a model. Hyperbranched polyesters are characterized by the presence of branch points or the presence of more than two end groups (ester groups) and comprise a class of polymers between linear polymers and polymer networks[103]

2.1.6.2 Preparation of hyperbranched polyester

Based on different repeating unit of monomer structure, hyperbranched polyesters can be classified into two major types, hyperbranched aromatic[103-107]and aliphatic polyesters[108-110], respectively. In most cases the hyperbranched polymers were synthesized via self-condensation of AB*x* monomers (*x*> 2). The theoretical growth of highly branched polymers was also obtained by self-condensation of ethylene group, multi-branched open-ring polymerization and polymerization of multi-functional comonomer etc. Like linear polyester, hyperbranched polyesters, hyperbranched polymers are prepared via the self condensation of an ABx monomer containing one 'A'

functional group, and two or more “B” functional groups(carboxylic or hydroxyl groups) that are capable of co-reaction through ester group.

2.1.6.3 Chemical Structure of hyperbranched polyester

Unlike linear polyesters, hyperbranched polyesters exhibit a randomly branched architecture, abundant functional end group, and hollow cavity like structures.

The structural features of a typical molecular architecture of hyperbranched polyesters were illustrated in **Figure 2.3**.

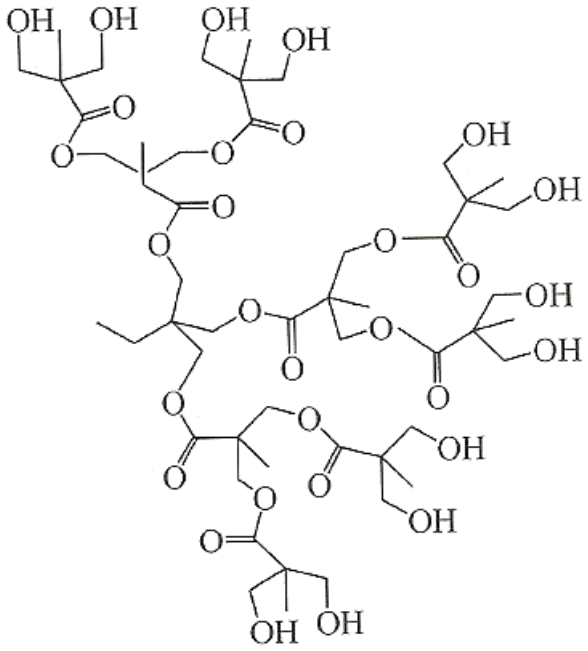

Figure2.3 The typical molecular structure of hyperbranched polyester

2.1.6.4 Properties of hyperbranched polyester

Hyperbranched polyesters exhibit some significant structure/property features as following:

(1) Good mobility

Relative to linear polyesters, the molecular architecture of HB polyesters exhibited even closer packed 3-dimensional spherical structures with Newtonian fluid flow pattern.[110]

(2) Low viscosity

Owing to spherical-like molecular structure, the entanglement between hyperbranched macromolecules is weak and the interaction among the HB molecules solely from the interaction between the functional end groups. Therefore, compared with linear polyesters, hyperbranched polyesters have lower melt and solution viscosity, particularly with nonpolar end groups.

(3) Multi-functionalities and good solubility

Hyperbranched polyester can have hydroxyl, carboxylic acid end group types in a large number and through modification of functional endgroups, hyperbranched polyester can provide a variety of functions. Due to the highly branched structure may significantly

improve the hyperbranched polyester solubility in organic solvents.

(4)Low crystallinity

The polarity of the linear polyester containing hydroxyl groups and flexible segments will be easy to make certain linear crystal, such as PET, PBT, etc. Hyperbranched polyester as the presence of highly branched nature, reduced the molecular chain of regular arrays, which eventually reduced crystallinity. In terms of transparency requirement in applications, hyperbranched polyester is very significant to this feature.

(5) Good weather resistance

Traditional linear polyester normally exhibited strong water sensitivity, mainly due to strong air exposure of ester group in molecular chain. This air exposure may cause ester hydrolysis. Hyperbranched polyester with highly branched molecular chains may embed ester group ester group effectively prevents direct contact with humid air, thereby reducing the probability of ester hydrolysis.

2.1.6.5 Applications of hyperbranched polyester

Hyperbranched polyester not only have the structure and property features of typical hyperbranched polymer but also consists of certain properties of the linear polyester,

making it shown broad prospects in many fields, and expected to make up for the poor performance of linear polyester in traditional application. Hyperbranched polyester modifications with multifunctional aspects diversify potential application of hyperbranched polyester.

Hyperbranched polyester can be expected to be the major focus in the application of biomedical materials, nonlinear optical materials, surface modification of solid particle, supramolecular chemistry and nano-materials.

2.2 Biodegradable polymer

2.2.1 Introduction

Biodegradable polymers are most widely used in terms of synthetic polymeric biomaterials. Biodegradable polymers are described as those that are hydrolyzed into small metabolizable compounds as a result of direct or indirect biological activity, and include both chemically or enzymatically catalyzed chemical reactions[113] The majority of biodegradable polymers comprise hydrolyzable functional groups. Hydrolytic biodegradation includes the reaction of hydrolyzable groups in polymer materials with water[114]. Factors in which affect the hydrolytic degradation behavior of biodegradable polymers are summarized in **Table 2**.[115]

Table 2 Factors affecting the hydrolytic degradation behavior of biodegradable polymers.

1.Water permeability and solubility (hydrophilicity/hydrophobicity)
2.Chemical structure (nature of hydrolytically unstable bonds)
3.Mechanism of hydrolysis (noncatalytic, autocatalytic, enzymatic)
4. Filler (acidic, basic, organic, inorganic species)
5.Morphology (crystalline or amorphous state)
6.Device dimensions (size, shape, surface to volume ratio)
7.Glass transition temperature (glassy and rubbery state)
8.Molecular weight and molecular weight distribution
9.Physico-chemical factors (ionic strength, pH)
10.Sterilization
11.Site of implantation

Technology in the field of petrochemical based polymers has brought substantial benefits. However, it is evident that ecosystems are considerably damaged as a result of the use of non-degradable polymeric materials for disposal[116]. In recent years biopolymers development, i.e., biodegradable polymers, have attracted more and more interest due to increasing environmental concern and less demand of fossil resources[117-119]. This trend motivates academic and industrial research to develop novel "environmental friendly" materials, i.e., materials produced from alternative resources, with low energy consumption, biodegradable and non-toxic to the environment. Since biopolymers are

biodegradable and the main productions are obtained from renewable resources such as agricultural resources, an interesting alternative route to common non-degradable polymers for short-life applications (packaging, agriculture, food processing etc.)[120]. Nevertheless, until now, most biopolymers are costly compared to conventional thermoplastic and they are sometimes not economical for practical applications. Therefore, it is necessary to improve these biopolymers in order to make them fully competitive with common thermoplastics.

There are three primary classes of polymer materials, which material scientists are currently focusing on. Consumers and industry usually refer to these polymer materials in the general class of plastics. The design strategy is in the approach of composite materials, where a polymer matrix (plastic material) forms a dominant phase around a filler material. The incorporation of filler materials used to improve mechanical properties and reduction in material costs.

Conventional plastics are highly resistant to biodegradation, as the surfaces area contact with the soil in which they are disposed are characteristically smooth[121]. Microorganisms within the soil are unable to degrade a portion of the plastic, which would, in turn, cause a rapid breakdown of the supporting matrix. This group of

materials usually has a petroleum based matrix, which is reinforced with carbon or glass fibers.

The second class of polymer materials under consideration is partially degradable. They are designed with faster degradation than that of conventional synthetic plastics. Production of this class of materials typically includes surrounding naturally produced fibers with a conventional (petroleum based) matrix. Microorganisms are able to consume the natural macromolecules within the plastic matrix upon disposal. A partially degraded material, with rough, open edges was formed and favorable for further degradation processing.

The final class of polymer materials is currently attracting a great deal of attention from both academics and industry. These plastics are designed to be completely biodegradable. The polymer matrix is derived from natural sources (such as starch or microbial grown polymers), and the fiber reinforcements are produced from common crops such as flax or hemp. Microorganisms are able to consume these materials completely, eventually leaving carbon dioxide and water as final degradation-products.

Materials must meet specific requirements set out by the ASTM and ISO in order to be

classified as biodegradable. In general, the likelihood of breakdown biodegradable materials is dependent upon the structure of the polymer. When examining polymer materials from a scientific point of view, there are certain ingredients that must be present in order for biodegradation to occur. Most importantly, the active microorganisms (fungi, bacteria, actinomycetes, etc.) must be present in the disposal site. The organism should be active under the appropriate degradation temperature, which usually falls between 20 to 60^{o}C. The disposal site must be in the presence of specific environments such as oxygen rich, highly moisture, and abundant mineral nutrients, while the site pH must be neutral or slightly acidic (5 to 7).

The positive and negative attributes and potential applications of each of these biodegradable plastics are summarized in **Table 3**.

Table 3: Biodegradable Polymers and Potential Applications[122]

Polymer (Class)	Positive Attributes	Negative Attributes	Potential Applications
(1) Starch & Starch blends	Low cost, rapid biodegradation	Hydrophilicity	Mulch film, compost bags, packing foams
(2) PVOH	Good oxygen barrier, rapid biodegradation	Solubility in water	Pesticide, fertiliser, detergent dispersal
(2) EVOH	Toughness, good oxygen barrier	Slow biodegradation	Food packaging
(2) PCL	Water stable, biodegradable, and hydrolysable, toughness	Low melting point	Compost bags, packaging for cold environments
(2) PLA	Tensile strength, clear films	Brittle, hydrolytically unstable	Injection Moulding, paper coating
(3) PHA	Rapid biodegradation, water stable	Cost	Paper Laminate

2.2.2 Biodegradable Polymers Classifications

Biodegradable polymers are a fast growing field. Various biodegradable polymers have been synthesized or are formed in nature during the growth cycles of all organisms. Some microorganisms and enzymes capable of degrading them have been studied extensively.

Depending on the synthesis process, classifications of the different biodegradable polymers have been proposed. **Figure2.4** shows an attempt at classification. We have 4 different categories. Only 3 categories (1 to 3) are obtained from renewable resources:

1. Polymers from biomass such as the agro-polymers from agro-resources (e.g., starch, cellulose),

2. Polymers obtained by microbial production, e.g., the polyhydroxy-alkanoates,

3. Polymers chemically synthesized and whose the monomers are obtained from agro-resources, e.g., the poly(lactic acid),

4. Polymers whose monomers and polymers are obtained conventionally, through chemical synthesis.We can also classify these different biodegradable polymers into two main families: the agro-polymers (category 1) and the biodegradable polyesters (categories 2 to 4).

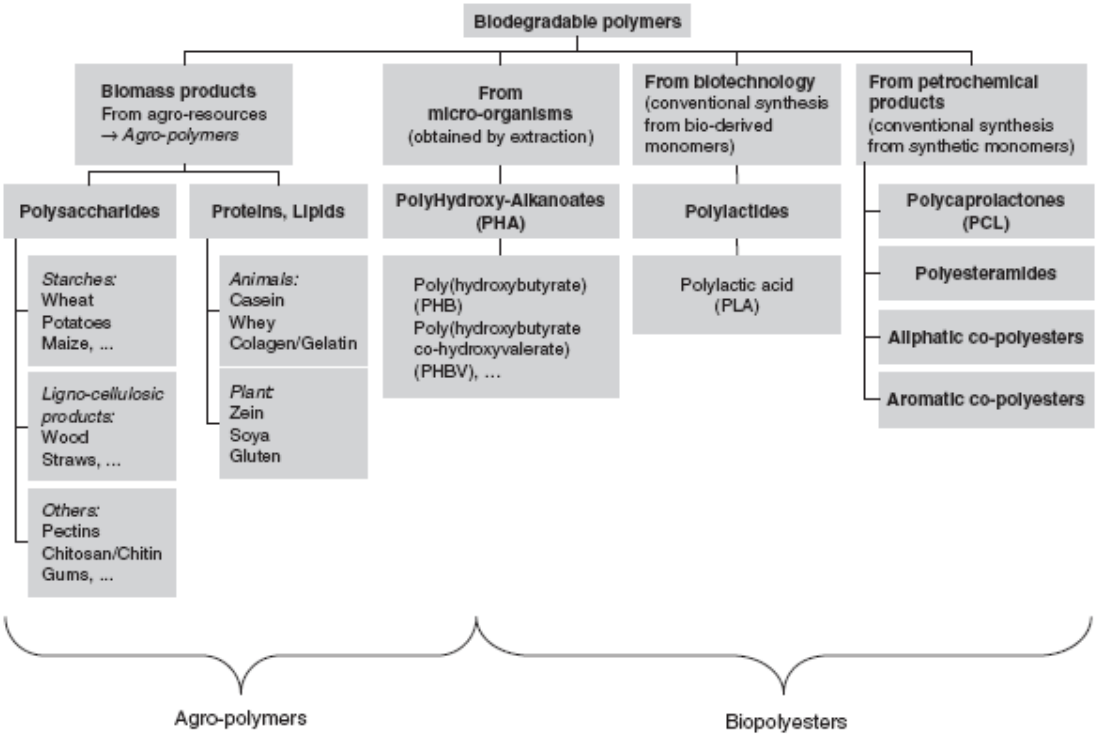

Figure 2.4 Classification of the biodegradable polymers.

2.2.3 Methods of biodegradation

The significant way in which a material formed is the way in which it is degraded. A general view on the breakdown of polymer materials is that it may be processed by microbial action, photo degradation, thermal and chemical degradation. All four methods are classified under biodegradation, as the end products are stable and found in nature. Degradation is normally characterized by a loss of molecular weight and initiates polymer erosion, which proceeds with the loss of newly-formed monomers and oligomers. For degradable polymers in biomedical application, chemical degradation in the form of hydrolysis is the most common mode of degradation, which leads to the

hydrolyzed products that are absorbed by the body with minimal tissue reaction. Many biopolymers are designed to discard in landfills, composts, or soil. Normal soil bacteria and water are generally required for the degradation of biopolymer. Polymers that are based on naturally grown materials (such as starch or flax fiber) are susceptible to degradation by microorganisms. The material may or may not decompose rapidly under aerobic conditions, depending on the formulation used, and the type of microorganisms.

Another approach to microbial degradation of biopolymers involves growing microorganisms for the specific degradation of polymer materials. This is a more intensive process that ultimately costs more, and circumvents the use of renewable resources as biopolymer feed stocks. The microorganisms are designed to breakdown petroleum based plastics [123]. This method may reduce the waste volume without aid in the preservation of non-renewable resources.

Photodegradable polymers undergo degradation from the action of sunlight [124]. In many cases, polymers are attacked photochemically first and subsequently. microbial degradation will be achieved for true biodegradation. Polyolefins (a type of petroleum-based conventional plastic) are the polymers found to be most susceptible to photodegradation. Proposed approaches for developing photodegradable biopolymers

includes incorporating additives that accelerates photochemical reactions (e.g. benzophenone), modifying the composition of the polymers with incorporation with more UV absorbing groups (e.g. carbonyl), and synthesizing new polymers with light sensitive substituents[123]. Biopolymers, which experience both microbial and photodegradation, can be applicable in the use of disposable bioproduct.

Some biodegradable polymer materials experience a rapid dissolution when exposed to (chemically based) aqueous solutions. As mentioned earlier, Environmental Polymer's product Depart is soluble in hot water. Once the polymer dissolves, the remaining solution consists of polyvinyl alcohol and glycerol. Similar to many photodegradable plastics, full biodegradation of the aqueous solution occurs later, through microbial digestion. These appropriate microorganisms are conveniently found in wastewater treatment plants[125]. Procter & Gamble has developed a product similar to Depart, named Nodax PBHB. Nodax is alkaline digestible, meaning that exposure to a solution with a high solution pH causes a rapid structural breakdown of the material[126]. Biopolymer materials, which disintegrate in aqueous solutions, are desirable for the disposal and transport of biohazards and medical wastes. Industrial "washing machines" are designed to dissolve and rinse away the aqueous solutions for further microbial digestion.

Most of the biodegradable polymers developed during the last two decades contain hydrolysable linkages such as ester, amide, anhydride and urethane linkages along the polymer backbone. Take poly(esters) for example; two distinct stages in the degradation process have been determined. The first stage is restricted to random hydrolytic cleavage of ester linkages. The resulting decrease in the molecular weight generates some changes in mechanical properties and morphology, but not weight loss. The second stage of degradation involves measurable weight loss in addition to chain cleavage. It begins when the molecular weight of the polymer has decreased to the point that the chain scission produces an oligomer small enough to diffuse from the bulk polymer. Dramatic loss of mechanical strength can occur during this second stage.

Degradability of biodegradable polymer: *Where X= O, N, S*

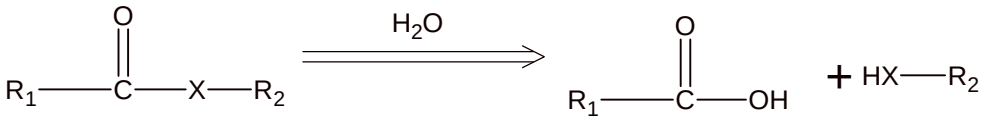

Figure 2.5 Polymer degradation process by hydrolysis

Polymers prepared by polycondensation can be susceptible to hydrolysis. Rate of hydrolysis is Anhydride > ester >>amide >>> ether.

The type of hydrolysable functional groups, polymer crystallinity, chemical composition, molecular weight and its distribution, pH and temperature of the degradation medium can affect the degradation rate. With regard to polymer crystallinity, amorphous regions degrade faster than crystalline domains. Polymer composition makes a strong contribution to the degradable rate. Copolymers and stereocopolymers generally degrade faster than homopolymers and the degradation rates can be modified through varying the chemical composition. Molecular weight and molecular weight distribution are also a critical factor in degradation process. Polymers with lower molecular weight degrade faster than those with higher molecular weight. Alkaline and acidic media, as well as high temperatures, may well enhance polymer degradation.

2.2.4 Applications of biodegradable polymers

Research and development in the application of biodegradable polymeric materials is still at a early stage. The design of such biodegradable materials usually in a conceptual means. It is usually considered as replacement of an existing material, or a complementary one. Sectors where applications for biopolymers have introduced include (but are not limited to) medicine, packaging, agriculture, and the automotive industry. Many developed and commercialized materials are applied in more than one of these categories. Biopolymers that may be employed in packaging continue to

receive more attention than those designated for any other application. All levels of government, particularly in China and Germany[127], are endorsing the widespread application of biodegradable packaging materials in order to reduce the volume of inert materials currently being disposed to the landfills, occupying scarce available space. It is estimated that 41% of plastics are used in packaging, and that almost half of that volume is used to package food products. BASF, a world leader in the chemical and plastic industry, is working on further development of biodegradable plastics based upon polyester and starch[128]. Ecoflex is a fully biodegradable plastic material that was introduced to consumers by BASF in 2001. The material is resistant to water and grease, making it appropriate for use as a hygienic disposable wrapping, fit to decompose in normal composting systems. Consequently, Ecoflex has found a number of applications as a packaging wrap.

Environmental-friendly Polymers (Woolston, Warrington, UK) has also developed a biodegradable plastic materialknown as Depart, in which the polyvinyl alcohol product is designed for extrusion, injection molding, and blow molding. Depart is highly soluble in water, which is determined by the formulation employed. Dissolution occurs at a preset temperature, allowing the use of Depart in a variety of applications. Examples include hospital laundry bags which are “washed away” allowing sanitary laundering of

soiled laundry, as well as applications as disposable food service items, agricultural products, and catheter bags[129]. The renewable and biodegradable characteristics of biopolymers are what render them appealing for innovative uses in packaging. The end use of such products varies widely. For example, biodegradable plastic films may be employed as garbage bags, disposable cutlery and plates, food packaging, and shipping materials[130]. Mechanical properties of the material are adequate, and true biodegradability is achieved. The biopolymer materials suited for packaging are often used in agricultural products. Ecoflex, in particular, sees use in both areas. Young plants, which are particularly susceptible to frost, may be covered with a thin Ecoflex film. At the end of the growing season, the film can be worked back into the soil, where it will be microbial degradable,[131] concluded that the use of a clear plastic mulch cover immediately following seeding increases the yield of spring wheat if used for less than 40 days. Therefore, plastic films that begin to degrade in average soil conditions after approximately one month are ideal candidates as crop mulches. Agricultural applications for biopolymers are not limited to film covers. Containers such as biodegradable plant pots and disposable composting containers and bags are areas of interest[132]. The pots are seeded directly into the soil, and breakdown as the plant begins to grow. Fertilizer and chemical storage bags, which are biodegradable, are also applications that material scientists have examined. From an agricultural standpoint,

biopolymers, which are compostable, are important, as they may supplement the current nutrient cycle in the soils where the remnants are added

Biodegradable polymers can be applied in the medical, biomedical and pharmaceutical field where degradation can bring about the desired effect. In biomedical field, biodegradable polymers are used as resorbable sutures, plates and screws. In bioengineering field, biodegradable polymers such as collagen, copoly(ester-ester), poly(carbonate), poly(ε-caprolactone), poly(glycolic acid), poly(imino carbonate), poly(lactic acid) and poly(orthoester) have potential use as scaffolding device for the growth and repair of tissues and organs. Biodegradation times ranged from days to months are achieved using these polymers as well as copolymers of these materials. In pharmaceutical applications, biodegradable polymers are used as drug carriers for the delivery of bioactive agents. Lactide/glycolide polymers, polyanhydrides, poly(ε-caprolactone) and its copolymers, poly(orthoesters) have been studied for applications in controlled drug release. With the use of a biodegradable device, problems associated with permanent metallic devices, such as second surgical procedure to remove the implant, are avoidable. In addition to avoid a second surgery, orthopedic fixation devices made from synthetic biodegradable polymers have advantages over metal implants in that they transfer stress to the damaged area as a function of time,

permit effective healing of the tissues, and lead to a lower tendency in the re-fracture of the healing bone tissue structures. When the polymers are biodegradable, such as poly(L-lactic acid) or poly(glycolic acid), the polymer support material degrades slowly. However, it is possible to engineer the biodegradable polymers with adhesion sites that act as cell hosts for shaping tissue replacements. However, the biopolymers used in medical applications must be compatible with the tissue they are found in, and may or may not be expected to break down after a given time period. Mukhopadhyay (2002) reported that researchers working in tissue engineering are attempting to develop organs from polymeric materials, which are fit for transplantation into humans. The polymers would require injections with growth factors in order to encourage cell and blood vessel growth in the new organ.

Not all biopolymer applications in the field of medicine are as involved as artificial organs. The umbrella classification of bioactive materials includes all biopolymers used for medical applications. One example is artificial bone material that adheres and integrates onto bone in the human body. The most commonly employed substance in this area is called Bioglass [133]. Another application for biopolymers is in controlled release delivery of medications. The bioactive material releases medication at a rate determined by its enzymatic degradation[134]. PLA materials were developed for medical

devices such as resorbable screws, sutures, and pins. These materials reduce the risk of tissue reactions to the devices, shorten recovery times, and decrease the number of doctor visits needed by patients.

The automotive sector is responding to societal and governmental demands for environmental responsibility. Biobased cars are lighter, making them a more economical choice for consumers, as fuel costs are reduced. Natural fibres are substituted for glass fibres as reinforcement materials in plastic parts of automobiles and commercial vehicles [135]. An additional advantage of using biodegradable polymer materials is that waste products may be composted. Natural fibres (from flax or hemp) are usually applied in formed interior parts. The components do not need load-bearing capacities, but dimensional stability is important. Research and development in this area continues to be enthusiastic, especially in European countries.

There are a number of novel applications for biopolymers, which do not fit into any of the previous categories. One such example is the use of biopolymer systems to modify food textures. For example, biopolymer starch (gelatin-based) fat replacers possess fat-like characteristics of smooth, short plastic textures that remain highly viscous after melting. Research continues into high pressure being used to manipulate biopolymers

into food products. The eventual goal is improved physical characteristics such as foaming, gelling, and water- or fat-binding abilities. Biopolymer materials are currently incorporated into adhesives, paints, engine lubricants, and construction materials[136]

2.2.5 Poly(ε-caprolactone)

2.2.5.1 Structure of PCL

Poly(ε-caprolactone) is synthesized by a ring-opening polymerization of ε-caprolactone which is catalyzed by stannous octoate at 140ºC[137]. The chemical structure of PCL is shown in **Figure 2.6.**

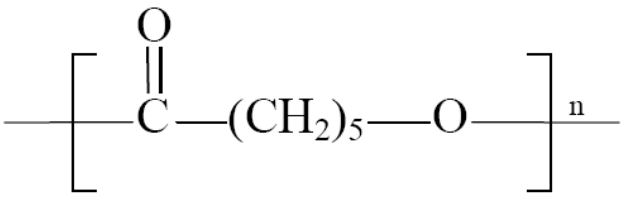

Figure 2.6 Schematic diagram of poly(ε-caprolactone)

2.2.5.2 Properties of PCL

PCL is noted to be an easily processable polymer due to its low melting temperature, low melt viscosity, thermoplasticity and excellent ability to form blends with other polymers[138]. Additionally it is reported to have high permeability and is degraded *in vivo* over several years by random hydrolytic chain scission at the ester linkages[139-140].

In addition, PCL has excellent compatibility with various polymers, making possible in well preparation of composite blends[141-144]. However, PCL has been reported to be well miscible with a number of polymers [145-147], particularly with the existence of hydrogen bonding[148-151] or other polar interactions with the second polymer. PCL shows a very low *T*g (61°C), a low melting point (65°C), which could be a disadvantage in some applications.

2.2.5.3 Degradability of PCL

Poly(ε-caprolactone) is aliphatic polyester and obtained through petrochemical processes. Nevertheless, it is degradable in several biotic environments, including aquatic resources, sewage sludge, farm soil, compost and various sediments. Further, it is non-toxic after degradation. PCL is therefore suitable for many applications, providing its mechanical and environmental properties are concerned. Particularly, it has been demonstrated that the molecular weight and crystallinity have significant effect on its biodegradability,[152] Tokiwa and Suzuki[153] have discussed the hydrolysis of PCL and biodegradation by fungi. They have shown that PCL can be enzymatically degraded.

2.2.5.4 Applications of PCL

PCL is considered to be a non-toxic and tissue compatible material and has a long history

of regulatory approval for use in biomedical applications[138]. These properties have allowed the polymer to be used as a subdermal sustained release drug delivery device for contraceptive steroids[139], such as the implantable Capronor system, which has been commercially available in Europe and the USA for almost 20 years. In addition to drug delivery devices, PCL is currently being evaluated for its applicability in wound dressings, biodegradable staples, bone cements and as the matrix component in bone replacement biocomposites [138,154,155]. PCL was found to have some potential applications based on its biodegradable character in domains such as biomedicine (e.g., drugs controlled release) and environment (e.g., soft packaging). The toxicology of the various molecular weights of poly(ε-caprolactone) in addition to its monomer, ε-caprolactone, have been extensively researched and have been found to be non-toxic and tissue compatible[137-140,154-155]. The chemical structure of PCL has been modified by sodium hydroxide treatment to incorporate more polar functional groups, which has been shown to improve its interfacial properties with calcium phosphates[156-157]. However, this approach cleaves the PCL at its ester linkages resulting in a lower molecular weight polymer.

2.2.6 Poly(lactic acid)

2.2.6.1 Structure of PLA

The synthesis of PLA is a multistep process that starts from the production of lactic acid and terminates with its polymerization[158-162].

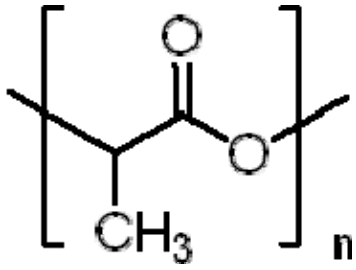

Figure 2.7 Schematic diagram of poly(L-lactic acid).

2.2.6.2 Properties of PLA

Poly(lactic acid) (PLA) has received major interest over the recent years in both the scientific and industrial realms. It demonstrated excellent physical properties, good processability, and a typical example in the research of alternative biodegradable polymers. PLA is a linear aliphatic thermoplastic polyester, andmainly synthesized by ring-opening polymerization of cyclic lactide dimer and the polycondensation of lactic acid monomers which are derived from the fermentation of corn and sugar feed stocks[163]. Generally, PLA products are copolymers of poly(L-lactic acid) (PLLA) and poly(D, L-lactic acid) (PDLLA), which are produced from L-lactides and D, L-lactides, respectively. The ratio of L- to D, L-enantiomers is known to affect the properties of

PLA, such as the melting temperature and the degree of crystallinity[144]. For example, The L-enantiomorph of PLA is a hard, transparent crystalline polymer. Among many biodegradable thermoplastics available, poly(L-lactic acid) (PLLA) has been the most popular biodegradable thermoplastics due to its high mechanical strength, which can be potentially applicable as structured materials [164] . However, brittleness of PLA may occur due to slow crystallization rate and cause strong reduction in toughness. Toughness in nanocomposites is significant to ensure the minimization in both delamination and crack propagation. To overcome the brittleness of PLA, considerable efforts have been made to improve the toughness of PLA so as to compete with low-cost and flexible polymers. Different modifications were carried out either by incorporation of biocompatible plasticizers, or through blending PLA with other polymers. Various types of chemical modifiers have been used include citrate esters,[165] glycerol,[166] poly(ethylene glycol), [167] glucose monoesters and fatty acids[168]. These small molecules can cause significant changes in both thermal and thermomechanical properties of PLA. Moreover, due to the boiling temperatures of these plasticizers are similar or closed to the melting temperature of PLA, their concentrations could vary due to different evaporation rate during processing. With long-term use of the composites, the plasticizers might result in leaching, which would eventually cause embrittlement. An alternative to plasticizers is the use of larger polymeric modifiers to perform similar functions.

2.2.6.3 Degradability of PLA

The main phenomena involve thermal and hydrolysis degradations during the life cycle of the material. The thermal stability of biopolyesters is not significantly high, a fact that inevitably limits their range of applications. The PLA decomposition temperature is lies between 230°C and 260°C. PLA hydrolysis is an important phenomenon since it leads to chain fragmentation [169-171], and can be associated with thermal or biotic degradation. This process can be affected by various parameters such as the PLA structure, its molecular weight and distribution, its morphology (crystallinity), the shape of its samples and its thermal and mechanical history (including processing), as well as, of course, the hydrolysis conditions. Hydrolytic degradation is a phenomenon, which can be both desirable (*e.g* . during the composting stage) or undesirable (*e.g* . during processing or storage). The hydrolysis of aliphatic polyesters starts with a water uptake phase, followed by hydrolytic splitting of the ester bonds in a random way. The amorphous parts of the polyesters have been known to undergo hydrolysis before their crystalline regions because of a higher rate of water uptake. The initial stage is therefore located at the amorphous regions, giving the remaining non-degraded chains more space and mobility, which leads to their reorganization and hence an increased crystallinity. In the second stage, the hydrolytic degradation of the crystalline regions of the polyester leads to an increased rate of mass loss and finally to complete resorbtion[172] .

The PLA degradation in an aqueous medium has been reported by Li *et al.*[172] to proceed more rapidly in the core of the sample. The explanation for this specific behavior is an autocatalytic effect due to the increasing amount of compounds containing carboxylic end-groups. These low molar mass compounds are unable to permeate the outer shell. The degradation products in the surface layer are dissolved in the surrounding buffer solution [172]. As expected, temperature plays a significant role in accelerating this type of degradation.

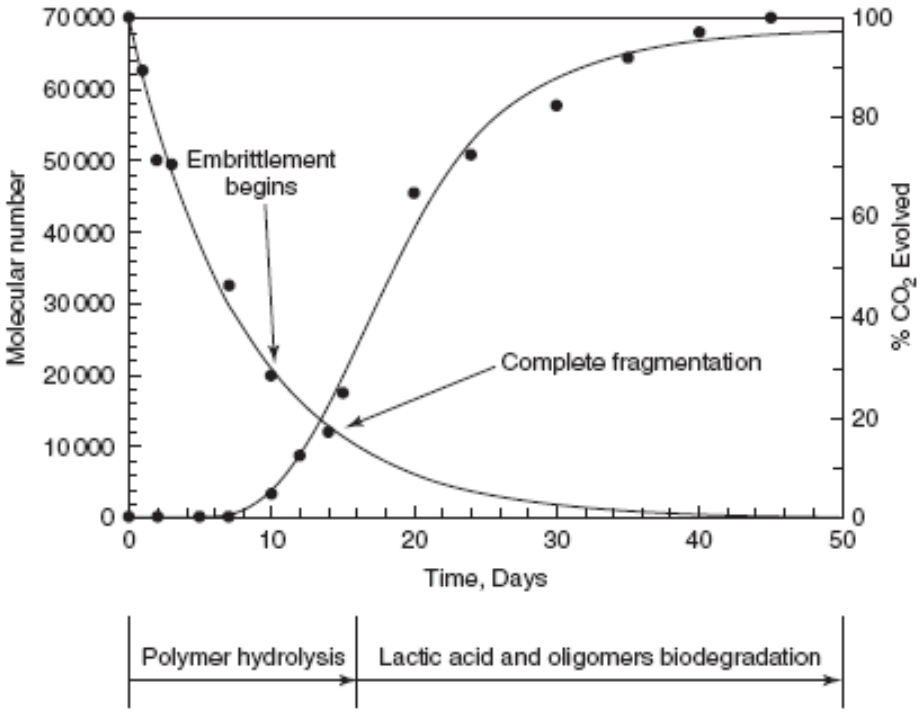

Figure 2.8 A biotic and biotic degradations during composting stage. (Adapted from Reference 176.)

The biodegradation of aliphatic biopolyesters has been widely reported in the literature.[170,171,173] The biodegradation of lactic acid-based polymers for medical applications has been investigated in a number of studies *in vivo*[174] and some reports can also be found on their degradation in other biological systems [175]. The *in vivo* and *in vitro* degradations have been evaluated for PLA-based surgical implants [174]. *In vitro* studies have shown that the pH of the solution plays a key role in the degradation and that this analysis can be a useful predicting tool for *in vivo* PLA degradation [169]. Enzymes, such as proteinase K and pronase, have been used to bring about the *in vivo* PLA hydrolysis, although, enzymes are unable to diffuse through the crystalline parts. As expected, little enzymatic degradation occurs at the beginning of the process, but pores and fragmentation are produced, widening the accessible area to the different enzymes. **Figure 2.8** shows that during the composting stage, PLA degrades in a multistep process with different mechanisms [171]. Primarily, after exposure to moisture by abiotic mechanisms, PLA degrades by hydrolysis. First, random non-enzymatic chain-scissions of the ester groups lead to a reduction in molecular weight, with the consequent embrittlement of the polymer. This step can be accelerated by solution pH and is affected by both temperature and moisture levels [176]. Then, the ensuing PLA oligomers can diffuse out of the bulk polymer and be attacked by microorganisms. The biotic degradation of these residues produces carbon dioxide, water and humus (mineralization).

Studies on PLA-based multiphase materials have been carried out. Gattin *et al.* [177] have found that the physical and morphological properties of the polymer blend play an important role in its degradation process, as in the case of comparative study of the degradation of PLA with and without plasticized starch materials [177]. Sinha Ray *et al.*[178] prepared PLA nano-biocomposites using montmorillonite as filler and studied and characterized their biodegradability.

2.2.6.4 Applications of PLA

PLA-based materials are mainly referenced on three different markets, namely, the biomedical (initial market), the textile (mainly in Japan) and the packaging (mainly food, *i.e* . short-term applications) . For instance, reported types of manufactured products are blow-moulded bottles, injection-moulded cups, spoons and forks, thermoformed cups and trays, paper coatings, fibres for textile industry or sutures, films and various molded articles[179].

Biomedical applications

PLA has been widely studied for use in medical applications because of its bioresorbability and biocompatible properties in the human body. The main reported examples on medical or biomedical products are fracture fixation devices like screws,

sutures, delivery systems and micro-titration plates[179]. PLA-based materials are developed for the production of screws and plates. As the bone healing progresses, it is desirable that the bone is subjected to a gradual increase in stress, thus reducing the stress-shielding effect. This is possible only if the plate loses rigidity in *vivo* environment. To meet this need, researchers introduced resorbable polymers for bone plate applications. PLA resorbs or degrades upon implantation into the body, but most of its mechanical properties are lost within a few weeks [174]. Tormala *et al* .[180] proposed fully resorbable composites by reinforcing matrices with resorbable PLLA fibres and calcium phosphate ($CaPO_4$)-based glass fibres. One of the advantages often quoted for resorbable composite prostheses is that they do not need to be removed with a second operative procedure, as with metallic or non-resorbable composite implants. To improve the mechanical properties, PLA is reinforced with variety of non-resorbable materials, including carbon and polyamide fibres. Carbon fibres/PLA composites possess very high mechanical properties before their implantation, but they rapidly lose *in vivo* because of delamination. The long-term effects of resorbed products, and biostable or slowly eroding fibres in the living tissues are not fully understood, and yet to be resolved [174]. Although PLA fibres are used in different textile applications as, for example, non-woven textile for clothes, they achieved their first commercial success as resorbable sutures. One of the first commercially available fibre-formed bioresorbable medical

products is based on copolymers of GA in combination with l -lactide (Vicryl) [181]. Fibres can be produced both by solvent and by melt-spinning processes and drawn under different conditions to orient the macromolecules[170]. Micro- and nanoparticles are an important category of delivery systems used in medicine, and the use of PLA is interesting due to its hydrolytic degradability and low toxicity. The most important properties of the micro- and nanoparticles are the controllable drug release rate and the matrix degradation rate, which are affected by the particle design and the material properties[170]. Copolymers of GA and rac-lactide[173] seem to be the most appropriate for use as drug delivery matrices. Porous PLA scaffolds have been used as reconstruction matrices for damaged tissues and organs. There are several techniques reported for the manufacturing of such materials[170].

Packaging applications

Commercially available PLA packaging materials can provide better mechanical properties than polystyrene and have properties more or less comparable to those of PET [169,179]. Market studies show that PLA is economically feasible for packaging. With its current consumption, it is at the present the most important market in volume for biodegradable packaging[169,179]. Due to its high cost, the initial use of PLA as a packaging material has been in high value films, rigid thermoforms, food and beverage

containers and coated papers. One of the first companies to use PLA as a packaging material was Danone (France) in yoghurt cups for the German market. During the last decade, the use of PLA as a packaging material has increased all across Europe, Japan and the US, mainly in the area of fresh products, where PLA is being used as a food packaging for short shelf-life products, such as fruit and vegetables. Package applications include containers, drinking cups, sundae and salad cups, wrappings for sweets, lamination films, blister packages and water bottles [182,183]. Currently, poly(lactic acid) is used in compostable yard bags to promote national or regional composting programs. In addition, new applications such as cardboard or paper coatings are being pursued, for example, the fast-food market (cups, plates and the like) [182,183]. However, to cater for a larger market, some PLA drawbacks must be overcome, such as its limited mechanical and barrier properties and heat resistance, and, in order to meet market expectations, the world production of PLA must be substantially increased.

2.3 Biodegradable Polymer Blends

2.3.1 Introduction

Due to their technological importance, polymer blends have attracted considerable attention during the past decade. For thermodynamic reasons, most polymer pairs are immiscible and their degree of compatibility is of underlying importance to the

microphase properties and consequently, to the mechanical properties of the blend.

A polymer blend is "a mixture of at least two polymers or two copolymers"[184]. Synthetic polymers, including polymer blends, 'are useful in designing tailor made materials with improved properties, processability and price/performance ratio[185]. Currently, many engineered biodegradable polymers have excellent product properties and performance. However, their widespread use is limited by high cost. There are many commercially available polymer blends and common ones include PVC/NBR a blend of poly(vinyl chloride) (PVC) and acrylonitrile rubber (NBR), acrylonitrile-butadiene-styrene copolymer (ABS) and starch/polyethylene. According to[184], the most sought after properties for engineering blends are high impact strength, processability and tensile strength. Quite notably, biodegradability is not listed under any of the categories. Blending to achieve biodegradability is only a relatively new concept and is still in the developmental phase. However, 'starch-based materials are now industrial products and are leading the market of biodegradable products'[186].

The first class of biodegradable materials, as classified by [132], is the blends of polymers and additives. To date, most research into biodegradable blends has concentrated on blends containing a non-biodegradable component, making them not fully 100%

biodegradable. There are many examples of starch in these types of blends including starch and polyethylene[187]. However, only a few studies have been undertaken into the blending of 100% biodegradable blends.

Some research into 100% biodegradable blends has been undertaken into starch/PCL blends [188,,189]. This produced preliminary results which indicate that a 'small amount of functionalised PCL significantly improves properties of the final product' [188]. Other starch/polyester blends investigated include starch/PLA by[190] and starch/Bionolle by[191]

.

2.3.2 Blends and compatibilization of Poly(ε-caprolactone)

Poly(3-hydroxybutyrate) (PHB) is a thermoplastic polyester with great potential because of features like biodegradation, bioreabsorbation and biological synthesis from a renewable source.[195] Despite these characteristics, the applications of this polymer are very restricted, due to its high crystallinity, and the secondary crystallization that occurs after processing, which leads to a material with poor mechanical properties.[196] Another drawback of this material is the thermal instability above the melting point, around 175 C[197].

Poly(e-caprolactone) (PCL) is a semi-crystalline polymer with potential to be used as biomaterial, it presents good mechanical properties, and has a melting point around 55 °C [198,5] and, thus, be a good option to develop PHB modified PCL blends maintaining its biodegradability and bioreabsorption properties.[199]

Blends of PHB and PCL prepared from chloroform solution have been described as imiscible, based on DSC and viscosimetry measurements.[200,201] Blends prepared from a polymer mixture followed by compression molding were also considered immiscible.[198]

A fascinating feature for polyesters blends is the potential for transreactions. This kind of reaction depends strongly on the initial polymer miscibility and blending conditions including temperature, mixing time, preparation method and presence of catalyst. Kotliar has reviewed interchange reactions involving the condensation polymers, polyester and polyamides[202]. In polyesters blends the possible reactions are intermolecular alcoholysis or transesterification (involving hydroxyl end-groups), intermolecular acidolysis (involving carboxyl end-groups) and interchange reactions between ester groups. In the literature there is few reports on the transreactions in the molten state involving PHB, probably due to its thermal instability at temperatures above 180 °C and its narrow window of processability. The thermal degradation is accompanied by decrease in the molar mass and consequently in mechanical properties of

the polymer. Due to this fact, the majority of the PHB blends had been prepared in solution to avoid thermal degradation[203]. Recently researchers studied the transreactions between PHB and amorphous PET, PETG conducted in an internal mixer and in presence of catalyst. The extension of transreactions was found to be more dependent on the catalyst concentration than the processing time[204]

As chitosan decomposes before undergoing melt flow, blending of this polymer has to be performed by dissolution in a common solvent. Although it is difficult to blend PCL with chitosan at a miscible level, several efforts have been made[205-213]. The main problem in solution blending chitosan and PCL has been a scarcity of common solvents. Honma et al. [206] produced PCL/CHT blend films casting from a 1,1,1,3,3,3-hexa-fluoro-2-propanol (HFIP) solution. Although it was proven that it is possible to process PCL/CHT blends using HFIP, it is not very advantageous since it is an extremely expensive solvent and is very difficult to remove. Another strategy adopted to produce biodegradable blend in film form by solvent casting was using 0.5 M acetic acid to dissolve chitosan and glacial acetic acid to dissolve PCL[209]. Blend membranes were obtained from low concentration solutions of both polymers. Sarasam et al.[209] stated that the blends were miscible for all compositions and that the mechanical properties were not improved due to the low concentrations of the solutions used.

However, as the concentration was increased, phase separation was detected, as noted by Cruz et al[205]. These phase-separated structures have been studied [214] in terms of their biological response, namely their protein and cell behaviour, indicating that such a system could be of interest in the biomedical application.

Starch-Polycaprolactone (SPCL) blend is one of the most used biodegradable polymers used for packaging. The addition PCL to starch produces an increase in tensile strength as a function of PCL content.[215,216] PCL has been selected among the different biopolymer commercially available for composite processing.

The development and biodegradable properties starch blended with PCL has been well documented in the literature[217-226]. Starch helps to lower the cost of the ultimate product as well as to give some biodegradable characteristics to PCL. Recently, starch-PCL blend has been proposed for biomedical applications, including tissue engineering scaffolds,[227-229] and different orthopaedic purposes.[227,230] Besides adequate physical properties, starch-modified PCL blend exhibits good biocompatibility[228,231,34,37] and low inflammatory response.[232]

In order to extend applications of PCL blend as primary packaging materials, current research has focused on starch blends especially starch-polyester biodegradable for

polycaprolactone blend with starch. Since starch is immiscible with poly(caprolactone), a reactive compatibilization process is required to synthesize starch–polyester blends especially at high starch levels (e.g. >20 wt%). In this process, existing or new functional groups on starch/PCL are reacted to produce a covalently bonded starch–PCL molecule. This reaction is well controlled so that a small amount of this molecule acted as a compatibilizer between unmodified starch and PCL results in the formation of the bulk structure of the matrix. An example of this kind of product is Envar,[233] that is being manufactured as compost bags. Envar is a reactive blend of starch, PCL, and a third polymer starch-*g*-PCL that was produced by addition of PCL to starch backbone during extrusion[233]

Recent studies of biodegradable polyester blend could be cellulose ester derivatives has been suggested[234,235]. Cellulose esters exhibit a fairly high glass transition temperature (*T*g), good optical transparency, high flexural and tensile strengths and a high modulus; they are also potentially biodegradable[236-240].

For cellulosics, it has been reported that a few cellulose derivatives show good miscibility with PCL; Brode and Koleske reported miscibility of nitrocellulose with PCL over a wide composition range,[241] and cellulose acetate butyrate (CAB) was also suggested as being

able to form miscible blends with the polyester.[242] However, Hubbell and Cooper (1977) claimed that the miscibility of nitrocellulose-PCL blends was restricted to a limited composition range of ~50% PCL, and that CAB-PCL blends were mostly phase separated, but with one phase having nearly equal proportions of the two polymers.[243] The mutually inconsistent observations by the two research groups for the same binary systems may be attributed primarily to the difference in the degree of ester substitution of hydroxyls between the cellulosic samples employed in the respective studies.

2.3.3 Blends and compatibilization of Poly(lactic acid)

Although polylactic acid (PLA) has an excellent balance of physical and rheological properties, many additives have been utilized to extend the range of properties achievable and thus optimize the material for specific applications. Traditionally, additives incorporated in PLA matrix can be classified as fillers and fibers. The most common fibers that have been combined with PLA are glass fibers and a limited selection of natural fibers including wood fibers, and certain renewable plant fibers such as flax. Fillers that have been have studied to afford beneficial properties with blended with PLA include talc, mica, kaolin, glass (milled)), a variety of inorganic carbonates and sulfates, as well as starch. Nanocomposites of PLA with various angstrom sized inorganic particles and platelets have been reported in the literature,[244]

In order to derive the benefit from the fiber or filler additives, several factors must be considered. Regardless of the additive, good (uniform) dispersion must be achieved. This is normally obtained by controlled addition of the additive during melt mixing in a twin screw extruder or batch mixing device[245]. Visual inspection can evaluate poor mixing, but often electron microscopy techniques are required to assure that the additives are not associated in macro-clumps, which can lead to rheological problems or a decrease in toughness. The particle size of the filler is important and generally particle sizes from 0.1-10 μm are used[246]. Smaller sizes have less detrimental effect on toughness and morphology, but generally lead to dust handling and high cost problems.

Interfacial compatibility of the filler/fiber is also important in obtaining maximum benefits from the additive, which will assist in dispersion and help minimize micron-sized defects in parts that can cause embrittlement. Coupling agents are often used with glass fibers[244] or coated fillers are used to enhance the interfacial adhesion of the additive to the matrix polymer. This is very common when polar additives are combined with non-polar polymers, but can be very useful in most systems. Silane and titanate coupling agents with various structures, depending on the polymer into which it will be blended, are often coated onto glass fibers and inorganic particulate fillers.

These coupling agents can have beneficial effects on dispersion, toughness, rheology and often permit higher levels of incorporation.

Many articles have been published during the last few decades on PLA-based blends[247-250], in terms of biodegradable blend with polysaccharides, a significant amount of work has been done optimizing PLA-starch blends for environmental friendly and short-term use. Besides reducing costs, starch has been reported to act as a nucleating agent for PLA[251] as well as enhancing the heat resistance and modulus of the material. Generally compatibilization of the starch with the PLA is necessary to obtain an overall improvement in both thermal and mechanical properties.

Native starch, which is composed of semi-crystalline granules, can be physically blended with PLA, but remains in a separate conglomerate form in the PLA matrix[252]. Thus, starch is typically characterized as solid filler with poor adhesion with PLA. Such biodegradable composites are used as a model to test (e.g. carbohydrate–PLA compatibilization[253]). Such a processable material is obtained by the disruption of the granular starch and the transformation of its semi-crystalline granules into a homogeneous, amorphous-like material with the destruction of hydrogen bonds between the macromolecules.

From the approach of the compatibilizer addition, which can be achieved by the modification of at least one of the polymers initially present in the blend. Maleic anhydride grafted systems[254] and addition of third component compatibilizing polymers such as polyvinyl alcohol,[255] and polycaprolactone[256] have shown beneficial effects on the interfacial adhesion of the starch and improvement in toughening properties. The amount of the compatibilizer and its molecular weight affect the balance of properties in the blends. The effect of the amylose content of the starch in PLA blends has also been studied and high-amylose content starches enhance water absorption and accelerate bio-degradation.[257]

For natural fiber used in the modification of PLA, walnut shell flour, pine wood flour, and other sources of cellulose fiber have been blended with PLA at levels up to ca. 60% while increasing stiffness and obtaining up to 10^{o}C improvement in heat resistance. Applications such as seedling planters for trees, which require bio-degradation in a short period of time, are ideal applications for cellulose-type fillers[258]. Short fibers of less than 1 mm in length were found with both injection molding and extrusion processes. However , in kenaf fibers, lengths up to 20 mm have been reported using the vast portion of the fiber[259]. Commercial products have already been introduced combining PLA and natural fibers. To increase the compatibility of natural fibers with PLA, the fibers

should be degreased and chemically modified on the surface by acylation or coated with silane coupling agents[260]. Natural fiber-PLA composites are reported to have the environmental advantage of being based on 100% renewable resources[261]. Other approaches to incorporate cellulose fiber include the use of up to 25% recycled paper, with blending temperature up to 230^{o}C resulting in a pressed sheet with good stiffness.[262]

It is known that PLA forms miscible blends with polymers such as poly(ethylene glycol (PEG).[263] PLA and PEG are miscible with each other when the PLA fraction is below 50 per cent.[263] The PLA/PEG blend consists of two semi-miscible crystalline phases dispersed in an amorphous PLA matrix. Melt mixing of PLA and PEG at various concentrations displayed that PEG acted as an efficient plasticizer for PLA. A blend containing 30 wt % PEG resulted in a material with a glass transition temperature (Tg) well below room temperature and allowed for higher elongation at break and lower modulus values as compared to neat PLA[263-267]. However, the low *T*g rendered the blend unstable over time resulting in an increase in modulus accompanied by a decrease in the elongation at break[266]. This was attributed to the enhanced crystallization of the PEG chains, which caused phase separation, gradually enriching the amorphous phase in PLA and increasing its *T*g[265,267]. Cooling the blend from the melt state at a rate of 5°C/min or low degree of crystallization of both PLA and PEG to occur. This also

resulted in a gradual increase of the *T*g. However, both the aging and the crystallization ceased when the *T*g reached ambient temperature[264]

PHB/PLA blends are miscible over the whole range of composition[268-276]. The elastic modulus, stress at yield, and stress at break decrease, whereas the elongation at break increases, with increasing polyhydroxybutyrate (PHB) content[277]. Both PLA/PGA and PLA/PCL blends give immiscible components,[278,286] the latter being susceptible to compatibilization with P(LA- *co* -CL) copolymers or other coupling agents.

2.3.4 Modification of biodegradable polymer (PCL and PLA) by hyperbranched polymer-based nanostructures

Hyperbranched polymer is a class of three-dimensional and artificially built molecules produced by multiplicative growth from small organic molecules. Hyperbranched polymers usually show low viscosities through high molecular weights, and as rheology modifiers for improving polymers melting fluidity[287]. Especially, hyperbranched polymers with abundant reactive chemical end groups such as hydroxyl and carboxyl groups in PLA may be used to act as surface modifier or toughening additives[288-290]. These functional end groups introduced effective hydrogen bonding interactions to improve the toughness of the polymers. Hyperbranched polymers blended with PLA

may be employed to enhance the mechanical properties of the matrix through molecular interactions. In addition, research studies have been made to reduce the crystallinity of polymers in order to increase the ductility of the blend[291]. The potential interaction between hyperbranched polymers and PLA is able to constrain the mobility of PLA macromolecules and thus would reduce the crystallinity of PLA.[294-296]

However, there is no information concerning the study of incorporated hyperbranched polymers on the physical properties of PCL blend. In this thesis, the thermal and mechanical of novel HBP-PCL blend will be investigated in detail.

Chapter 3 Hyperbranched Polymer Synthesis and Characterization

3.1 Introduction

The concept of "hyperbranched" may be traced back to 50's in the 20th century. Owing to its unique structure and properties, HBPs have attracted many researchers so far. In order to obtain precisely controlled molecular structures such as those in dendritic polymers, multi step-growth polymerization was often utilized in the synthesis with tedious and complicated isolation procedures. Thus, the potential for commercial application is heavily restricted. In contrast to dendritic polymers, randomly HBPs can be synthesized by one-pot chain polymerization strategy. Hence the synthetic process can be simplified and the production cost can be reduced. Although the integrity of randomly hyperbranched structures is not as good as dendritic polymers', but randomly HBPs still achieve similar physical and chemical properties, which thus makes them very interesting in the field of polymer science.

Until now, randomly HBPs have been studied for nearly two decades under rapid development and expectedly, these polymers will become novel materials for many future applications.

Although, randomly HBPs may not have such fine and highly symmetric molecular structures as described in dendritic polymers, the highly branched structure is able to

maintain intrinsic properties of dendritic polymer, such as nanoscale cluster dimension, vast amount of reactive functional end groups located at molecular surface[292,293]. Thus, the obtained polymers with high degree of branching exhibit similar properties of dendritic polymers such as low viscosity, high solubility, multi-functional group attachment, high thermal stability, and low crystallinity. The specific properties allow randomly HBPs promising for many novel applications, where traditional polymers cannot consent.[15]

Hyperbranched polyesters are an important class of condensation polymers that have highly branched molecular conformation constructed by repeating branched unit with ester end group. The potential applications of hyperbranched polyester have been widely investigated in the field of chemical industry, materials science, life sciences, and medicine, etc[294-296]. In most cases, hyperbranched polyesters were synthesized from self-condensation of AB*x* monomers (*x*> 2). Due to the multi-functionality of B group (X >1), hyperbranched structure can be formed during the polyesterification reaction. Citric acid is A_3B type monomer. Several publications have been emerged using citric acid as the monomer to synthesize hyperbranched polyesters via polycondensation[297]. However, the resulting polymers were achieved with molecular weights in the order of 10^3. In this work, a group of hyperbranched poly(citric acid) [HBP(COOH)] was synthesized by a new method. The highest average molecular weight can reach Mw=758577.

Another type of monomer, 2,2-Bis(hydroxymethyl)propionic acid (bis-MPA), was

used to synthesize required HBP. The formation of HBP using bis-MPA as monomer were presented in the literature in which the highest average molecular weight achieved was about ten thousands[298-299,300-303]. Here, we employ a new method with minimal solvent used to synthesize hyperbranched poly(bis-MPA) [HBP(OH)], in which higher molecular weight products (higher Mw = 50466) can be obtained. In addition, introducing a controlled amount of allylamine can effectively control the molecular weight distribution.

3.2 Experimental

3.2.1 Materials

All reagents were used as received without further purification. Citric acid (CA, 99%), sulfuric acid (95-97%), 2,2-bis(hydroxymethyl)propionic acid (bis-MPA, 99%), and allylamine (99%) were purchased from Sigma Aldrich Chemical Co.

3.2.2 Synthesis of HBP with acid end-groups

HBP with acid end-groups was synthesized from citric acid and the polymerization was catalyzed by sulfuric acid. 10g citric acid was mixed with 20 ml THF and small amount of sulfuric acid and the reaction was maintained at 80^{o}C for controlled periods of time. The resulting products were subsequently purified through dialysis membranes with a MWCO value of 500.

3.2.3 Synthesis of HBP with hydroxyl end-groups

2,2-bis(Hydroxymethyl)propionic acid was polymerized using sulfuric acid as catalyst in THF. The reaction mixture of bis-MPA (10g), THF (20 ml), and sulfuric acid (small amount) was stirred at 120^{o}C for controlled periods of time. The resulting products were subsequently purified through dialysis membranes with a MWCO value of 500.

3.2.4 Control of hyperbranched polymerisation

Allylamine was added in order to control the polymerization reaction of 2,2-bis(hydroxymethyl)propionic acid. Appropriate mole ratios of bis-MPA to allylamine (e.g., 56.26:1) were fed into the reaction mixture to produce polymers with desired molecular weights. The resulting products were subsequently purified through dialysis membranes with a MWCO value of 500.

3.2.5 Structural identification by Nuclear Magnetic Resonance Spectroscopy

NMR analysis was carried out on Inova 500 NB NMR Spectrometer NMR spectrometer operating at 500 Hz. DMSO-d_6 was used as solvent. The data was collected at 300 K using 5 mm outer diameter (o.d) sample tubes. About 5 mg and 50 mg of sample were dissolved in 6 ml DMSO-d_6 for ^{1}H NMR and ^{13}C NMR measurements, respectively. A spinning frequency of 20 kHz was applied.

3.2.6 Fourier-Transform Infra-red spectroscopy (FT-IR)

Fourier transform infrared (FTIR) spectra were recorded on a Perkin Elmer Spectrum 100 spectrometer in reflective mode. The samples were mounted on the universal diamond ATR (Attenuated Total Reflectance) top-plate and scanned in the range 650-4000 cm^{-1}. 8 scans were collected with a spectral resolution of 1 cm^{-1}.

3.2.7 Gel Permeation Chromatography

Molecular weight of the HBPs was determined in THF by gel permeation chromatography (GPC, detector: Waters Series 2414 refractive index detector; pump: Waters Series 1515 Isocratic HPLC pump) using polystyrene as the standard. The specimen concentrations were ~0.03 g sample/10 ml THF, and the flow rate was 0.8 ml/min.

3.3 Results and discussion

3.3.1 Synthesis of HBP with acid end-groups

The reaction products with different molecular weights were synthesized by controlling the reaction time. GPC showed the molecular weights of the isolated products were Mw = 785 (HBP(COOH)-1), 2225 (HBP(COOH)-2), 16995 (HBP(COOH)-3), 45279 (HBP(COOH)-4), and 758577 (HBP(COOH)-5) (**Table 4**). The highest molecular weight achieved by this synthesis method was Mw = 758577.

Table 4. Gel Permeation Chromatography data of the HBPs

Type of HBP	Molecular weight range	Sample name	Molecular weight(M_w)	Polydispersity
HBP(COOH)	Low molecular weight range	HBP(COOH)-1	785	2.046
		HBP(COOH)-2	2225	2.922
	medium molecular weight range	HBP(COOH)-3	16354	2.477
	High molecular weight range	HBP(COOH)-4	45279	5.647
		HBP(COOH)-5	758577	
HBP(OH)	Low molecular weight range	HBP(OH)-1	906	1.814149
	medium molecular weight range	HBP(OH)-2	2044	2.511002
	High molecular weight range	HBP(OH)-3	50466	
Allylamine-capped HBP(OH)	HBP(OH: allylamine=56.26:1)		3303	

3.3.2 Synthesis of HBP with hydroxyl end-groups

Hyperbranched products bearing hydroxyl end-groups were successfully synthesized based on the reduced-solvent method. As shown in **Table 4**, molecular weights of the isolated products are Mw = 906 (HBP(OH)-1), 2044 (HBP(OH)-2) and 50466 (HBP(OH)-3), respectively.

3.3.3 Control of hyperbranched polymerisation

By controlling the amount of allylamine in the polymerization reaction of bis-MPA, a

controlled molecular weight HBP(OH) can be obtained. As shown in **Table 4**, an appropriate mole ratio of bis-MPA to alylamine (e.g., 56.26:1) can be fed into the reaction mixture to produce polymer with desired molecular weight (e.g., Mw=3303). Now, we are even able to figure out the difference between the theoretical molecular weight (Mw) of the product (=3795) and the experimental value determined by GPC (=3303). The real molecular weight of the polymer can be more accurately predicted by theory. Similar experiments with other ratios have also been tried, and the average molecular weight can also be manipulated within the expected range.

3.3.4 Chemical structure of HBP(COOH)

Each citric acid monomer has three tertiary carboxylic acid groups and one hydroxyl group. Through polycondensation of the two groups, HBP with acid end groups on the peripheral can be synthesized. As shown in **Figure 3.1**, a sterically hindered tertiary hydroxyl group is left at the core.

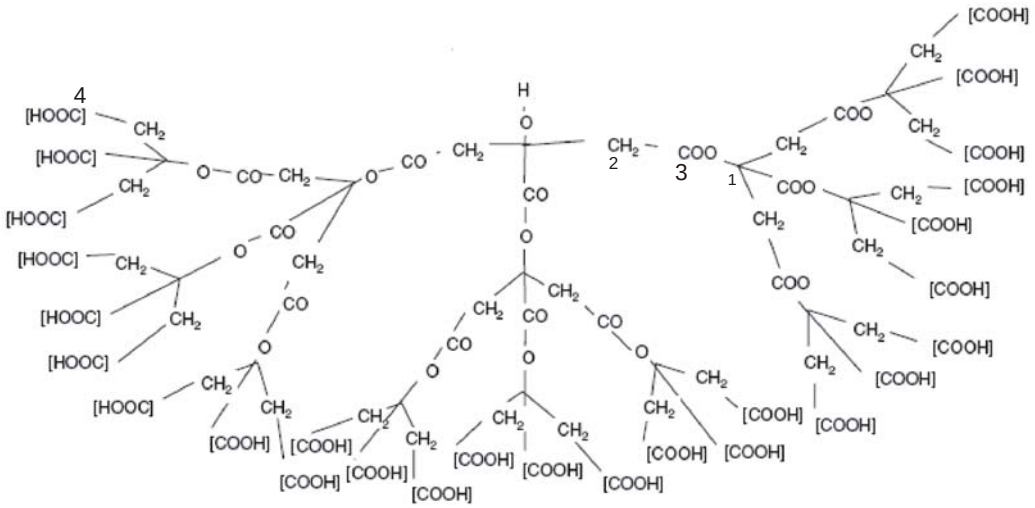

Figure 3.1 Schematic diagram of HBP(COOH)

3.3.5 Chemical structure of HBP(OH)

Bis-(MPA) monomer has two hydroxyl, and one carboxylic acid groups. Through polycondensation, hyperbranched polyester with hydroxyl groups on the peripheral can be obtained. As shown in **Figure 3.2**, an unreacted sterically hindered carboxylic acid group locates at the core of the polymer.

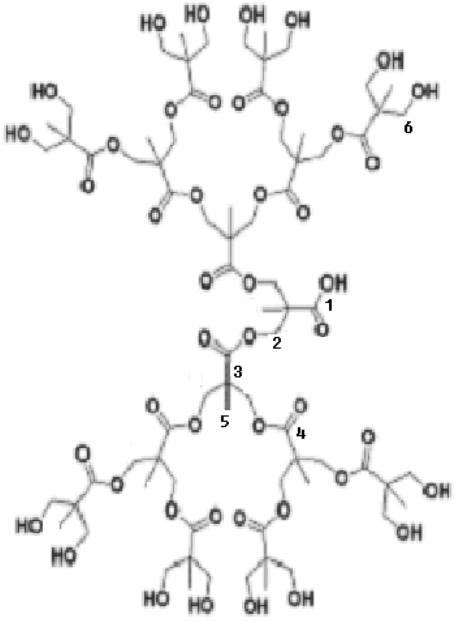

Figure 3.2 Schematic diagram of HBP(OH)

3.3.6 Chemical structure of allylamine-capped HBP(OH)

By mixing a controlled ratio of allylamine and bis-MPA, a capped HBP(OH) can be obtained. The amine group of allylamine can participant in the reaction to react with certain amount of bas-MPA. At the end of the polymerization process, allylamine will eventually become the core group of the formed polymer. The polymerization will terminate with enough amount of allylamine to limit the polymer chains to grow. Molecular structure of allylamine-capped HBP(OH) is shown in **Figure 3.3.**

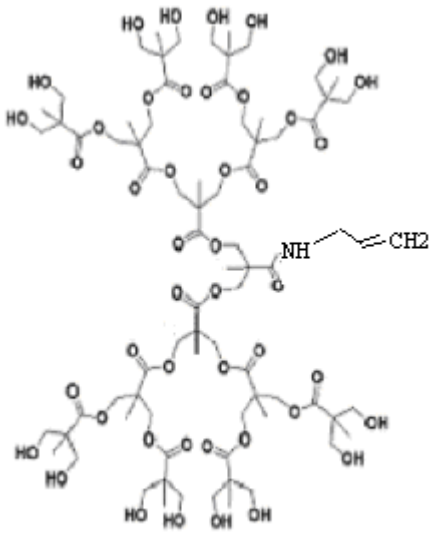

Figure 3.3 Schematic diagram of allylamine-capped HBP(OH)

3.3.7 Structural identification by NMR

Figure 3.4 shows the ^{1}H NMR specturm of HBP(COOH)-2. The signals at 3~4 ppm are related to the protons of the CH_2 system of citric acid units in the backbone of the polymer. The CH_2 peak at 3~2 ppm should be related to the end groups on the polymer shell.

Figure 3.5 shows the ^{13}C NMR spectrum of HBP(COOH)-2. The absorption peaks of the quaternary carbons are observed at 26.55, 27.66 and 44.43 ppm with each generation number. In contrast, the chemical shifts of the methylene (66.11, 71.31 and 74.05 ppm), carbonyl (171.11 and 172.815 ppm) and carboxyl carbons (176.06 ppm) absorption are independent on the generation number.

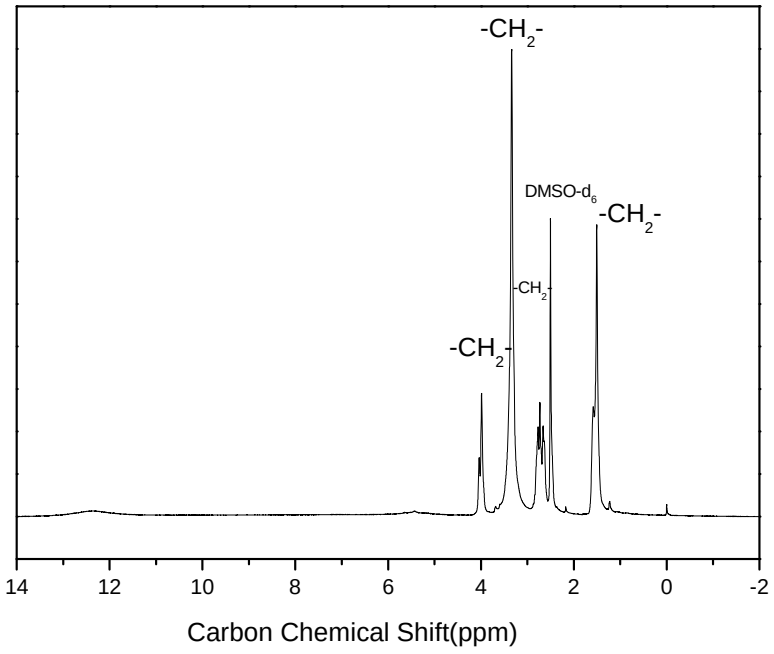

Figure 3.4 ^{1}H-NMR spectrum of HBP(COOH)-2

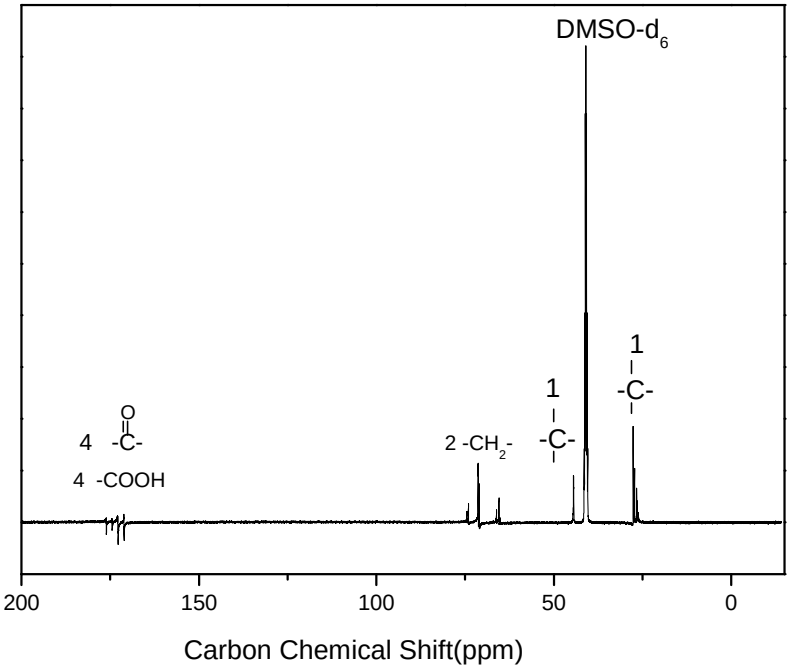

Figure 3.5 ^{13}C-NMR spectrum of HBP(COOH)-2

Figure 3.6 shows the 1H NMR specture of HBP(COOH)-3. The signals at 3~4 ppm are related to the protons of the CH_2 system of citric acids units in the polymer backbone. The CH_2 absorption peaks at 2~3 ppm should be related to the citric acid unit on the surface of the polymer.

Figure 3.7 shows the ^{13}C NMR spectrum of HBP(COOH)-3. The absorptions of the quaternary carbons are observed at 25.06, 28.94, and 43.82 ppm with each generation number. In contrast, the chemical shifts of the methylene (61.25, 64.49, 69.65 and 73.53 ppm), carbonyl (170.02, 171.76 and 173.29 ppm), and carboxyl carbons (175.21 ppm) absorptions are independent on the generation number.

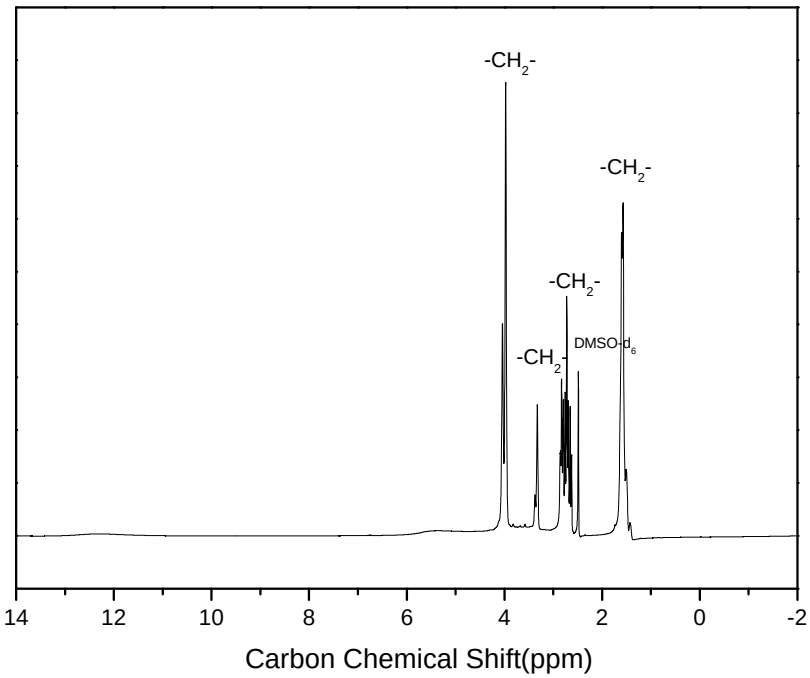

Figure 3.6 ^{1}H-NMR spectrum of HBP(COOH)-3

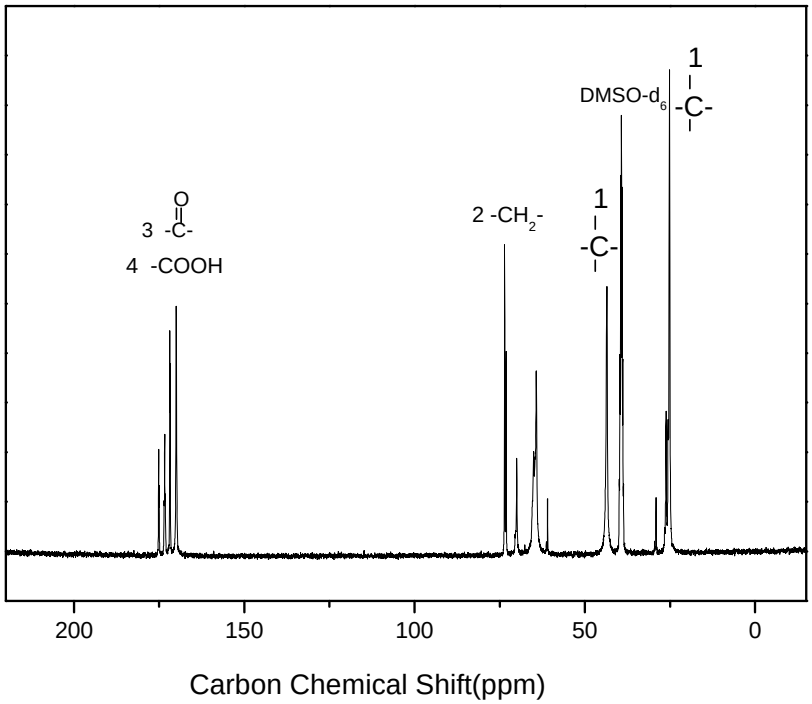

Figure 3.7 ^{13}C-NMR spectrum of HBP(COOH)-3

Figure 3.8 shows the 1H NMR specture of HBP(COOH)-4. The signals at 3~4 ppm should be related to the protons of the CH_2 system of citric acid units in the backbone of the polymer. The CH_2 absorption peaks at 3~3 ppm should be related to the citric acid unit on the polymer shell.

Figure 3.9 shows the ^{13}C NMR spectrum of HBP(COOH)-4. The absorptions of the quaternary carbons are observed at 25.18, 29.28, 39.71, and 43.51 ppm with each generation number. In contrast, the chemical shifts of the methylene (60.91, 64.39, 67.56, 70.08 and 73.56 ppm), carbonyl (170.08, 171.73, and 173.38 ppm) and carboxyl carbons (175.15 ppm) absorptions are independent on the generation

number.

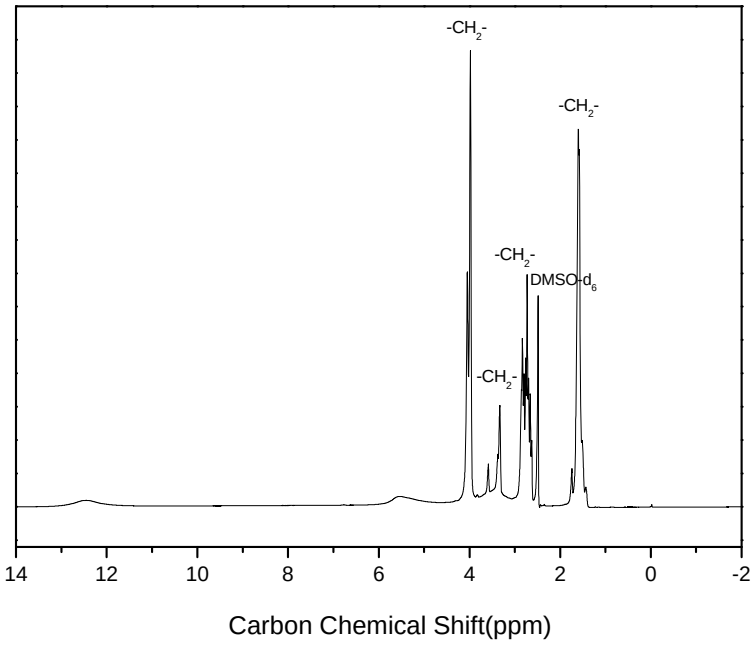

Figure 3.8 ^{1}H-NMR spectrum of HBP(COOH)-4

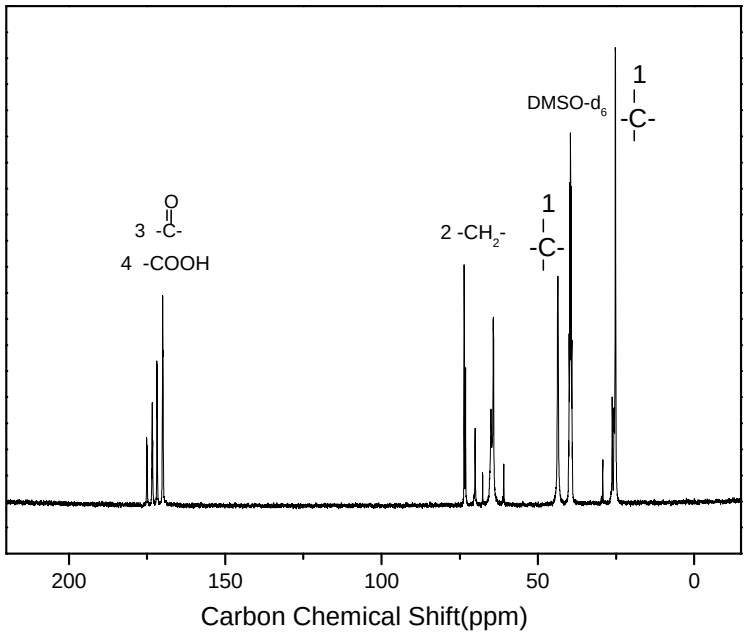

Figure 3.9 ^{13}C-NMR spectrum of HBP(COOH)-4

Figure 3.10 shows the 1H NMR spectrum of HBP(COOH)-5. The signals at 3~4ppm are related to the protons of the CH_2 system of citric acid units in the polymer backbone. The CH_2 absorption peaks at 2~3 ppm should be associated with the citric acid unit on the polymer surface.

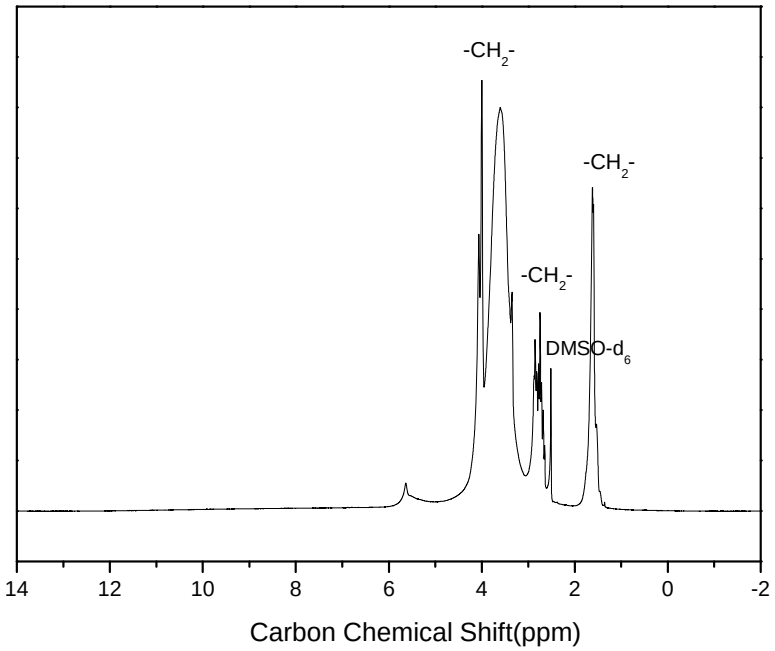

Figure 3.10 ^{1}H-NMR spectrum of HBP(COOH)-5

Figure 3.11 shows ^{1}H NMR spectrum of HBP(OH)-1 The signal at 1~1.4 ppm are related to the protons of methyl groups. The signals at 3~4.2 ppm should be attributed to the protons of the CH_2 system of MPA units in the polymer backbone. The CH_2 peak at ~3.5 ppm should be related to the MPA unit on the polymer surface.

Figure 3.12 shows the ^{13}C NMR spectrum of HBP(OH)-1. The absorptions of

methyl carbons appear at 17.5 ppm, and the quaternary carbons are at 48.21, 48.96, and 51.01 ppm with each generation number. In contrast, the chemical shifts of the methylene (65.73, 66.19 and 66.72 ppm), carbonyl (173.72 ppm) and carboxyl carbons (176.11ppm) absorption are independent on the generation number.

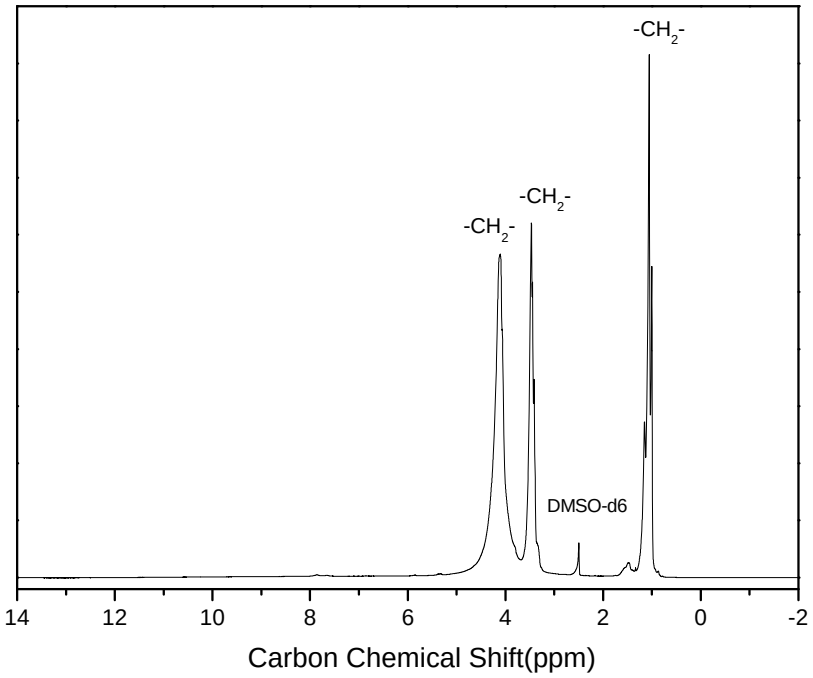

Figure 3.11 ^{1}H-NMR spectrum of HBP(OH)-1

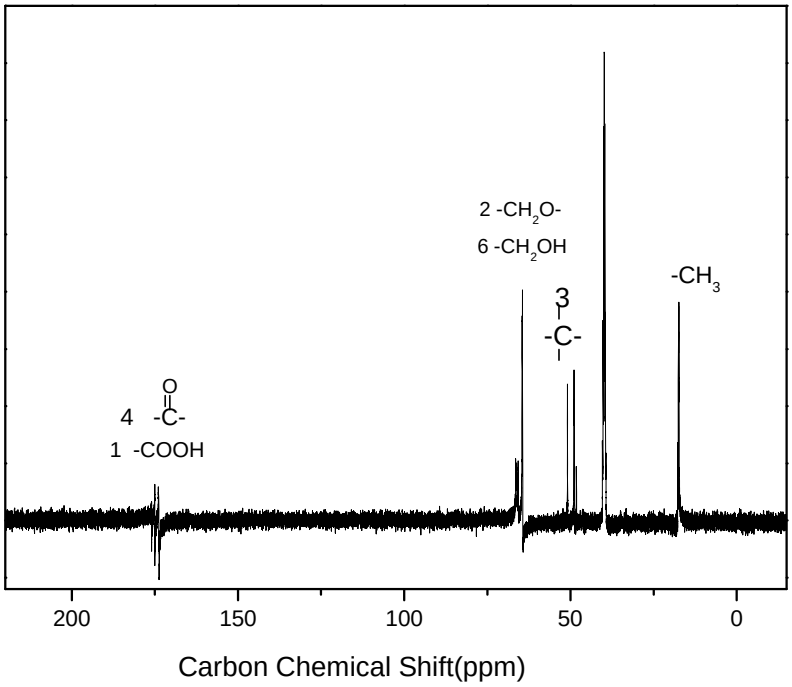

Figure 3.12 ^{13}C-NMR spectrum of HBP(OH)-1

Figure 3.13 shows the 1H NMR spectrum of allylamine-capped HBP(OH). The signals at 5~8ppm are related to the protons of allylamine group on the polymer. The ratio between the peaks at ~5.81 ppm and at 0.7~1.2 ppm associated with the allylamine and poly(bis-MPA) moieties of the polymer is 3.33:282. Hence, the ratio of allylamine monomer to bis-MPA monomer should be 1: 28.5. This result closely matches the actual mole ratio of the monomers applied for the synthesis. On the other hand, the result confirms the incorporation of allylamine can effectively control molecular weight of the hyperbranched product.

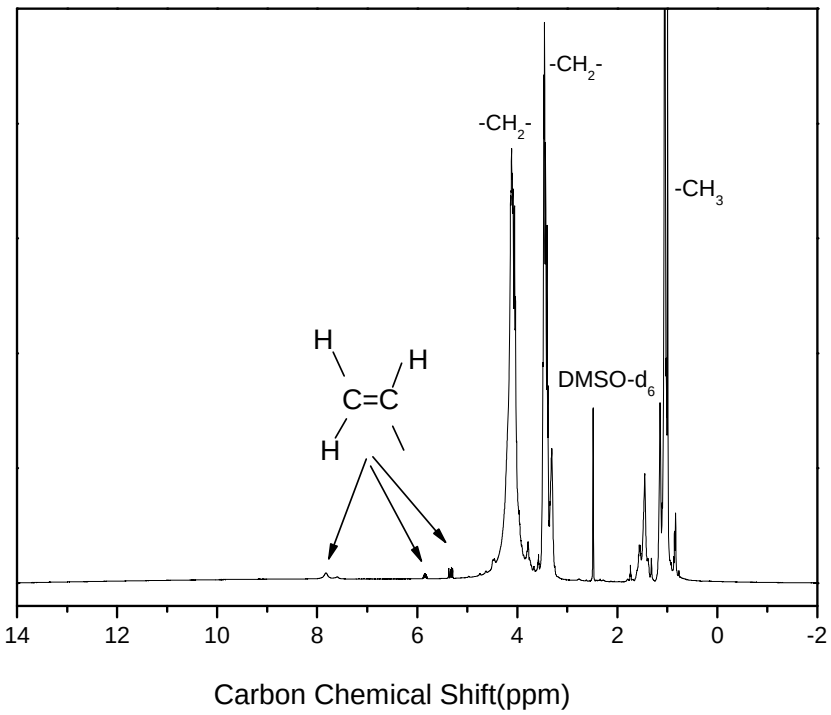

Figure 3.13 ^{1}H-NMR spectrum of allylamine-capped HBP(OH)

3.3.8 Fourier-Transform Infra-red spectroscopy (FT-IR)

Figures 3.14 and **3.15** show FT-IR spectra of HBP(COOH)-3 and HBP(OH)-1. From the spectrum of HBP(COOH)-3, the broad peak in the range of 3300-3600 cm^{-1} represents the stretching band of OH bond. Remarkably, a sharp peak at ~1720cm^{-1} should be attributed to the stretching of carbonyl (C=O) group on the polymer. Another strong and broad peak at 1184 cm^{-1} can be verified as O-H bond due to the intermolecular attraction.

From the spectrum of HBP(OH)-1, a broad peak at around 3300 cm^{-1} represents the

stretching band of OH bond. A sharp peak at ~1718 cm^{-1} should be attributed to the stretching of carbonyl (-C=O) group of the polyester. The peak wavenumber at 1470 cm^{-1} exhibits rocking vibration of -C-O-H bond. The peaks at 1396~1313 cm-1 and 1202~1037 cm-1 should be the results of the stretching of C-O and bending of O-H bond, respectively. In other words, both the bands comprised of C-O-H rocking vibration.

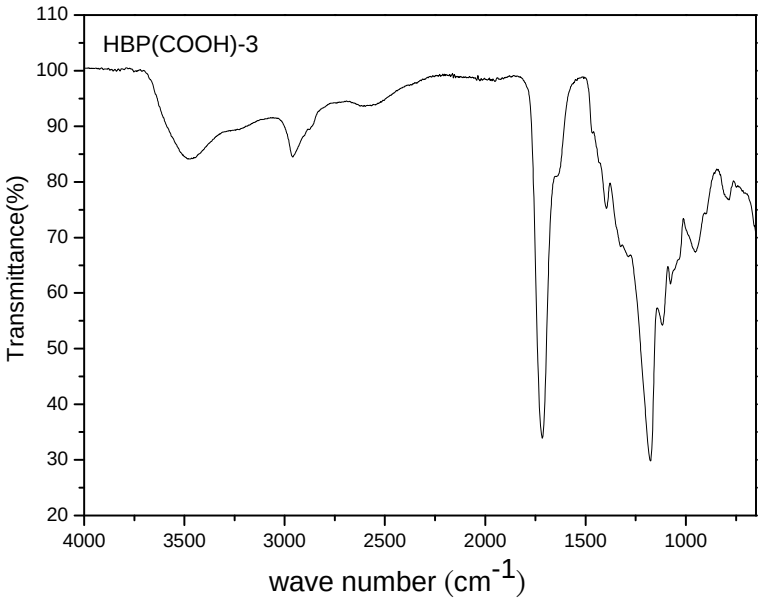

Figure 3.14 FTIR spectra of HBP(COOH)-3

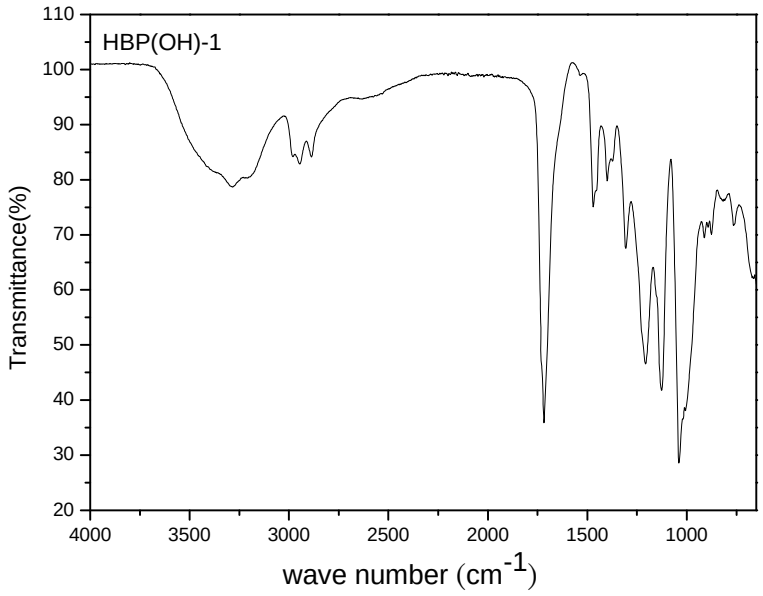

Figure 3.15 FTIR spectra of HBP(OH)-1

3.4 Conclusion

Hyperbranched products with acid and hydroxyl end group, respectively, have been successfully synthesized. The products obtained divides into different molecular weight products. The maximum molecular weights of HBP(COOH) and HBP(OH) achieved in this study were approx. 760000 and 50,000, respectively. The synthesized polymers were characterized by NMR, FT-IR, TGA and GPC.

Chapter 4: Fabrication and Characterization of HBP-reinforced PCL composites

4.1 Introduction

In recent years, biopolymers, i.e., biodegradable polymers, have attracted more and more attention due to increasing environmental concern and decreasing fossil resources[117-120]. Since biopolymers are biodegradable and their main productions are obtained from renewable resources such as agroresources, they represent an interesting alternative to common non-degradable polymers, particularly for short-life range applications (packaging, agriculture, etc.)[117-120]. Nevertheless, most biopolymers are sometimes too weak for practical use when compared to conventional thermoplastic polymers. Therefore, it appears necessary to improve the biopolymers to make them fully competitive with common thermoplastics.

Nano-biocomposites are very promising materials as they show improved properties with preservation of the native material biodegradability, without causing eco-toxicity. The properties of the materials can be considerably improved by the strong polymer-nanofiller interactions.

The unique physical properties and high peripheral functionalities of HBPs offer a variety of pathways for polymer modification. HBPs can thus play an important role as novel

building blocks for generating new nanostructures ranging from core shell type to network morphologies[2]. When HBPs containing hydrogen bondable surface groups are blended into a polymer matrix, their outer shells may strongly interact with the polymer molecules. Combining these nanostuffs to improve performances of aliphatic polyesters and other promising biodegradable materials would be an opportunity. The inter-play between their various effects/constituents may give birth to a new generation of biodegradable materials valuable to replace the traditional plastics.

4.2 Experimental

4.2.1 Materials

PCL (M_n=70,000~90,000, GPC standard) was purchased from Sigma Aldrich Chemical Co.

4.2.2 Fabrication of PCL composites

HBP(COOH)-2, HBP(COOH)-3, HBP(COOH)-4, HBP(OH)-1 and HBP(OH)-2 were used to blend with PCL to form composite materials in the study. Hyperbranched polymer in the amounts of 3% (0.15g), 6% (0.3g), or 10% (0.5g), 15 %(0.75g) and 20 % (1g) with respect to same PCL content (dry weight = 5g) were added to the THF solvent (150 mL) during its preparation. After complete solvent evaporation, the resultant sheet of composite in dry weight was determined before DSC analysis. Blends of both

hyperbranched polymers with PCL were co-mixed in THF well prior to forming composite sheets. The sheets were casted on TEFLON molds and the solvent was allowed to evaporate at 40°C. The films were further dried in vacuum at room temperature for two days. The resultant sheets were peeled off from the casting surface.

4.2.3 Tensile tests

Tensile tests were performed on a screw-driven universal testing machine (instron 4411, Canton, MA) equipped with a 10 kN electronic load cell and mechanical grips. The test specimens were cut into the dimension as indicated from sample size below. The thickness of the specimen was about 0.22 mm. The tests were conducted at room temperature using a crosshead rate of 10 mm/min. All tests were carried out according to the ASTM standard, and the data reported were the mean and standard deviation from four separated determinations.

(1) Sample size and geometry

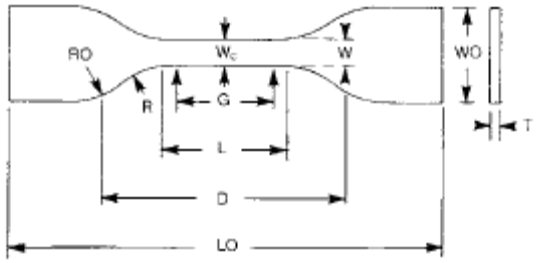

Dimensions (mm)	Rod sheet specimen
W-Width of narrow section	6
L-Length of narrow section	33
WO-Width overall	19
LO-Length overall	115
G-Gage length	25
Distance between grips	65
Radius of fillet	14
RO-Outer radius	25

4.2.4 Differential Scanning Calorimetry (DSC)

The effect of HBPs on crystallinity behaviour of the bulk polymers was investigated by DSC analysis. The experiments were performed on a Perkin Elmer Instruments Diamond DSC series under constant nitrogen flow (20 ml/min). The following thermal cycle was used:

1) Heat from -60.00 ^{o}C to 80.00 ^{o}C at 10.00 ^{o}C/min ; 2)Hold for 5.0 min at 80.00 ^{o}C 3)

Cool from 80.00 °C to -60.00 °C at 10.00 °C /min ; 4) Hold for 1.0 min at -60.00 °C. 5) Heat from -60.00 °C to 80.00 °C at 5.00 °C /min. 6) Hold for 5.0 min at 80.00 °C 7) Cool from 80.00 °C to -60.00 °C at 5.00 °C /min 8)Hold for 1.0 min at -60.00 °C. The samples were weighed such that all of the samples had an identical PCL content. The sample weight was maintained at low levels (5-7mg) for all measurements in order to minimize any possible thermal lag during the scans. The machine calibration and background subtraction were done according to the Perkin Elmer instrument protocols. The results of the DSC thermograms were used from the data in second heating-cooling cycle.

4.2.5 Dynamic Mechanical Analysis (DMA)

DMA analysis of HBP(COOH)/PCL composites

DMA experiments were performed on a Perkin Elmer Diamond DMA Lab system equipped with a film tension clamp. The instrument was programmed to measure G' (storage modulus) over the range of -100°C to 40°C at 3°C /min heating rate and 1 Hz constant frequency. Calibrations for force, mass, position and temperature were made in accordance with Perkin Elmer procedures. The specimen sheets were cut with dimensions W x H x L = 5 x 0.22 x 15 mm) and mounted on a dual-cantilever geometry in order to guarantee uniform strain on the sheet under tension. The applied strain (0.02

% - 0.05 %) was well within the linear viscoelastic region of the samples and the collected data were reproducible. Storage modulus (G'), and tan δ were recorded as a function of temperature.

DMA analysis of HBP(OH)/PCL composites

DMA experiments were performed on a Perkin Elmer DMA 8000 apparatus equipped with a film tension clamp. The instrument was programmed to measure G' (storage modulus) over the range of -100^{o}C to 40^{o}C at 2^{o}C /min heating rate and 1 Hz constant frequency. The specimen sheets were cut with dimensions W x H x L = 6 x 0.15 x 12 mm) and mounted on a dual-cantilever geometry in order to guarantee uniform strain in the sheet under tension.

4.2.6 Scanning Electron Microscopy (SEM)

SEM examined tensile fractured surfaces of the neat polymers and the blends. A JEOL 5339F field emission scanning electron microscope (JEOL, Japan) equipped with an EDS (energy dispersive X-ray spectroscopy) system was used to capture high-resolution images of the cross-sectional fracture surface after tensile test. All samples were sputter-coated with gold (5 nm) to provide enhanced conductivity prior to imaging analysis.

4.2.7 Transmission electron microscopy (TEM)

TEM was employed to evaluate the morphology and distribution of HBP particles in the PCL matrix. The blends were first stained with an aqueous solution of uranyl acetate (2wt%) and dried overnight before TEM observation. Uranyl acetate selectively stained the carboxyl group present in hyperbranched (citric acid) and appeared darker than the PCL phase in the TEM micrographs. TEM bright field imaging was performed on a JEOL 100 CX II microscope using 100 kV accelerating voltage.

4.2.8 Degradation

The composite samples were weighed and immersed in two different aqueous media, respectively. The specimens were kept at 37 ^{o}C for given time periods. The media are listed as below[304].

(a) PBS solution: phosphate-buffered saline (PBS) at pH 7.5 (KH_2PO_4 0.0087 M, Na_2HPO_4 0.0304 M and NaCl 0.154 M).

(b) NaOH solution: 0.01 M of NaOH solution.

PBS solutions adjusted at pH 7.4 were appropriate incubation buffers (typical bacterial culture medium) for an accurate simulation of the *in vivo bio*degradation of

biodegradable polymers. In order to apply biodegradable polymer (PCL and PLA) in biomedical application such as tissue engineering scaffold, the study of biodegradability is necessary using PBS buffer solution as working medium. In conventional chemical degradation experiment, the rate of degradation is higher in solution with higher alkalinity , for example, NaOH. OH^- ions play significant role in hydrolysis reaction in both hyperbranched polyester and biodegradable polymer system.

Each degradation test was performed in triplicate under sterile conditions. For this purpose, the samples were kept in absolute ethanol overnight before immersing in the degradation media. The NaOH and PBS solutions were renewed every week. Once a week up to 35 days, the samples were collected, washed with distilled water, vacuum-dried at room temperature and weighed. The % of weight loss of the samples was calculated according to the equation below:

$$\%weight\ loss = \frac{(W_o - W_t)}{W_o} \times 100\%$$

where W_t is the dry weight remaining at a given degradation time t and W_o is the initial weight.

Molecular weight distributions of the hyperbranched polymers were determined by gel permeation chromatography (GPC, detector: Waters Series 2414 refractive index detector; pump: Waters Series 1515 Isocratic HPLC pump) using THF as eluent and polystyrene as

the standard. Specimen concentration was 0.03 g sample/10 ml, and the flow rate was controlled at 0.8 ml/min

4.3 Results and discussion

4.3.1 Fabrication of PCL composite specimens

Figure 4.1 illustrates a sample film obtained by solvent blending HBP(COOH) with PCL. All the films prepared from this method possessed smooth and homogeneous texture.

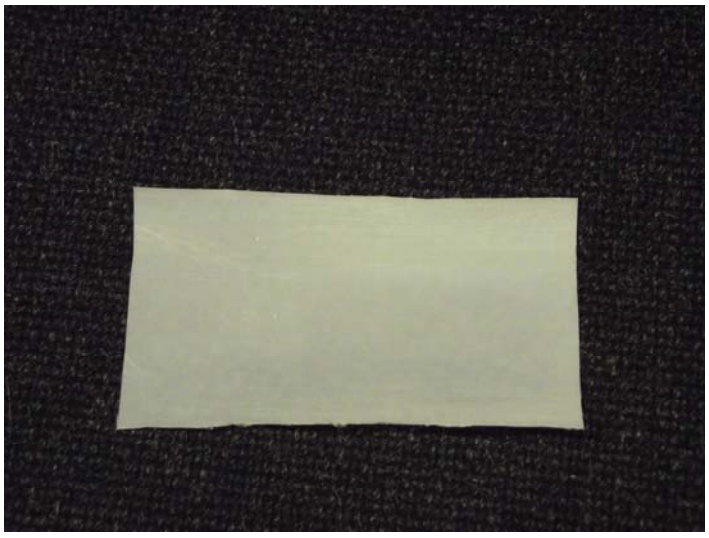

Figure 4.1 A sample of a HBP(COOH)/PCL composite

4.3.2 Mechanical properties

4.3.2.1 Tensile test of HBP(COOH)-reinforced PCL nanocomposites

Stress-strain dependence of HBP(COOH)-2-blended PCL nanocomposite specimens is shown in **Figure 4.2**. It can be seen that all the composite samples are weaker than pure

PCL.

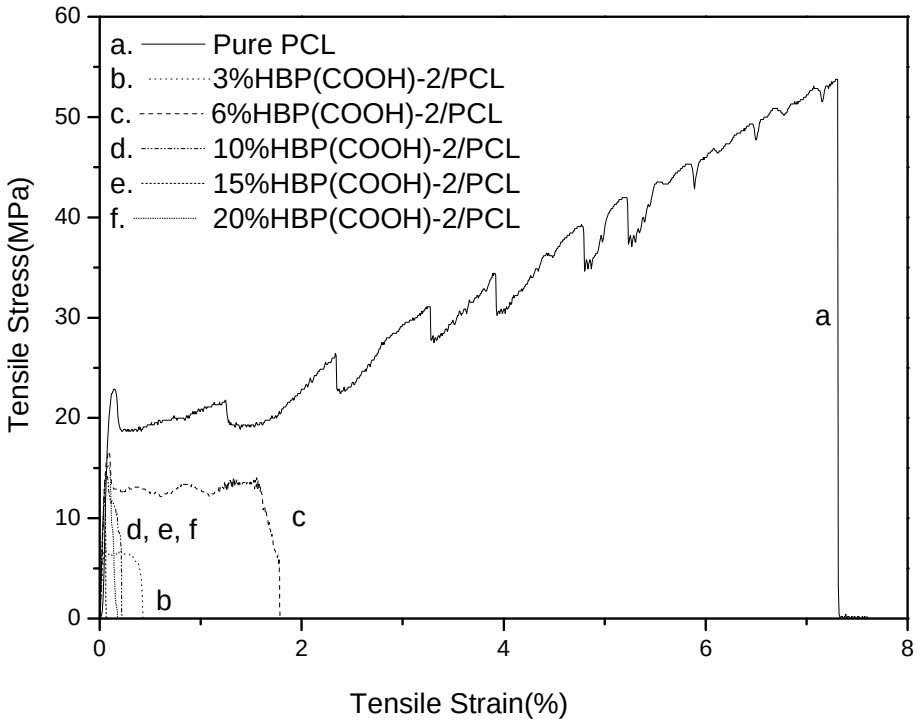

Figure 4.2 Tensile stress-strain curves of the PCL composite with different HBP(COOH)-2 contents

Stress-strain dependence of HBP(COOH)-3 modified PCL nanocomposites is shown in **Figure 4.3**. The samples with weight ratios of both 3 wt. % and 6 wt. % HBP(COOH)-3 exhibits better tensile strength than does pure PCL. Among those samples, 3 wt. % HBP(CA)-3 gives the maximum tensile strength. However, for the samples with filler content in the range of 10~20 wt. %, the tensile strengths were weaker than that of pure PCL. In **Figure 4.4**, the average values of tensile stress and elongation

at break of the samples with various filler ratios are presented. It is found that 3 wt. % HBP(COOH)-3 presents an ideal strain at break for the material, which is increased by 15.5% compared to pure PCL.

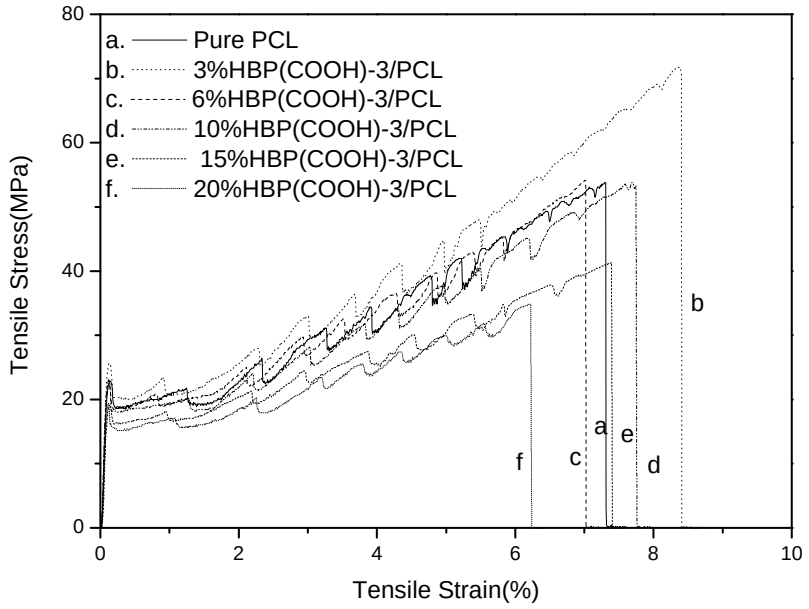

Figure 4.3 Tensile stress-strain curves of the PCL composite with various HBP(COOH)-3 contents

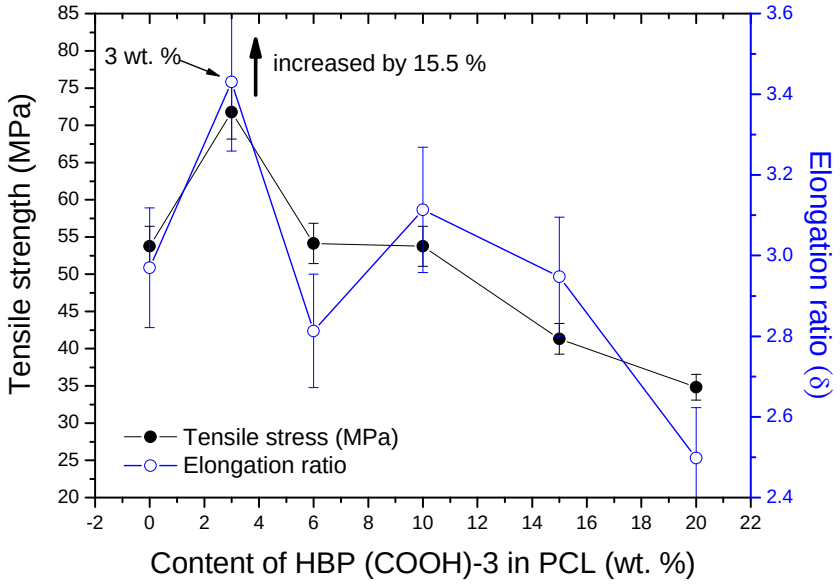

Figure 4.4 Mechanical properties of PCL with various HBP(COOH)-3 concentrations

Stress-strain dependence of HBP(COOH)-4 modified PCL nanocomposites is given in **Figure 4.5**. Their average values of tensile stress and elongation at break are presented in **Figure 4.6**. It can be seen that the weight ratios of 3 wt. %, 6 wt. %, and 10 wt. % exhibit better tensile strength results. Among those samples, 6 wt. % HBP(COOH)-4 gives the maximum tensile strength. However, further increasing filler content to 15~20 wt. % results in a decrease of tensile strength. On the other hand, the sample with 6wt. % of HBP(COOH)-4 presents the best elongation at break, which is increased by 14.9%

compared to pure PCL.

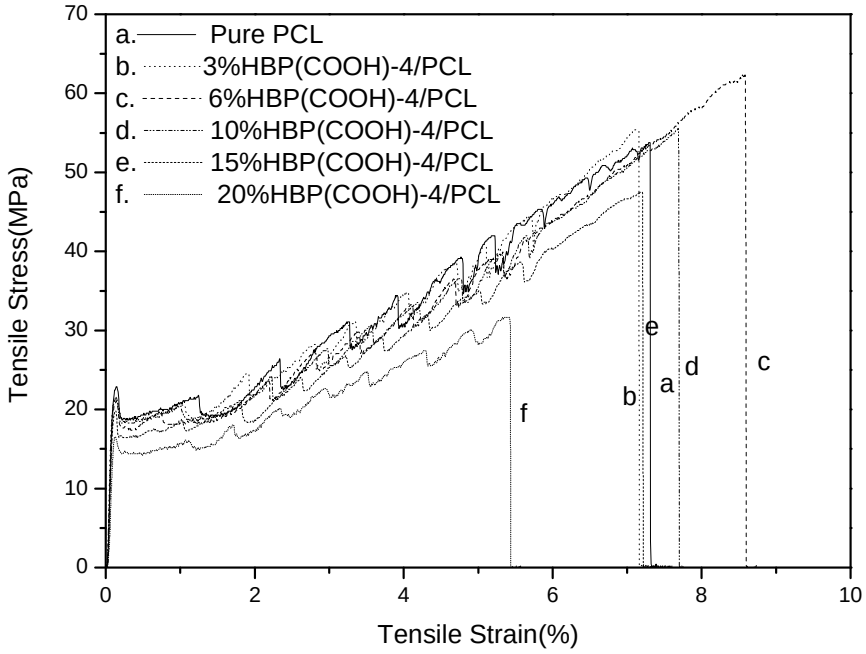

Figure 4.5 Tensile stress-strain curves of the PCL composite with different HBP(COOH)-4 contents

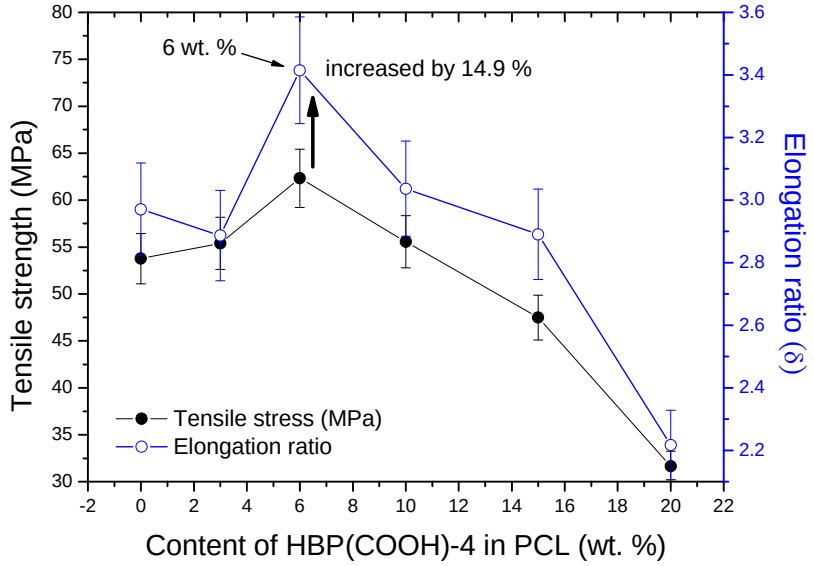

Figure 4.6 Mechanical properties of PCL with various HBP(COOH)-4

concentrations

It seems that the tensile stress-strain behaviour depends on two factors. One is the filler content, and another is the molecular weight of HBP. For samples with low molecular weight HBP(COOH), relatively poor mechanical properties are always resulted. For those with medium molecular weight HBP(COOH) at an optimum level, better properties can be realized. For example, introduction of 3 wt. % HBP(COOH) can improve the mechanical properties of PCL significantly. For the high molecular weight specimens, the best toughness results can be obtained at filler content of ~6 wt. %. High molecular weight HBA(COOH) is also found to be the best toughness modifier in this system among the others.

From theoretical point of view, the component polymers with similar viscosity should have the behavior to be mixing well as the other conditions were unchanged. Moreover, It was shown that a change in the viscosity ratio for the blend composition had a significant effect on mechanical property and on the blend phase morphology. The viscosity of PCL was much higher than that of hyperbranched polymer, and whereas hyperbranched polymer has a lower viscosity. It should be point out that the viscosity of PCL with addition of HBP decreased drastically compared to that of pure PCL. On the other hand, ester group of PCL should interact with the hydroxyl group of HBP, and then form weak

hydrogen bond. These two effects have the abilities to improve compatibility of HBP and PCL, and deduce the increasing of the tensile strength of the blends. However, the high degree of entanglements within hyperbranched polymer due to the formation of larger hyperbranched cluster-like particles resulted in poor dispersion in biodegradable polymer matrix. Thus, the addition of excessive HBP was not favorable to increase the tensile strength of the blends, and so the tensile strength of the blends should be decreased, as the weight percentage of the HBP is 20 wt. %. Therefore, HBP can be used to improve the poor inter-phase adhesion and high interfacial tension between the two phases of PCL blends and the tensile strength of blends reach the maximum value when the blends consists of 3~6 wt. % HBP. The more HBP should be unfavorable to increase the mechanical property due to the reason mentioned above.

4.3.2.2 Tensile test of HBP(OH)-reinforced PCL nanocomposites

Stress-strain dependence of the blends with various HBP(OH)-1 contents is shown in **Figures 4.7** and **4.8**. The samples with 3 wt. % and 6wt. % of HBP(OH)-1 exhibit better tensile strength than pure PCL. Among the samples, 6 wt. % HBP(OH)-1 gives the best tensile strength value. The strain at break value of the material is also improved by 21% in comparison to neat PCL. However, for those with 10~20 wt. % of HBP(OH)-1, there is a drop in tensile strength when compared with neat PCL.

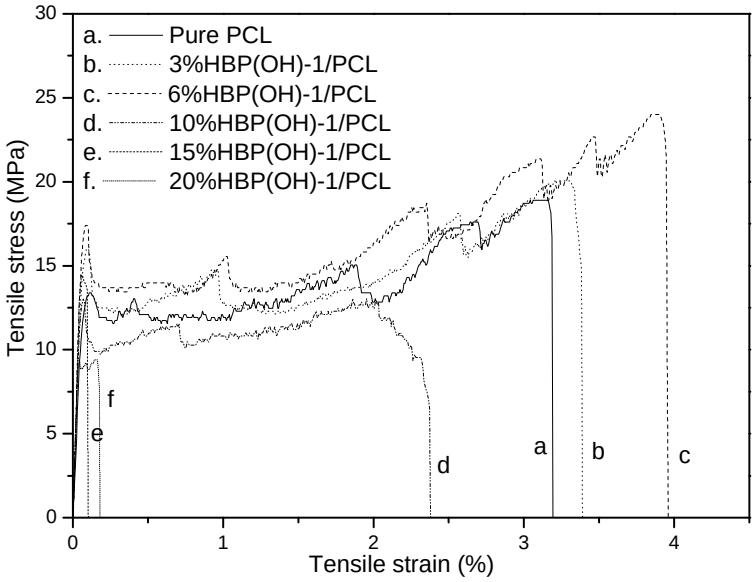

Figure 4.7 Tensile stress-strain curves of the PCL composite with various HBP(OH)-1 contents

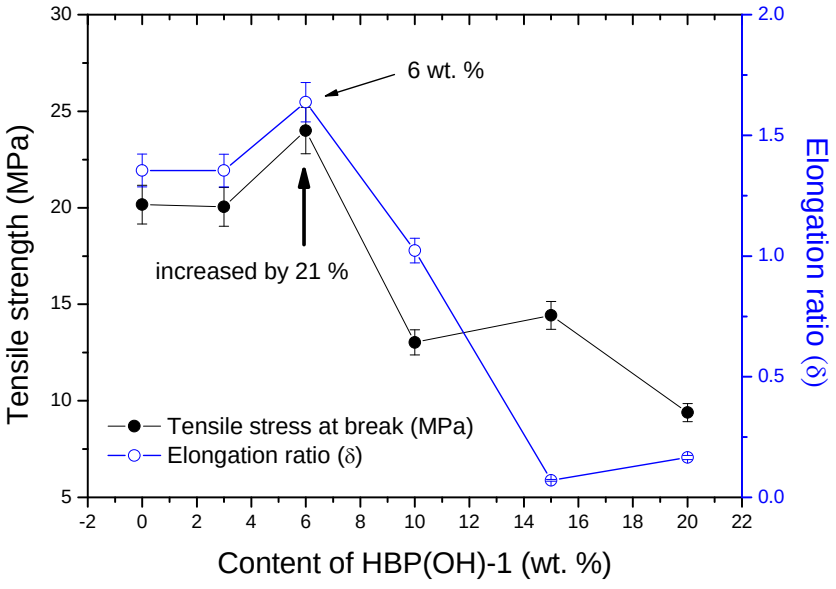

Figure 4.8 Mechanical properties of PCL with various HBP(OH)-1 weight percentages

Stress-strain dependence of HBP(OH)-2 modified PCL nanocomposites is shown in **Figures 4.9** and **4.10**. Apparently, the addition of HBP(OH)-2 affords only mild effect to the system when below filler content of ~6wt. %. Above 6wt. %, adverse effect can be found.

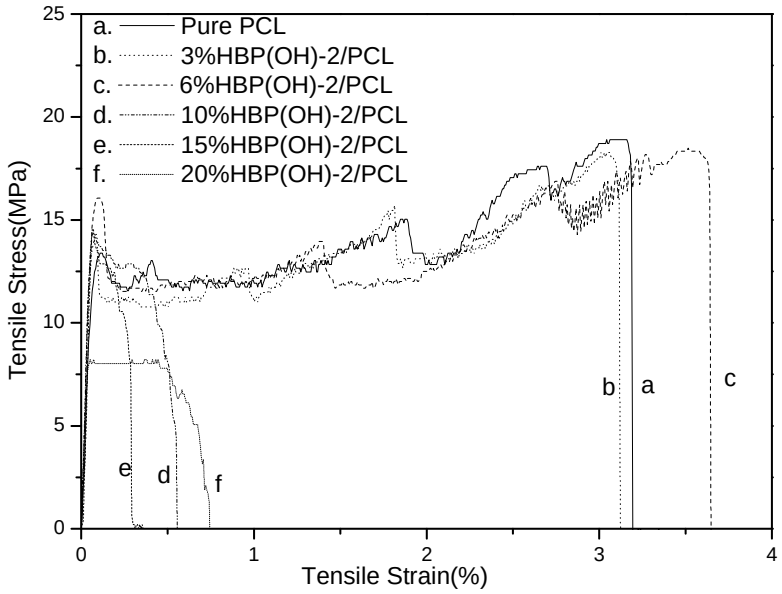

Figure 4.9 Tensile stress-strain curves of the PCL composite with various HBP(OH)-2 contents

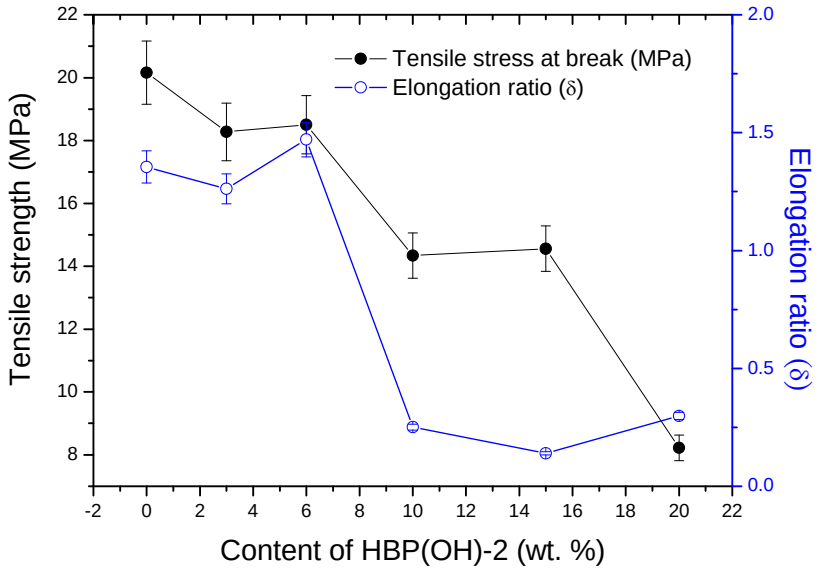

Figure 4.10 Mechanical properties of PCL with various HBP(OH)-2 concentrations

Similar to the previous system, the tensile stress-strain behaviour of the HBP(OH)-modified system depends on two factors, the filler content and the molecular weight of HBP. In comparison, low molecular weight HBP(OH) has better effect than the one with larger molecular weight for the blends. The filler content of 6 wt. % is found to be the optimum level for the system, where improved mechanical properties can be realized.

4.3.3 Thermal and thermomechanical studies

4.3.3.1 Differential Scanning Calorimetry (DSC)

DSC was used to determine nonisothermal crystallization behavior of the blends. The useful parameters corresponding to their crystallization behaviors can be obtained from the curves as well as using the following formula:

$$X_c(\%) = \frac{\Delta H_c}{\Delta H_{100}} \times 100$$

where X_c is the degree of crystallinity, ΔH_c is the cool of crystallization of the sample, and $\Delta H_{100,c}$ is the cool of crystallization for a 100% crystalline PCL, which is taken as -136.4 J/g.

4.3.3.1.1 DSC of HBP(COOH) modified PCL nanocomposites

Figures 4.11 to 4.13 show the DSC cooling curves of the samples. The T_m、ΔH_h、Tp 、ΔH_c and X_c values of HBP(COOH)/PCL composites are summarized in **tables 5~7.**

It can be observed from **Table 5** that T_m decreases 1~2 ^oC as the content of HBP(COOH)-2 increases from 3 to 20 wt. %. The peak temperature fluctuates in small amplitude. Compared to pure PCL, the degree of crystallinity of the 3 wt. % HBP(COOH)-2 sample reduces by about 5 %. However, the Xc value is enhanced as

the content of HBP(COOH)-2 increases. When the weight percentage of HBP(COOH)-2 reaches 20 wt. %, the Xc value increases by 22.5 %.

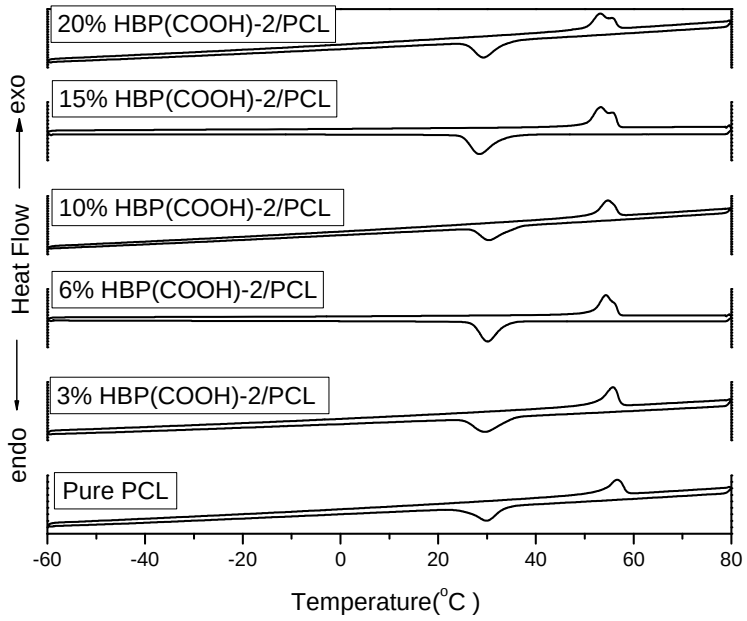

Figure 4.11 DSC thermograms for pure PCL and HBP(COOH)-2 modified composites

Table 5 DSC data of HBP(COOH)-2/PCL blends

HBP(COOH)-2/PCL	0%HBP	3%HBP	6%HBP	10%HBP	15%HBP	20%HBP
Tm (^{o}C)	56.55	55.72	53.33	54.73	53.23	53.20
ΔH_h(J/g)	48.0388	50.2618	54.2406	52.0080	62.2611	59.8141
Tp (^{o}C)	29.98	29.64	30.12	30.44	28.43	29.32
ΔH_c(J/g)	-57.6559	-54.7752	-61.8087	-62.4078	–69.4060	-70.5862
X_c(%)	42.26	40.15	45.31	45.76	50.88	51.75

It can be observed from **Table 6** that Tm decreases 1~3 ^{o}C as the content of HBP(COOH)-3 increases from 3 to 20 wt. %. The peak temperature fluctuates in small amplitude. When a small amount of HBP(COOH)-3 (~3 wt. %) is introduced to the blend, the Xc value dramatically decreases by 22.6 % as compared with pure PCL. The Xc bounds back to the value close to that of neat PCL as the weight percentage of HBP(COOH)-3 gradually increases to 20 wt. %.

When addition of HBP weight percentage of 3-6 %. The decrease in degree of crystallinity could improve the mechanical properties of the PCL blends due to the decrease particle size of hyperbranched molecules and the increase of compatibilization at the interface between HBP and PCL. A further increase in HBP weight percentage to 20 wt. % did not produce high dispersity of hyperbranched particles in the bulk PCL matrix, thus not contribute to the reduction of interfacial tension between HBP and PCL, This reduction in interfacial tension between HBP and PCL resulting in more chain segment mobility of PCL chains. Thus, the degree of crystallinity (Xc) is closed to PCL with HBP addition.

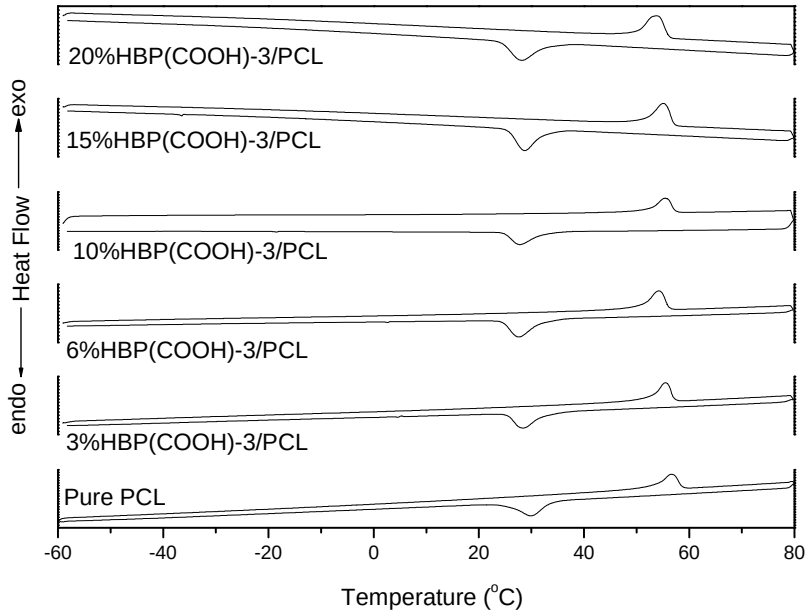

Figure 4.12 DSC thermograms for pure PCL and HBP(COOH)-3 modified composites

Table 6 DSC data of HBP(COOH)-3/PCL blends

HBP(COOH)-3/PCL	0%HBP	3%HBP	6%HBP	10%HBP	15%HBP	20%HBP
Tm (°C)	56.55	55.52	54.18	55.37	55.06	53.88
ΔH_h(J/g)	48.0388	40.6433	42.0766	45.4391	47.3032	50.7251
Tp	29.98	28.47	27.65	27.84	28.69	28.10
ΔH_c(J/g)	-57.6559	-44.6230	-48.6990	-51.0806	-52.2246	-56.5910
X_c(%)	42.27	32.71	35.70	37.44	38.28	41.49

It can be observed from **Table 7** that Tm decreases 1~3 ^{o}C as the content of HBP(COOH)-4 increases from 3 to 20 wt. %. The peak temperature fluctuates in small amplitude. When a small amount of HBP(COOH)-4 (3 ~6wt. %) is introduced, the Xc value of the blend dramatically decreases by 17.9 % as compared with pure PCL. The Xc comes back to the value close to that of neat PCL as the weight percentage of HBP(COOH)-4 further increases to 20 wt. %

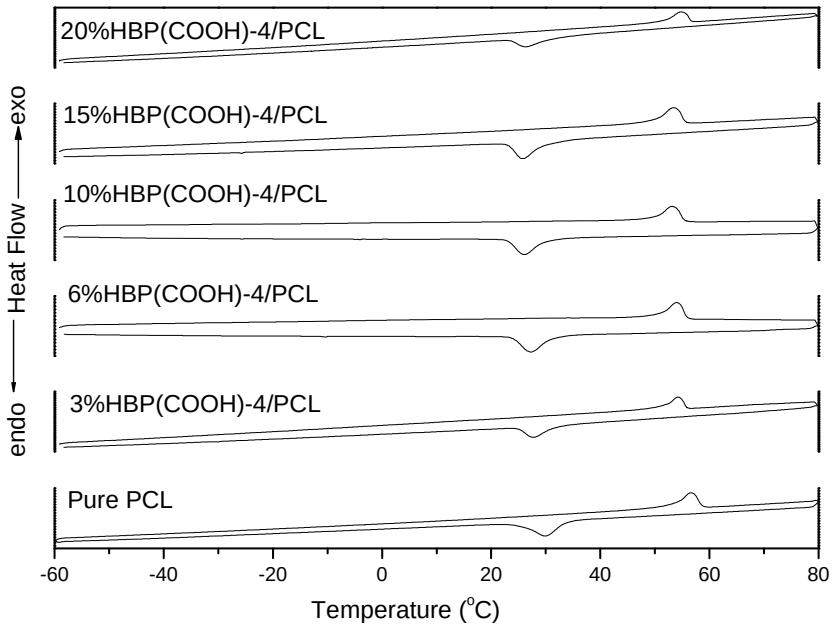

Figure 4.13 DSC thermograms for pure PCL and HBP(COOH)-4 modified composites

Table 7 DSC data of HBP(COOH)-4/PCL blends

HBP(COOH)-4/PCL	0%HBP	3%HBP	6%HBP	10%HBP	15%HBP	20%HBP
Tm (^{o}C)	56.55	54.24	53.96	53.12	53.43	54.74
ΔH_h(J/g)	48.0388	41.2171	40.5653	42.8379	43.9911	50.5296
Tp	29.98	27.80	27.34	26.09	25.82	26.45
ΔH_c(J/g)	-57.6559	-47.7578	-47.3584	-52.9189	-50.7280	-55.584
X_c(%)	42.27	35.01	34.71	38.80	37.19	40.75

As illustrated from the DSC data, there is no change in crystalline phase when HBP(COOH) is incorporated, however, there is a dramatic change in Xc. When small amount of HBP(COOH) (3 wt. %) is introduced, particularly HBP(COOH)-3 and HBP(COOH)-4, the Xc value was reduced. As the content of HBP(COOH) further increases in the blend, the Xc value likely rebounds back to the original level. It can be seen that only a small percentage of HBP(COOH) is able to interfere with the crystallization behavior, resulting in improvement of brittleness of the blends. However, an excess amount of HBP(COOH) may cause heterogeneous mixing, thus leading to deterioration in mechanical properties.

4.3.3.1.2 DSC of HBP(OH) modified PCL nanocomposites

Figures 4.14 and **4.15** show the DSC cooling curves of the samples. The T_m、ΔH_h、Tp、ΔH_c, and X_c values are summarized in **Tables 8** and **9**.

It can be observed from **Table 8** that the peak temperature fluctuates 2~3°C as the content of HBP(OH)-1 increases from 3 to 20 wt. %. The T_m fluctuates in small amplitude. Compared to pure PCL, the Xc value of he blends increases as the content of HBP(OH)-1 increases from 3 to 20 wt. %. The Xc value is at the minimum when the weight percentage of HBP(OH)-1 reaches 6 wt. % in the blend.

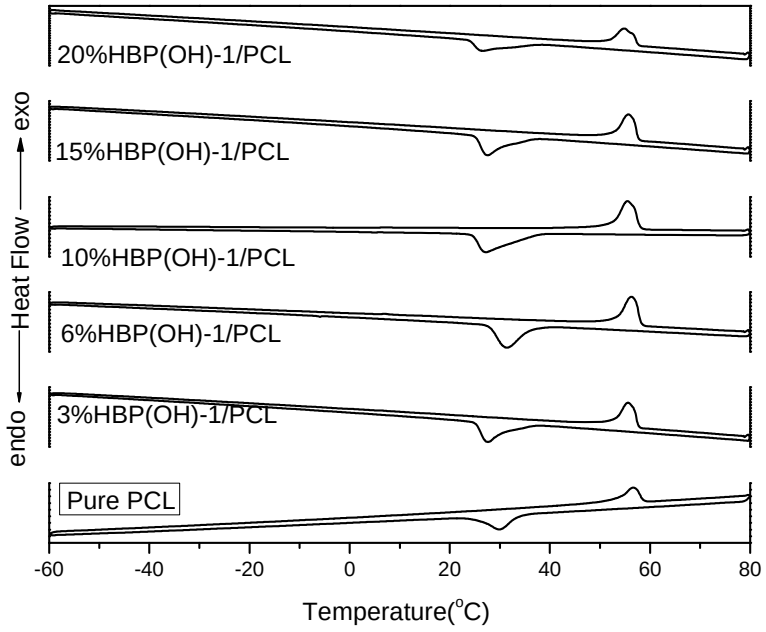

Figure 4.14 DSC thermograms for pure PCL and HBP(OH)-1 modified composites

Table 8 DSC data of HBP(OH)-1/PCL blends

HBP(OH)-1/PCL	0%HBP	3%HBP	6%HBP	10%HBP	15%HBP	20%HBP
Tm (^{o}C)	56.55	55.33	56.29	55.52	55.72	54.87
ΔH_h(J/g)	48.0388	59.7030	55.4819	56.0435	63.5323	66.9464
Tp (^{o}C)	29.98	27.58	31.32	27.21	27.49	26.47
ΔH_c(J/g)	-57.6559	-63.9765	-60.985	-61.9534	-67.9137	-69.8130
X_c(%)	42.27	46.91	44.71	45.42	49.79	51.8750

It can be observed from **Table 9** that $T_{m,}$ the peak temperature, and the Xc value fluctuate in small amplitude as the content of HBP(OH)-2 increases from 3 to 20 wt. %.

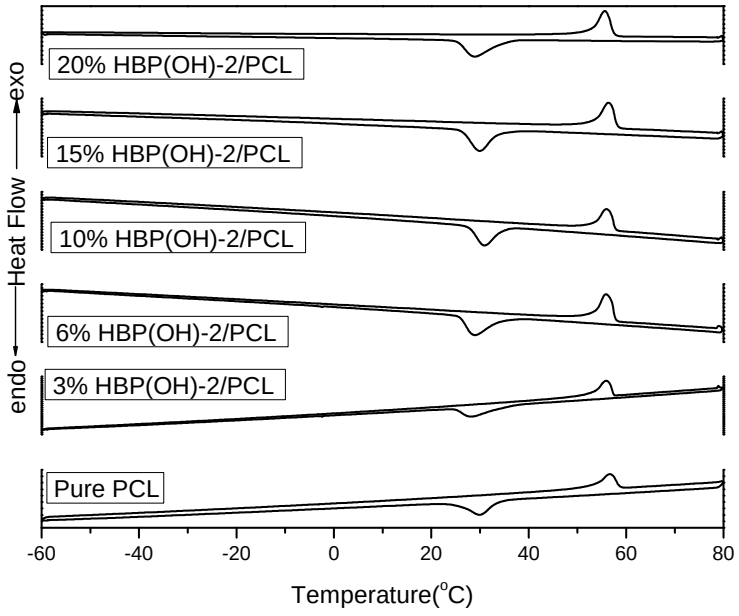

Figure 4.15 DSC thermograms for pure PCL and HBP(OH)-2 modified composites

Table 9 DSC data of HBP(OH)-2/PCL blends

HBP(OH)-2/PCL	0%HBP	3%HBP	6%HBP	10%HBP	15%HBP	20%HBP
Tm (^{o}C)	56.55	55.87	55.89	56.03	56.36	55.61
ΔH_h(J/g)	48.0388	48.6347	52.0604	53.9132	53.2345	52.3478
Tp	29.98	28.39	28.90	30.90	29.88	28.88
ΔH_c(J/g)	-57.6559	-58.7450	-56.0606	-57.8568	-58.4961	-57.9303
X_c(%)	42.26	43.07	41.10	42.42	42.88	42.47

As shown in **Table 8**, there is no significant change in Tm when HBP(OH)-1 is incorporated but the Xc value is enhanced. Overall speaking, the enhancement of tensile strength of the modified composites can be attributed to the synergistic effect of HBP(OH)-1 added and the increase in degree of crystallinity**.** On the other hand, it seems that excess amount of HBP(OH)-1 incorporated into PCL matrix results in poor dispersion of the filler, leading to interrupting the interaction between HBP-OH and the PCL matrix.

4.3.3.2 Dynamic Mechanical Analysis (DMA)

4.3.3.2.1 DMA of HBP(CA) modified PCL nanocomposites

DMA for pure PCL and the modified PCL blends were conducted and the influence of

temperature on their storage modulus (G') and loss factor (tan δ) were presented in **Figures 4.16** and **4.17**, respectively. As shown in **Figure 4.16**, the peaks in the range of -60 to -30 ^{o}C should be attributed to glass transition temperature (Tg) of PCL, showing a characteristic of semi-crystalline polymers. The peaks at ~0 ^{o}C should be attributed to Tg of HBP(COOH). For 3 % HBP sample (refer to Figure 4.16), the peak still exists due to the much smaller scale compared to the higher percentage of hyperbranched polymer (10 and 20 %). If we specifically enlarged the scale of tan δ at 0^{o}C, the peak can be identified for small percentage of incorporated HBP.

Tg of PCL in the blend increases as the weight percentage of HBP(COOH)-3 increases (maximum Tg achieved is –43.24^{o}C at 20 wt. % HBP(COOH)-3). Tg of HBP(COOH)-3 also increases as the weight percentage of HBP(COOH)-3 increases (maximum Tg achieved is –1.76^{o}C at 20 wt. % HBP(COOH)-3).

As shown in **Figure 4.17**, G' decreases with increasing temperature for each sample, especially in zone nearly their glass transitions. The G' value of the composite decreases first and then increase when the filler content gradually increases in the blend. It is found that G' is at the maximum when the weight percentage of HBP(COOH)-3 reaches 20 wt. %.

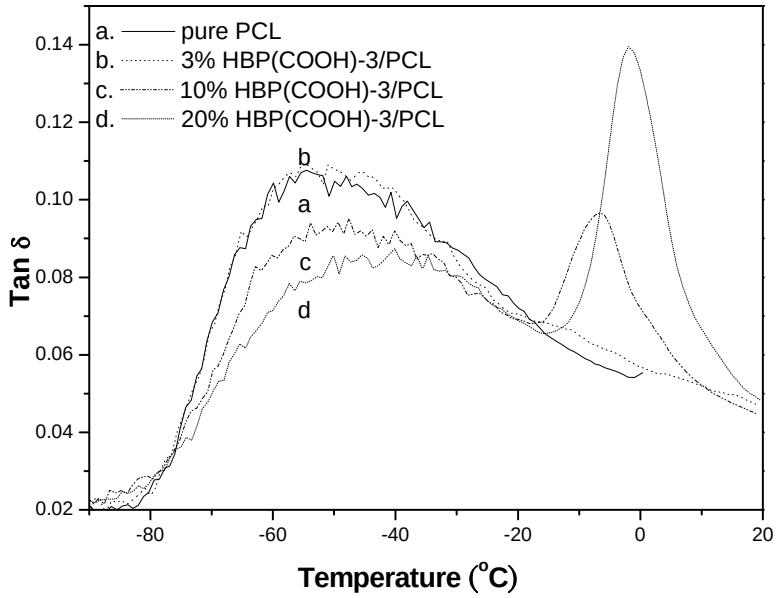

Figure 4.16 Tan δ vs. temperature curves of pure PCL and HBP(COOH)-3 modified PCL composites

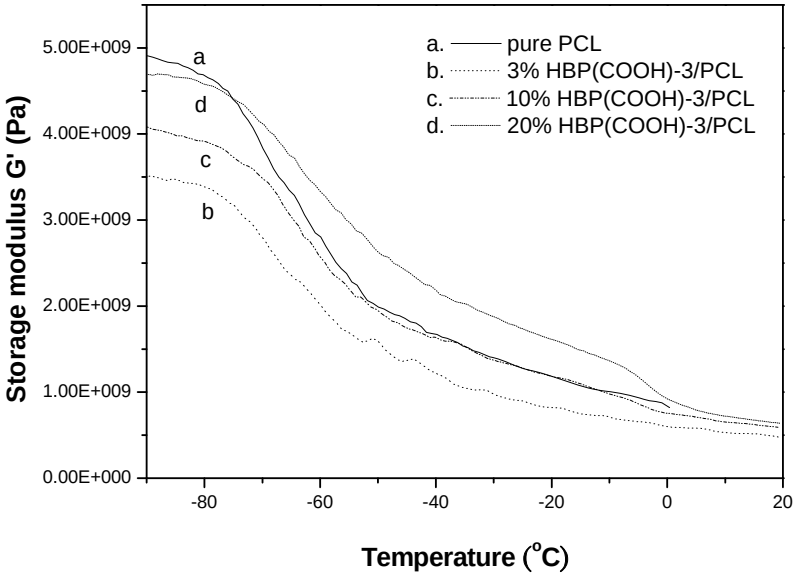

Figure 4.17 Storage modulus G' vs. temperature curves of pure PCL and HBP(COOH)-3 modified PCL composites

Similar study was also conducted for the HBP(COOH)-4/PCL system. As indicated in **Figure 4.18**, Tg of PCL increases as the weight percentage of HBP(COOH)-4 increases (maximum Tg achieved is –46.86^{o}C at 20 wt. % HBP(CA)-4). Tg of HBP(COOH)-4 also increases as the weight percentage of HBP(COOH)-4 increases (maximum Tg achieved is –3.54^{o}C at 20 wt. % HBP(COOH)-4).

For each composite, G' decrease with increasing temperature, especially in the zone nearly their glass transitions. As shown in **Figure 4.19**, their G' value decrease first and then increase when the filler content increases from 3 to 20 %. It is found that the G' value is at the maximum when the weight percentage of HBP(COOH)-4 reaches 20 wt. %..

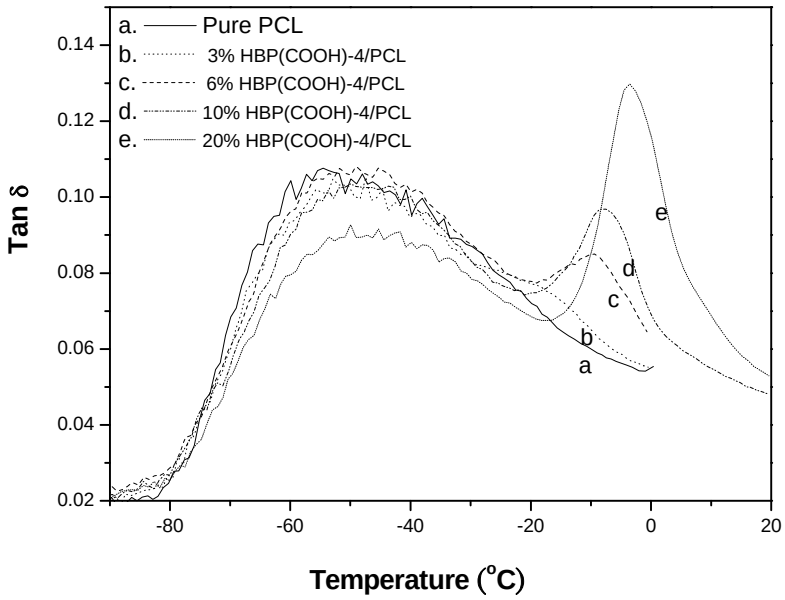

Figure 4.18 Tan δ vs. temperature curves of pure PCL and HBP(COOH)-4modified PCL composites

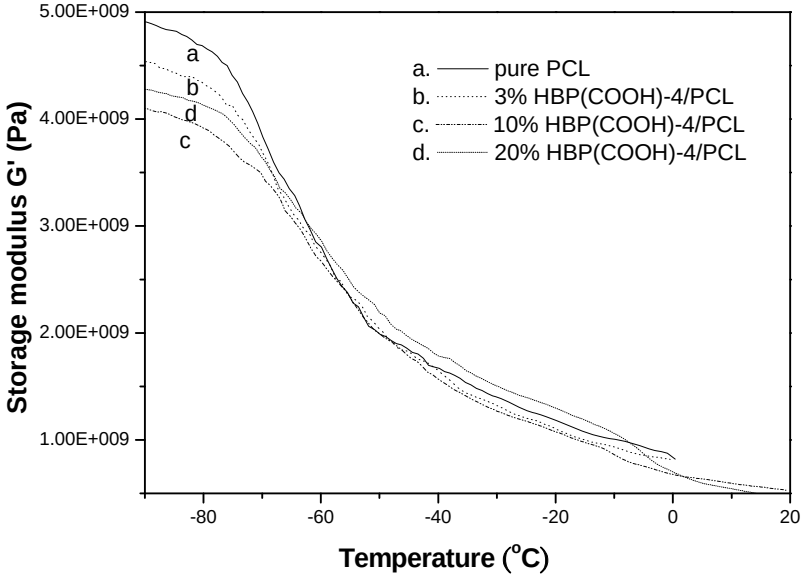

Figure 4.19 Storage modulus G' vs temperature curves of pure PCL and HBP(COOH)-4 modified PCL composites

The interactions between HBP and the polymer matrix should be enhanced as more HBP(COOH)-3 is introduced. Due to the enhanced interactions, Tg values of both HBP and PCL change correspondingly. When small amount of HBP(COOH) is introduced, G' of the material reduces significantly. This explains that HBP(COOH) even in a very diluted state (3-6 wt. %) is able to interfere with the crystallinity behavior in the PCL matrix. As the content of HBP(COOH)-3 and HBP(COOH)-4 subsequently increases to 10-20 wt. %, G' rebounds. This is because when more HBP is introduced, crystallization will reoccur and the degree of crystallinity is back to the original level. However, the excess amount of HBP(COOH) causes an increase in Tg of PCL. The increases in both Tg and degree of crystallinity may eventually lead to the enhancement in G'.

4.3.3.2.2 DMA of HBP(OH) modified PCL nanocomposites

The DMA spectra of neat PCL and the blends are presented in **Figures 4.20** to **4.23**, where the influences of temperature on G' and tanδ of the materials were present. The peaks in the range of -60 to -30^{o}C are attributed to Tg of PCL, showing a characteristic of semi-crystalline polymers. In general, Tg of the blends slightly changes with different amounts of the filler added, as illustrated in **Figure 4.20**.

From **Figure 4.21**, it is found that G' decreases with an increase in temperature for each sample, especially in the zone nearly their glass transition. The G' value decreases first and then increase when the content of HBP(OH)-1 increases in the composite system. G' is at the maximum when HBP(OH)-1 achieves 6 wt. %. For 6 wt. % HBP(OH)-1, the tan δ peak indicated from Figure 4.20 represent a sharp glass transition temperature at approx. –53 ^{o}C corresponding to rapid reduction in storage modulus. The decrease in shear storage modulus exhibited the rapid release of elastic energy of the composite.

Tg increases with increasing content of HBP(OH)-1 in the blend. When small amounts of HBP(OH)-1 (3wt. %~10 wt. %) are introduced, the G' value significantly increases. This is due to an increase in Tg of the blends. However, the G' decreases as the HBP(OH)-1 content increases to more than 10 wt. %.

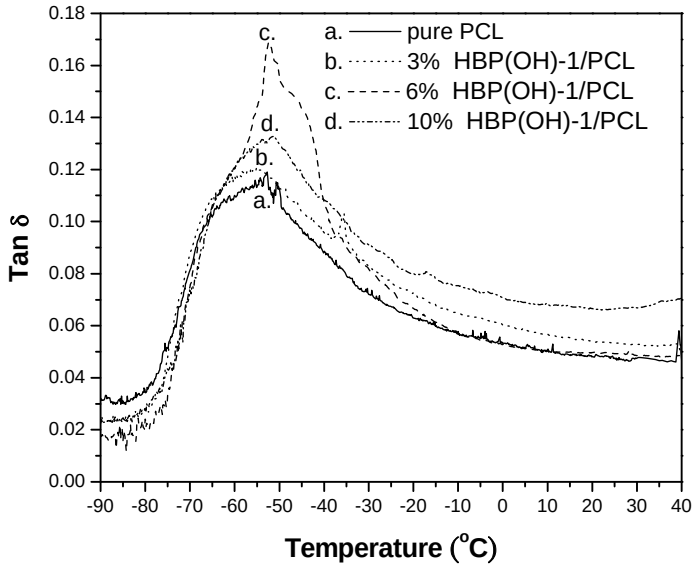

Figure 4.20 Tanδ vs. temperature curves of pure PCL and HBP(OH)-1 modified composites

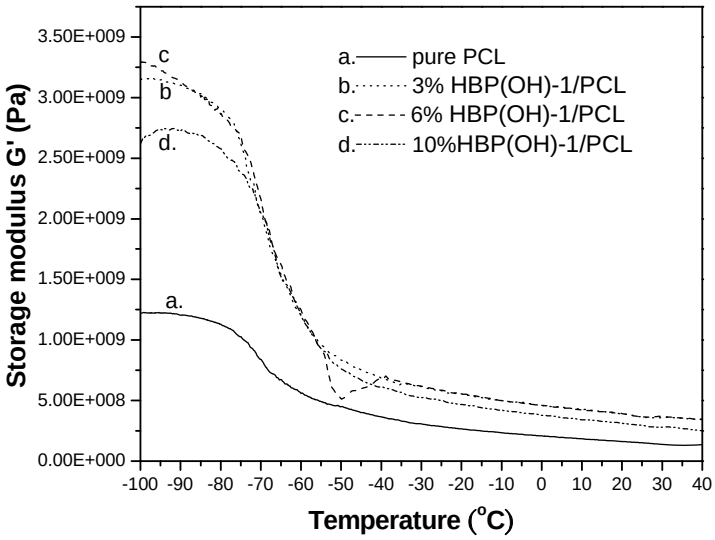

Figure 4.21 Storage modulus G' vs temperature curves of pure PCL and HBP(OH)-1 modified PCL composites

Similarly, as shown in **Figure 4.22**, Tg of PCL in the HBP(OH)-2 system increases with the weight percentage of HBP(OH)-2 (maximum Tg achieved is –47.02^{o}C at 10 wt. % HBP(OH)-2). From **Figure 4.23**, it is found that G' increases for the blends with filler content ranging from3 to 10 wt.%. G' is at the maximum when HBP(OH)-2 reaches 10 wt. %.

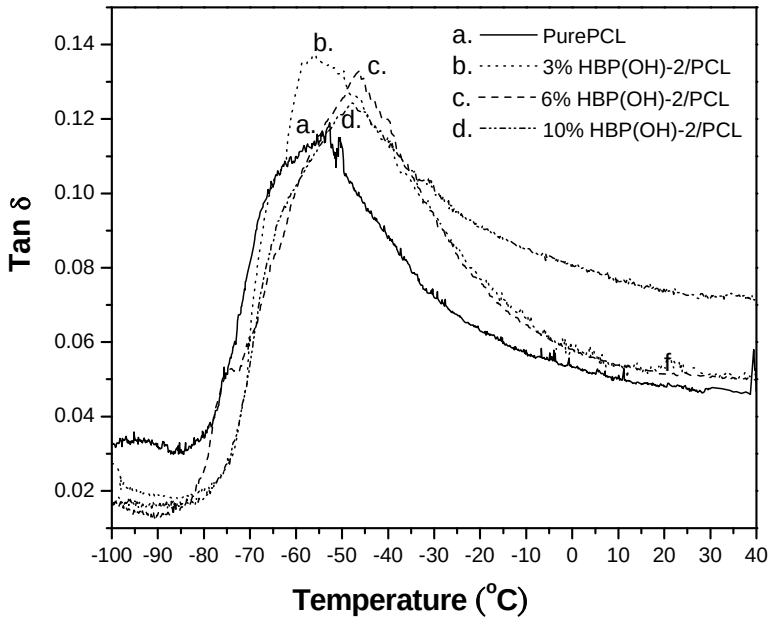

Figure 4.22 Tan δ vs. temperature curves of pure PCL and HBP(OH)-2 modified PCL composites

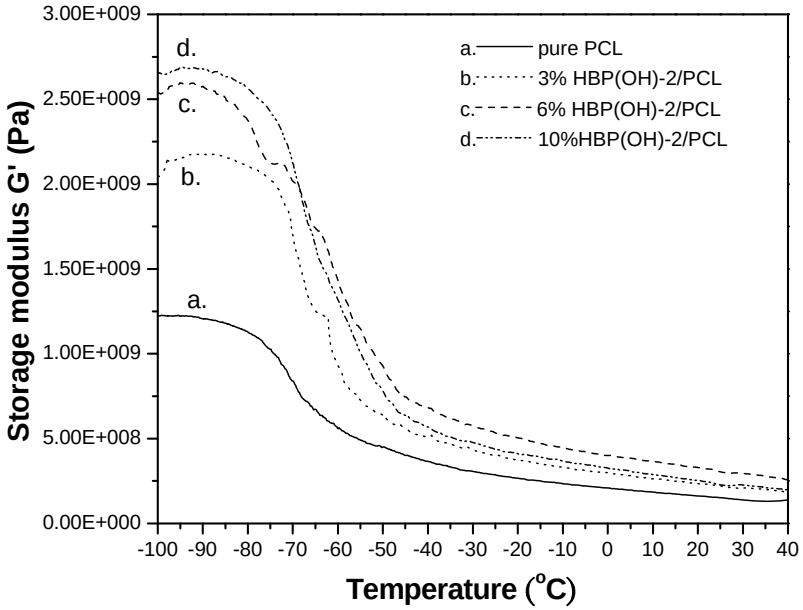

Figure 4.23 Storage modulus G' vs temperature curves of pure PCL and HBP(OH)-2 modified PCL composites

4.3.4 Scanning Electron Microscopy (SEM)

4.3.4.1 SEM of HBP(COOH) modified PCL nanocomposites

Figure 4.24 shows FE-SEM images of the fracture surface of the samples containing different amounts of HBP(COOH)-3. The surface of neat PCL is microscopically flat, indicating the brittle failure of PCL under tensile loading. The tensile fractured surface of 3 wt. % HBP(COOH)-3 modified PCL composite reveals considerable ductile tearing and surface roughness. The increased surface area of fractured surface of the blend suggests that the crack paths are highly splitted, and the crack propagation absorbs

considerable strain energy before failure. This is an indication of an effective adhesion arisen from the effect of intermolecular attractions between the filler end groups and the PCL matrix. The in-situ cross-linking of HBP(COOH)-3 (3~6wt. %) in the PCL matrix dramatically changes its surface characteristic after the tensile induced deformation. As the amount of HBP(COOH)-3 increases to 10wt. %, the fractured surface reveals a less homogeneous morphology, which contains fused particles and absence of ductile tearing. As the weight percentage of HBP(COOH)-3 further increases to 20 wt. %, separate phase domains are distinguishable. The surfaces become increasingly rough, with more threads found between the PCL domains, inducing a weak-toughening effect. The occurrence of phase separation may account for the fact that the HBP molecules can strongly interact with each other. Through this debonding process, the PCL matrix can deform more easily to realize a toughening effect.

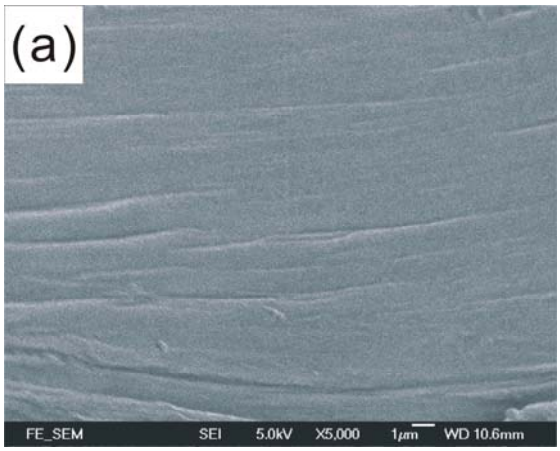

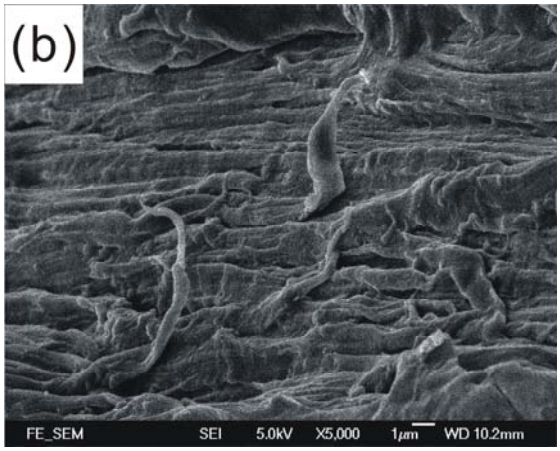

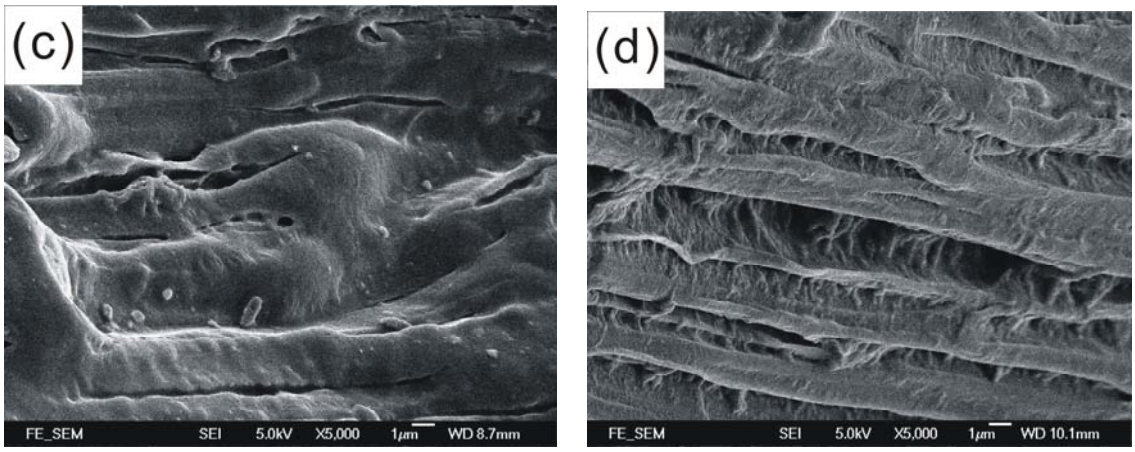

Figure 4.24 FE-SEM images of the fracture surface of PCL composite samples with different weight ratios of HBP(COOH)-3 and PCL: (a) 100/0; (b) 97/3; (c) 90/10; (d) 80/20 (The magnifications are ×5000)

The fractured surface of 6 wt. % HBP(COOH)-4 modified PCL composite after the tensile test reveals considerable ductile tearing and surface roughness. As shown in **Figure 4.25**, the thread-like structure of the fractured surface suggests that there is no distinct phase separation. The interfacial interactions between HBP(COOH)-4 and PCL is believed to play an important role in the toughening mechanism. As the weight percentage of HBP(COOH)-4 increases to 10 wt. %, the fractured surface of the blendexhibits some signatures of phase separation and less homogeneous. The poor homogeneous surface implies a non-uniform dispersion of HBP(COOH)-4 particles in the PCL matrix. On the other hand, with 20 wt. % HBP(COOH)-4, the fractured surface becomes less ductile, leading to lower strain energy release rate.

From SEM micrographs, it is found that good miscibility can be realized in both HBP(COOH)-3/PCL and HBP(COOH)-4/PCL blends. This is an indication of strong interactions between HBP and the polymer matrix, leading to better mechanical properties. When the weight percentage of HBP(COOH) increases to 20 wt. %, the mutual interactions between the HBP molecules become dominate, thus resulting in phase separation in the blend. This phenomenon is no good for toughening.

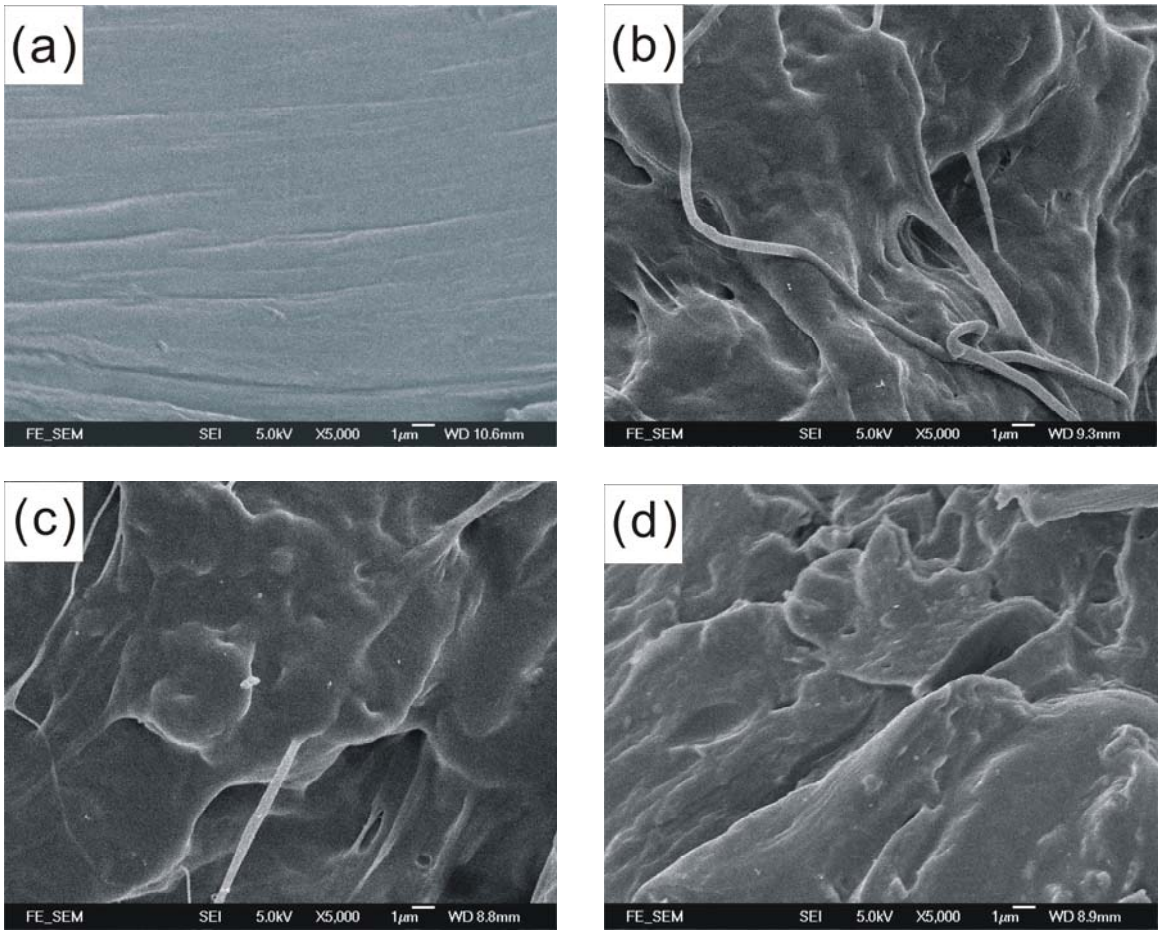

Figure 4.25 FE-SEM images of the fracture surface of PCL composites with different weight ratios of HBP(COOH)-4 and PCL: (a) 100/0; (b) 94/6; (c) 90/10; (d) 80/20 (The magnifications are ×5000)

4.3.4.2 SEM of HBP(OH) modified PCL nanocomposites

Figure 4.26 shows FE-SEM images of the fracture surface of the HBP(OH)-1/PCL samples. The occurrence of plastic deformation was present in the fractured surface of the samples containing 3 and 6 wt. % HBP(MPA)-1, revealing a elongated fibrillar morphology. In comparison with the non-modified, exposed fibrous structure for discrete phase of the blend is observed, which would interfere with the crack propagation occurred through the fiber matrix interface. In this case, the bonding between the fiber and the polymer matrix reflects the delamination occurred through the fiber interface. As the weight percentage of HBP(OH)-1 increases to 10 wt. %, a co-continuous structure is observed. No fiber laminate structures are seen. The formation of this co-continuous structure is possibly attributed to the hyperbranched cluster coalescence within the PCL matrix. The smooth-like topography of the cross-sectional surface resembles to the material with low ductility, but not to the same extent as the unmodified PCL. Of a 10 wt. % blend, the fractured surface becomes less ductile and results in lower strength of the matrix, contributing to lower strain energy release rate. However, the crack propagation occurred along the fiber-matrix interface in the composites with 3 and 6 wt. % HBP(OH)-1. This reveals the higher resistance and high-energy release rate caused by ductile tearing of the PCL matrix at the interface. The increased strength of modified PCL composite contributes to a significant increase in fracture toughness at a

controlled filler range from 3 to 6% of HBP(OH)-1.

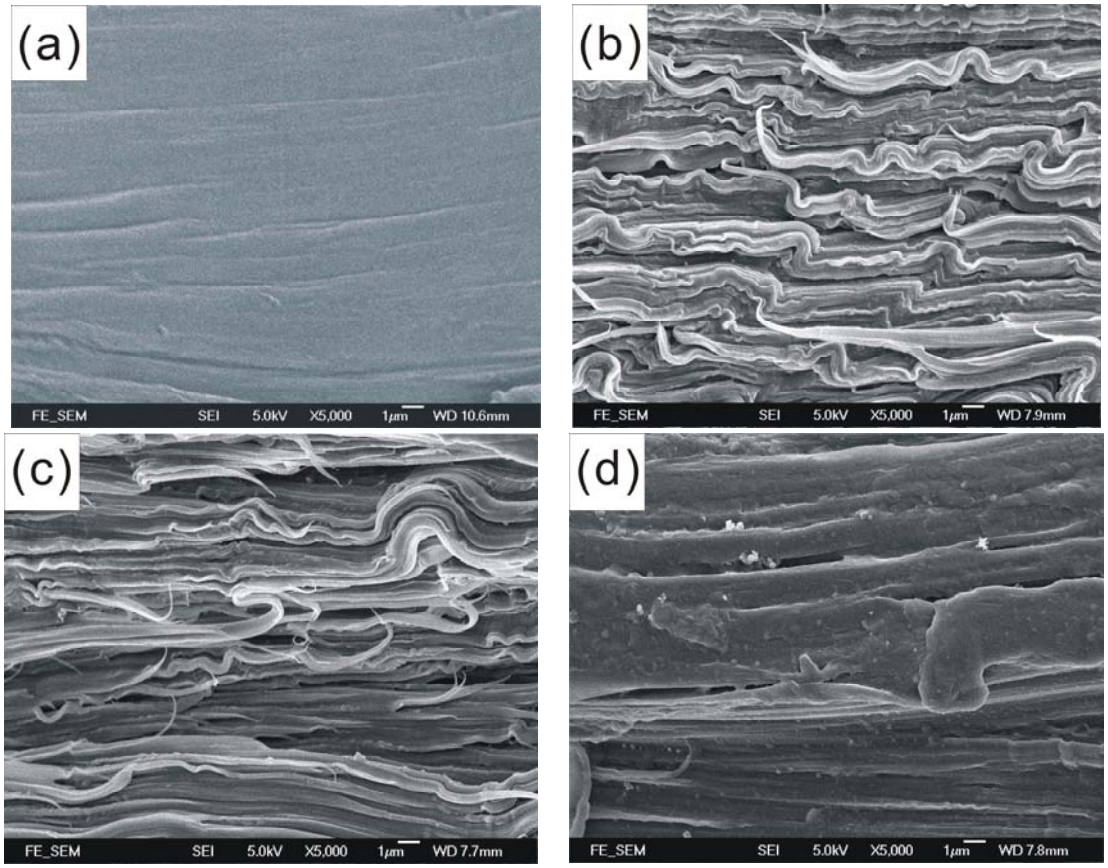

Figure 4.26 FE-SEM image of the fracture surface of PCL composites with different ratios of HBP(OH)-1 and PCL: (a) 100/0; (b) 97/3; (c) 94/6, and (d) 90/10 (The magnifications are ×5000)

It is found from the SEM micrographs that good miscibility can be realized between HBP and PCL. This is an indication of strong interaction between HBP(OH) and the PCL matrix, leading to better mechanical properties. As the weight percentage of HBP(OH)-1 increases to 10 wt. %, the mutual interaction between HB(OH)-1 molecules

increases in the system, leading to phase separation. Toughening is thus unsuccessful.

4.3.5 Transmission electron microscopy (TEM)

TEM examination was carried out to further evaluate the morphology and dispersion of the hyperbranched polymer clusters in the PCL matrix. The ultramicrotoned samples of the modified PCL blends were stained with 2 wt. % uranyl acetate solutions for 10 min. before the TEM observation.

4.3.5.1 TEM of HBP(COOH) modified PCL nanocomposites

Under TEM, the HBP clusters appeared as discrete agglomerations can be distinguished from the dark region due to the specific staining with uranium acetate. As illustrated in **Figure 4.27(a),** HBP(COOH)-3 clusters in diameter between 10 and 30 nm are observed and they exhibit in spherical-like domains in the PCL matrix. Similarly, as illustrated in **Figure 4.27(b)**, HBP(COOH)-4 clusters in diameter between 30 and 50 nm are also obtained and exhibit in spherical-like domains in the PCL matrix.

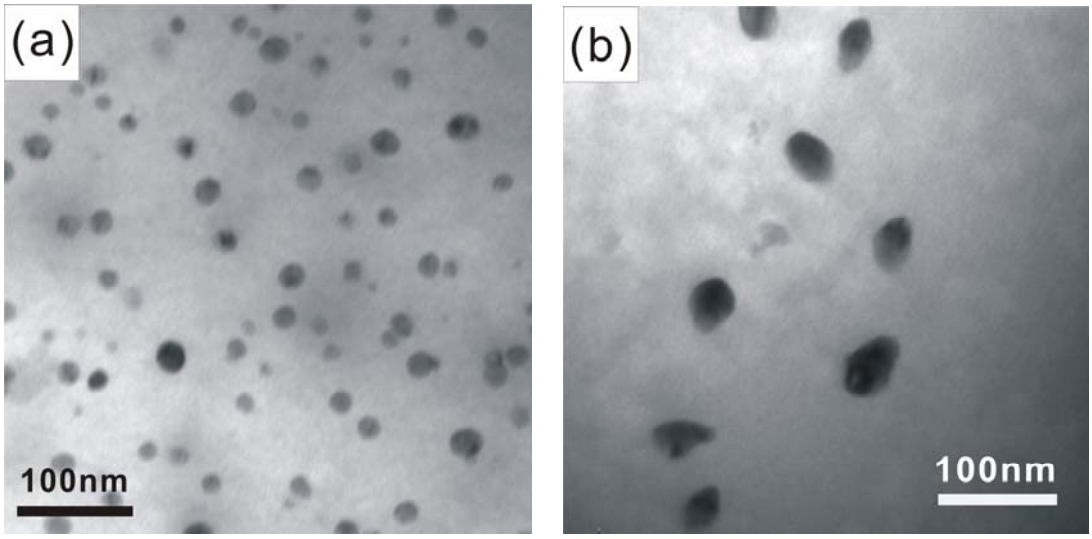

Figure 4.27 TEM micrographs of (a) 3 wt. % HBP(COOH)-3/PCL composite, (b) 6 wt. % HBP(COOH)-4/PCL composite

For both of the blends, the nanosize HBP clusters are well dispersed in the PCL matrix. It is believed that the nanoclusters formed play an important role in the toughening effect.

The morphology observed by SEM for different contents of HBP blended with the same ratio. The average minor-phase hyperbranched particle size in the PCL blends was given in TEM micrograph. The hyperbranched polymer exhibited spherical phase domains of PCL and weak interfacial adhesion, surrounded by the continuous PCL phase as shown in Figure 4.27. The SEM micrographs of HBP-PCL blends suggested that the minor-phase particle size of the dispersed phase decreased when hyperbranched compatibilizer concentration increased up to 20 wt/ %, and a co-continuous morphology when addition

of the amount of HBP was 3~6 wt. %. This change of morphology could effectively improve the mechanical properties of the HBP-PCL blends due to the decrease HBP particle size and the increase of compatibilization at the polymer/polymer interface. A further increase in hyperbranched polymer weight percentage did not decrease the size of dispersed particles, and indicated that wt. % compatibilizer was sufficient to occupy the interface between HBP and PCL As a result, an excess of compatibilizer remained in the bulk and did not contribute to the better interaction between HBP and PCL, which would not cause further improvement in HBP particle dispersion.

The change of the average minor-phase hyperbranched polymer particle weight percentage was in accordance with the compatibility of PCL blends. The mixing thermodynamics and the kinetics controlled the decrease in the average minor-phase particle size, in which the miscibility was increasing, The compatibility property can be induced by the third component that interacted physically with both phases or had specific interaction with one phase and physical contact with the other. The SEM micrographs demonstrated that the addition of the compatibilizer (3~6 wt. % HBP) suppress particle coalescence, and was in accordance with the mechanical and rheological result, suggesting the formation of an interfacial compatibilizer.

4.3.5.2 TEM of HBP(OH) modified PCL nanocomposites

As illustrated in **Figure 4.28**, HBP(OH)-1 clusters in diameter between 300 and 450 nm are observed and they exhibit in spherical-like domains in the PCL matrix. The darker region appears as discrete agglomerations. This can be attributed to the limit miscibility and inhomogeneous mixing between HBP-OH and PCL. The presence of strong intermolecular hydrogen bonding within the hyperbranched polymers arises from the high peripheral hydroxyl functional end groups.

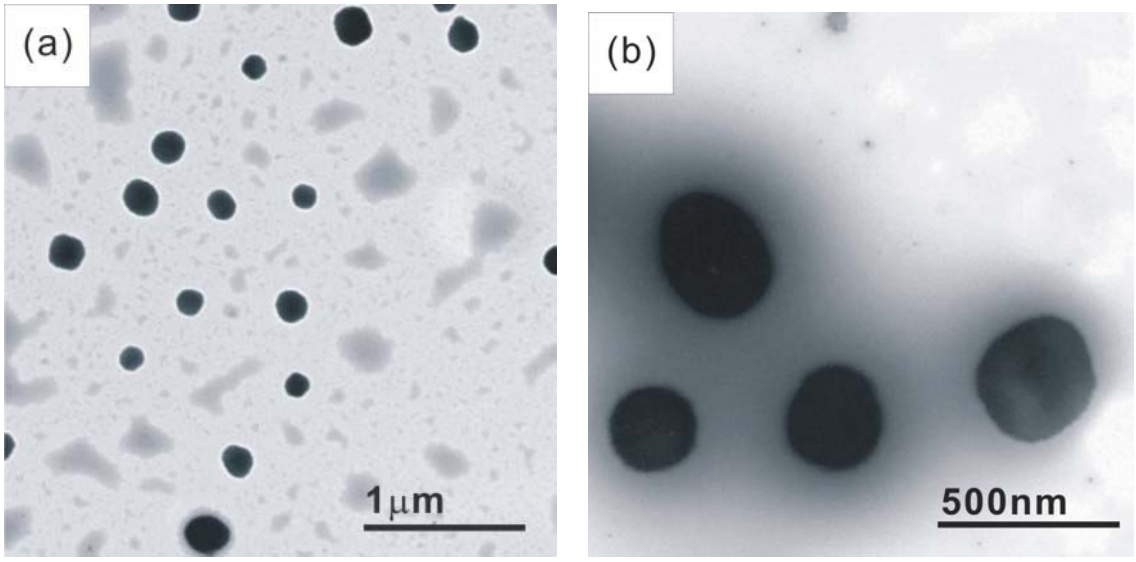

Figure 4.28 TEM micrographs of 6 wt % HBP(OH)-1 modified PCL sample

In the blends, the HBP molecules aggregate to form sub-micron scale clusters. The presence of the clusters is believed to be beneficial to the polymer modification.

4.3.6 Degradation study

4.3.6.1 Biodegradability of HBP(COOH)

Table 10 shows the degradation data for HBP(COOH)-3 and HBP(COOH)-4. In PBS solution, the measured molecular weight of HBP(COOH)-3 decreases from 16354 to 7265, while the molecular weight of HBP(COOH)-4 changes from 45279 to 6568. Similarly, in an alkaline medium (NaOH solution), the molecular weight of the hyperbranched polymers decreases significantly. The test proves that both the acid hyperbranched polymers are biodegradable.

Table 10 The degradation data of HBP(COOH)-3 and HBP(COOH)-4

	Solution	samples	Before degradation	After degradation
Molecular weight(Mw)	PBS solution	HBP(COOH)-3	16354	7265
		HBP(COOH)-4	45279	5957
	NaOH solution	HBP(COOH)-3	16354	6568
		HBP(COOH)-4	45279	3403

4.3.6.2 Biodegradability of HBP(COOH)/PCL composites

The composite samples before and after the degradation test are shown in **Figure 4.29**. The sample after the treatment still maintains in original shape but exhibits higher opacity and thinner.

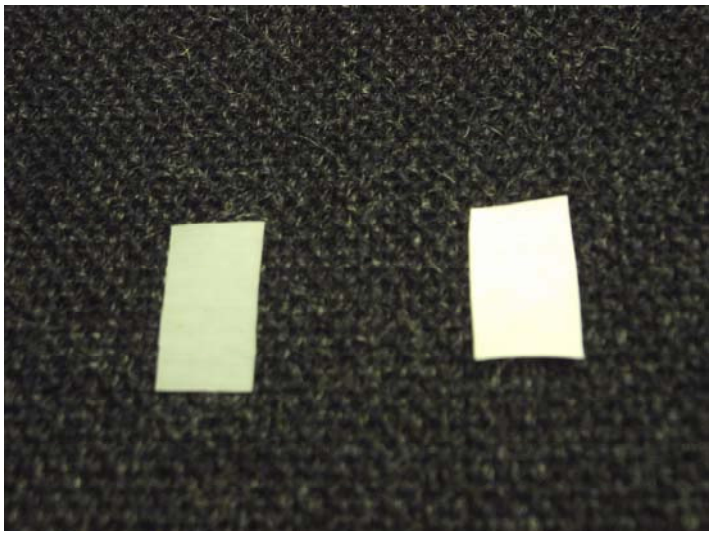

Figure 4.29 Photographs of a HBP/PCL composite sheet (left) before and (right) after the degradation test

The degradation test results of HBP(COOH)-3/PCL specimens in two different media are demonstrated in **Figures 4.30** and **4.31** and **Table 11**. It can be seen that the samples in both PBS and NaOH solutions degrade to lower molecular mass compounds. The more the amount of the HBP added, the higher the drop of the molecular mass. It indicates that the addition of HBP(COOH)-3 into PCL accelerates the degradation process significantly.

The degradation test results of HBP(COOH)-4/PCL specimens in two types of solutions are given in **Figures 4.32** and **4.33** and **Table 11**. In general, the composite specimens degrade smoothly to lower molecular mass compounds. The addition of HBP(COOH)-4 to PCL accelerates the degradation process significantly. The PCL blends in NaOH

exhibit slightly higher weight loss than in the phosphate solution. The overall degradation rate in NaOH is higher.

In terms of degradation rate, there is no definite difference between the blends with HBP(COOH)-3/PCL and HBP(COOH)-4/PCL in PBS buffer, indicating their similar degradation behaviors in a neutral medium. However, in an alkaline environment (0.01M NaOH solution, pH=12), it is found that the one with higher molecular mass HBP(COOH) (HBP(COOH)-4) degrades faster.

When the content of HBP(COOH) increases in the blend, the amorphous content will increase accordingly, which may account for the higher degradation rate observed. Another factor affecting the rate may refer to the H^+ ions released from HBP(COOH). The release of H^+ from the acid surface groups of HBP(COOH) could lead to a drop in pH that catalyzes the hydrolysis reaction[305].

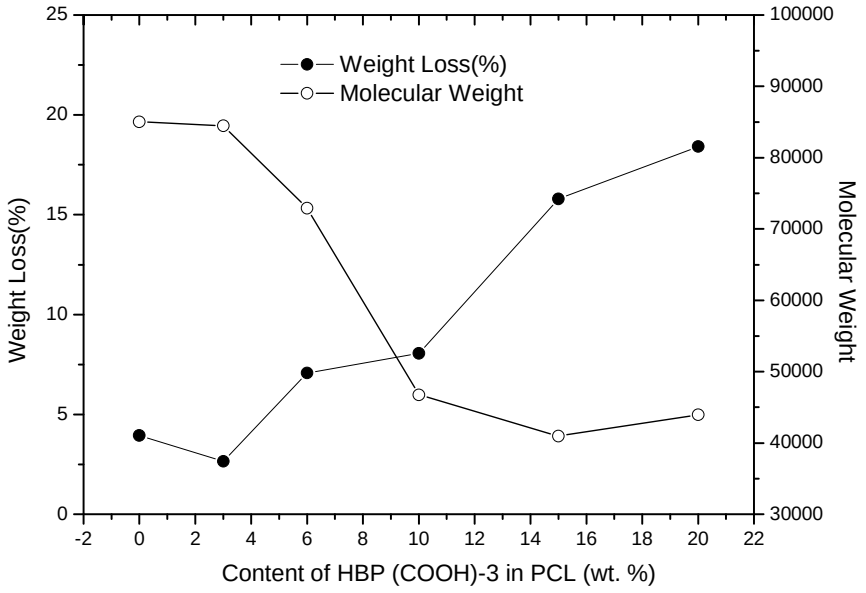

Figure 4.30 Weight loss and molecular weight of the blend vs. wt. % of HBP(COOH)-3 in PCL treated with PBS solution after the test

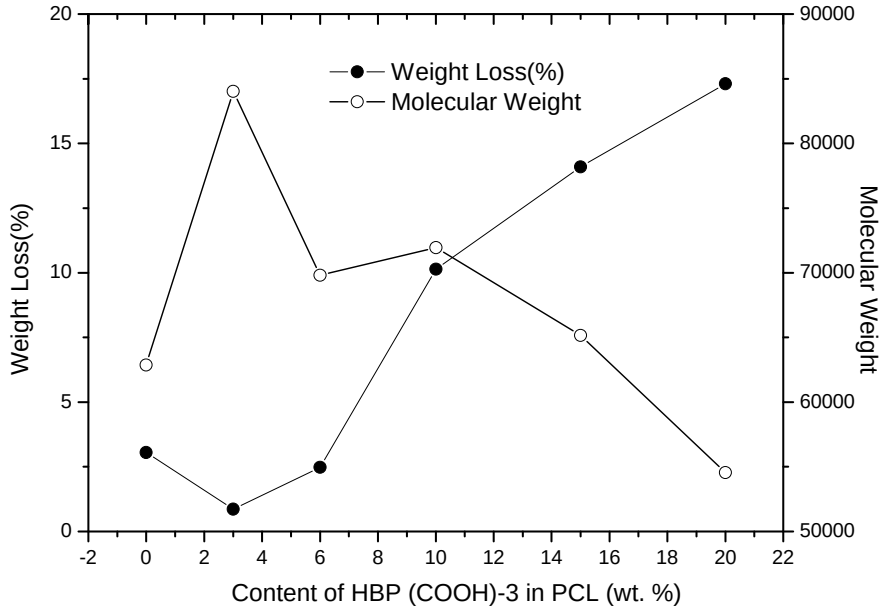

Figure 4.31 Weight loss and molecular weight of the blend vs. wt. % of HBP(COOH)-3 in PCL treated with 0.01M NaOH after the test

Table 11 The degradation data of HBP(COOH)-3/PCL and HBP(COOH)-4/PCL composites

Degradation solution		Samples	0%HBP	3%HBP	6%HBP	10%HBP	15%HBP	20%HBP
PBS solution	Weight loss (%)	HBP(COOH)-3/PCL	3.95	2.65	7.08	8.06	15.79	18.42
		HBP(COOH)-4/PCL	3.95	4.19	6.02	9.21	13.93	17.88
	Molecular weight(Mw)	HBP(COOH)-3/PCL	85014	84487	72924	46755	40962	43952
		HBP(COOH)-4/PCL	85014	53622	48767	53622	49201	42412
NaOH solution	Weight loss (%)	HBP(COOH)-3/PCL	3.05	0.87	2.48	10.14	14.09	17.30
		HBP(COOH)-4/PCL	3.05	5.73	8.28	10.23	14.29	18.95
	Molecular weight(Mw)	HBP(COOH)-3/PCL	62861	84027	69820	71936	65162	54561
		HBP(COOH)-4/PCL	62861	57475	65848	70657	80507	51948

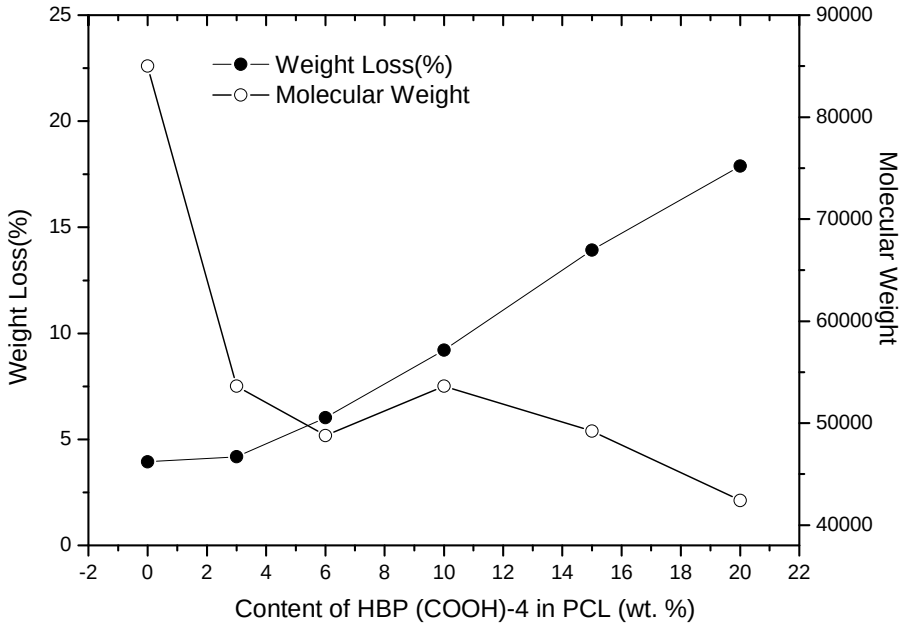

Figure 4.32 Weight loss and molecular weight of the blend vs. wt. % of HBP(COOH)-4 in PCL treated with PBS solution after the test

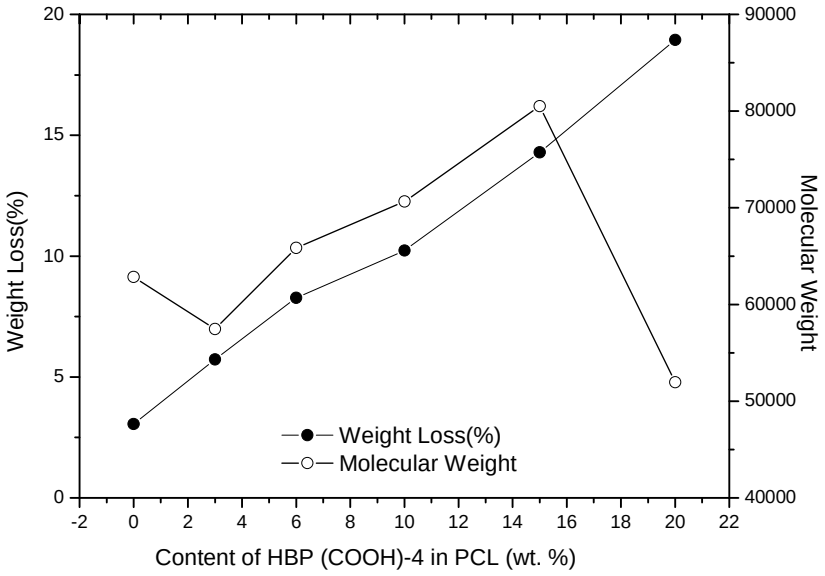

Figure 4.33 Weight loss and molecular weight of the blend vs. wt. % of HBP(COOH)-4 in PCL treated with 0.01M NaOH after the test

4.3.6.3 Biodegradability of HBP(OH)

As shown in **Table 12**, HBP(OH)-1 naturally degrades in PBS solution from 906 to 300. In NaOH, its molecular weight changes from 906 to 250.

Table 12 The degradation data of HBP(OH)-1

	Solution	Samples	Before degradation	After degradation
Molecular weight(Mw)	PBS solution	HBP(OH)-1	906	300
	NaOH solution	HBP(OH)-1	906	205

4.3.6.4 Biodegradability of HBP(OH)-1/PCL composites

The biodegradability test results of HBP(OH)-1/PCL composite are summarized in **Figures 4.34** and **4.35**. It is found that the samples in both the solutions degrade spontaneously to lower molecular mass compounds. The more the amount of the HBP added, the higher the reduction of the molecular mass. It indicates that the addition of HBP(OH)-1 to PCL does accelerate the degradation process. Besides, the degradation rate of the blend is also faster in NaOH than in PBS buffer.

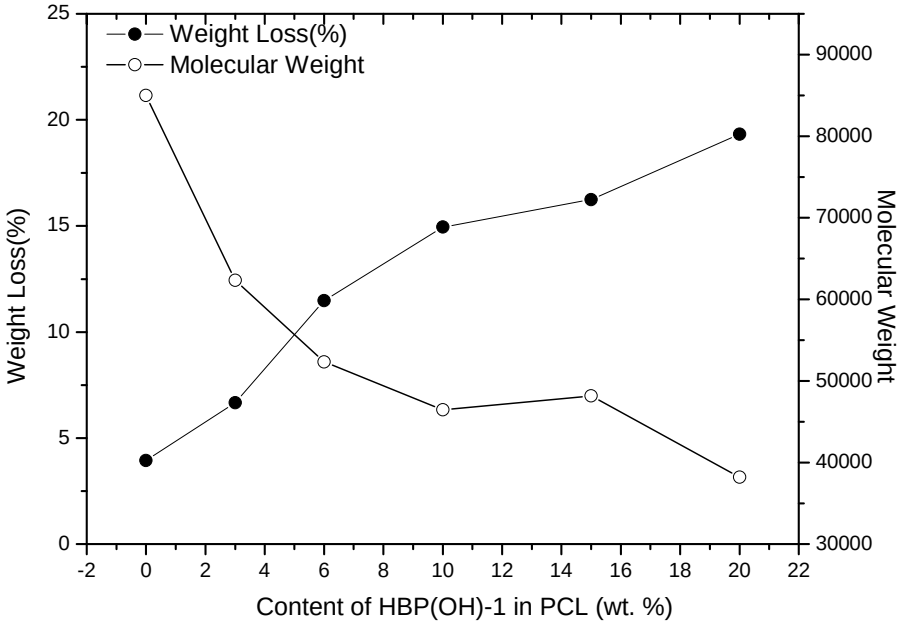

Figure 4.34 Weight loss and molecular weight of the blend vs. wt. % of HBP(OH)-1 in PCL treated with PBS solution after the test

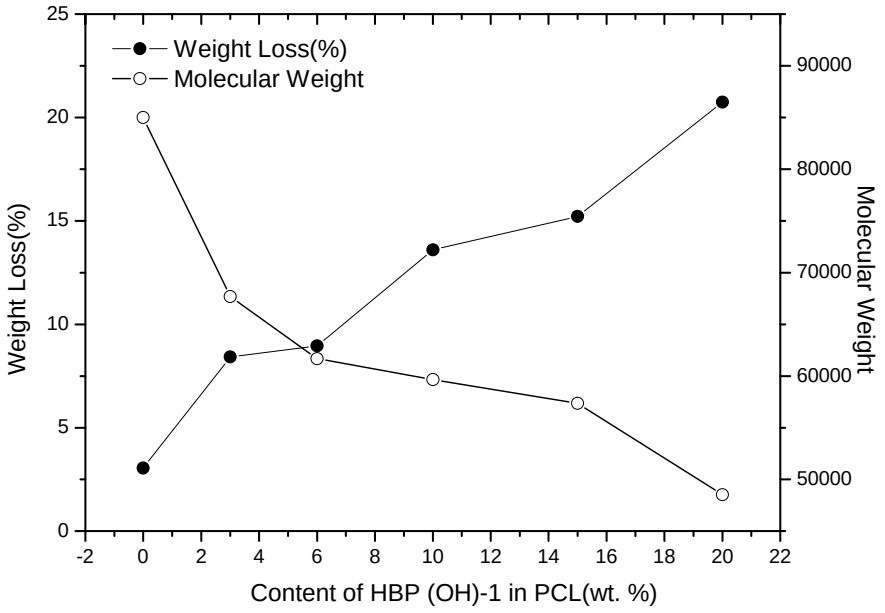

Figure 4.35 Weight loss and molecular weight of the blend vs. wt. % of HBP(OH)-1 in PCL treated with 0.01M NaOH solution after the test

4.4 Conclusion

Advanced biodegradable composite blends were prepared by solvent casting of PCL with biodegradable HBP(COOH) or HBP(OH). The incorporated modifiers have been comprehensively investigated with respect to their effects on physical, mechanical, thermal, and morphological properties of the end products [306-308].

Mechanical properties of PCL can successfully be improved by adding small amounts of HBP(COOH)-3, HBP(COOH)-4, or HBP(OH)-1. It is found that the HBPs are able to improve flexibility of the PCL matrix with a decrease in brittleness of the polymeric

blends. Optimal weight percentages of the fillers (HBP(COOH)-3: 3 wt. %; HBP(COOH)-4: 6 wt. %; HBP(OH)-1: 6 wt. %) can effectively enhance decrease in brittleness of PCL. SEM micrographs show that the addition of HBPs results in an increase in surface roughness and elongated fibrils as well as better interfacial adhesion between PCL and the fillers. A debonding-initiated shear yielding mechanism is probably involved in the toughening of the composite materials. It is found that good miscibility can be realized in the blends when the filler content is lower 10 wt. %. This is an indication of strong interactions between HBP and the polymer matrix, leading to better mechanical properties. When the filler percentage increases to 20 wt. %, the mutual interactions between the HBP molecules become dominate, thus resulting in phase separation in the blends. This phenomenon is no good for toughening.

Well-defined spherical HBP nanosized domains are found in the PCL matrix of the blends, as revealed by TEM investigation. The presence of the clusters in the blends is believed to be beneficial to the polymer modification. DSC and DMA studies reveal the existence of strong molecular interactions in the system. Both Xc and G' are sensitive to the content of the HBPs in the blends. The thermomechanical analysis can provide evidence that the increase in fracture decrease in brittleness was accompanied by an increase in strain energy release rate and loss modulus.

The incorporation of the organic fillers does affect the bio-stability of PCL, but the degree is subjected to factors such as concentration, type and molecular weight of the fillers, and degradation conditions. In general, higher molecular weight filler or higher filler content would likely induce an increase in biodegradable rate for the end materials. The degradation is faster in an alkaline medium than in a neutral environment. We have demonstrated that a better hydrophilicity makes the biodegradation to proceed faster.

Chapter 5: Fabrication and characterization of HBP-reinforced PLA composites

5.1 Introduction

Hyperbranched polymers (HBP) encompass highly branched nanostructures having high peripheral functional end groups[309]. They are synthesized by a one-step polycondensation reaction, producing molecules with a high degree of irregular branching and broad molecular weight distribution, and significantly lower viscosity compared with linear polymers of the same molecular weight[2]. They are polydisperse and can be prepared in a one-pot synthesis unlike dendrimers, making the former less expensive. The role of hyperbranched polymers is reported as branching agents, compatibilizers and tougheners for conventional biodegradable composite materials[1,83,310,311]. However, the unique physical properties and high peripheral functionalities of HBP offer a variety of pathways for polymer modification. HBP can play a role of novel building blocks for generating new nanostructures inside a polymer matrix ranging from core shell type to network morphologies.

In terms of thermal properties, HBPs are flexible polymers with low glass transition temperature (T_g often below room temperature) and the low melting temperature(T_m normally below 60^{o}C). Due to the high degree of branching, limited crystallization or

interchain entangling is possible. Consequently, this gives rise to poor mechanical properties but good solubility and reduced melt viscosity.[312]

Of the many biodegradable thermoplastics available, poly(L-lactic acid) (PLA) has been the most popular biodegradable plastics due to its high mechanical strength, which can be potentially applicable as structured materials.[313] The L-enantiomorph of PLA is a hard, transparent crystalline polymer. Brittleness may occur due to slow crystallization rate and cause strong reduction in toughness. Toughness in nanocomposites is significant to ensure the minimization in crack propagation. To overcome the brittleness of PLA, a large range of plasticizers has been used with some success. These include citrate esters,[165] glycerol,[166] poly(ethylene glycol),[167] glucose monoesters and fatty acids.[168] These small molecules can cause significant changes to the thermal and mechanical properties of PLA. However, due to the boiling temperatures of these plasticizers are similar or closed to the melting temperature of PLA, their concentrations could vary due to different degree of evaporation during processing. With long-term use of the composites, the plasticizers might result in leaching, which would eventually cause embrittlement. An alternative to plasticizers is the use of larger polymeric modifiers to perform the same functions. It is commonly practical to blend different polymers to alter their properties.

Although a great number of scientific publications have been contributed to the filed of biodegradable composites in the past decade, there is usually a lack of information on the potential use of such novel biocomposites using hyperbranched polymer as chemical modifier. The novel composite systems presented in this study are fully biodegradable. The use of HBP in PLA or other biodegradable polymer improved the stiffness of the nanocomposites. HBP also improved processing thermal conditions, by reducing the melting temperature. The use of HBP in PLA fibre as a hydrogen-bonding additive may produce favorable effects on the fracture toughness of the nanocomposites.

5.2 Experimental

5.2.1 Materials

PLA (M_n=100,000~110,000, GPC standard) was purchased from Hong Kong Henfen Chemical Co.

5.2.2 Fabrication of PLA composites

HBP(COOH)-1, HBP(COOH)-3, HBP(COOH)-4, HBP(OH)-1 and HBP(OH)-2 were used to blend with PLA to form composite materials in the study. Hyperbranched polymer in the amounts of 3% (0.15g), 6% (0.3g), or 10% (0.5g), 15 %(0.75g) and 20

% (1g) with respect to same PLA content (dry weight = 5g) were added to the THF solvent (150 mL) during its preparation. After complete solvent evaporation, the resultant sheet of composite in dry weight was determined before DSC analysis. Blends of hyperbranched polymers with PLA were co-mixed in THF well prior to forming composite sheets. The sheets were casted on TEFLON molds and the solvent was allowed to evaporate at 60 °C. The films were further dried in vacuum at room temperature for two days. The resultant sheets were peeled off from the casting surface.

5.2.3 Tensile tests

Tensile tests were performed on a screw-driven universal testing machine (Instron 4411, Canton, MA) equipped with a 10 kN electronic load cell and mechanical grips. The tests were conducted at room temperature using a crosshead rate of 1 mm/min. All tests were carried out according to the ASTM standard, and the data reported were the mean and standard deviation from four determinations.

5.2.4 Differential Scanning Calorimetry (DSC)

The effect of HBPs on crystallinity behaviour of the bulk polymers was investigated by DSC analysis. The experiments were performed on a Perkin Elmer Instruments

Diamond DSC series under constant nitrogen flow (20 ml/min). The following thermal cycle was used:

(1) Heat from0.00 ^{o}C to 120.00 ^{o}C at 10.00 ^{o}C/min ; 2)Hold for 5.0 min at 120.00 ^{o}C 3) Cool from 120.00 ^{o}C to 0.00 ^{o}C at 10.00 ^{o}C /min ; 4) Hold for 1.0 min at 0.00 ^{o}C. 5) Heat from 0.00 ^{o}C to 180.00 ^{o}C at 5.00 ^{o}C /min. 6) Hold for 5.0 min at 180.00 ^{o}C 7)Cool from 180.00 ^{o}C to 0.00 ^{o}C at 5.00 ^{o}C /min 8)Hold for 1.0 min at 0.00 ^{o}C. The samples were weighed such that all of the samples had an identical PLA content. The sample weight was maintained at low levels (5-7mg) for all measurements in order to minimize any possible thermal lag during the scans. The machine calibration and background subtraction were done according to the Perkin Elmer instrument protocols. The results of the DSC thermograms were used from the data in second heating-cooling cycle.

5.2.5 Dynamic Mechanical Analysis (DMA)

DMA experiments were performed on a Perkin Elmer Diamond DMA Lab system equipped with a film tension clamp. The instrument was programmed to measure G' (storage modulus) over the range of -60^{o}C to 80^{o}C at 3^{o}C /min heating rate and 1 Hz constant frequency. Calibrations for force, mass, position and temperature were made in accordance with Perkin Elmer procedures. The specimen sheets were cut with

dimensions W x H x L = 5 x 0.22 x 15 mm) and mounted on a dual-cantilever geometry in order to guarantee uniform strain on the sheet under tension. The applied strain (0.02% - 0.05 %) was well within the linear viscoelastic region of the samples and the collected data were reproducible. Storage modulus (G'), and tan δ were recorded as a function of temperature.

5.2.6 Scanning Electron Microscopy (SEM)

(Detail procedure refer to **Chapter 4.2.6**)

5.2.7 Transmission electron microscopy (TEM)

(Detail procedure refer to **Chapter 4.2.7**)

5.2.8 Degradation

(Detail procedure refer to **Chapter 4.2.8**)

5.3 Results and discussion

5.3.1 Fabrication of PLA composite specimens

Figure 5.1 illustrates a sample film obtained by solvent blending HBP(COOH) with PLA. All the films prepared from this method possessed smooth and homogeneous

texture.

Figure 5.1 A sample of a HBP(COOH)/PLA composite

5.3.2 Mechanical properties

5.3.2.1 Tensile test of HBP(COOH)-reinforced PLA nanocomposites

Stress-strain dependence of HBP(COOH)-1-blended PLA nanocomposite specimens is shown in **Figure 5.2**. It can be seen that all the composite samples are less toughened than that in pure PLA.

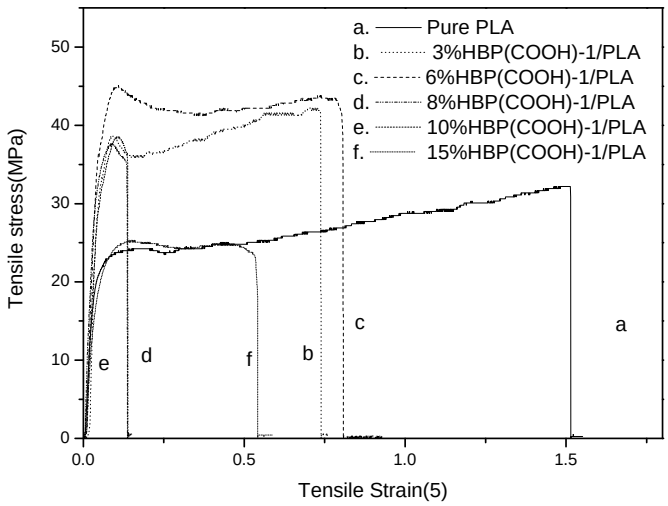

Figure 5.2 Tensile stress-strain curves of the PLA composite with different HBP(COOH)-1 contents

Stress-strain dependence of HBP(COOH)-3 modified PLA nanocomposites is shown in **Figure 5.3**. The samples with weight ratios from 3 wt. % to 15 wt. % HBP(COOH)-3 exhibits better tensile strength than does pure PLA. Among those samples, 6 wt. % HBP(COOH)-3 gives the maximum tensile strength. However, for the samples with filler content of 20 wt. %, the tensile strength was weaker than that of pure PLA. In **Figure 5.4**, the average values of tensile stress and elongation at break of the samples with various filler ratios are presented. It is found that 6 wt. % HBP(COOH)-3/PLA presents an ideal strain at break for the material, which is increased by 90.3% compared to pure PLA.

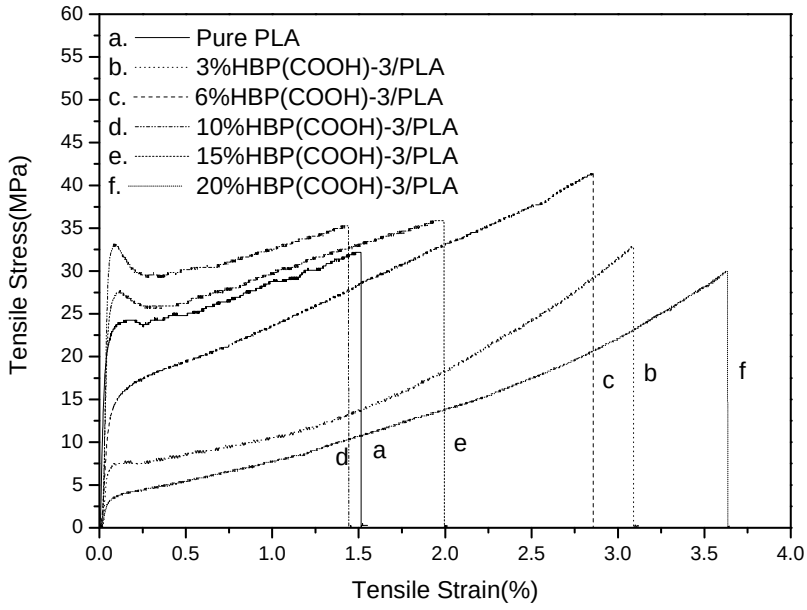

Figure 5.3 Tensile stress-strain curves of the PLA composite with various HBP(COOH)-3 contents

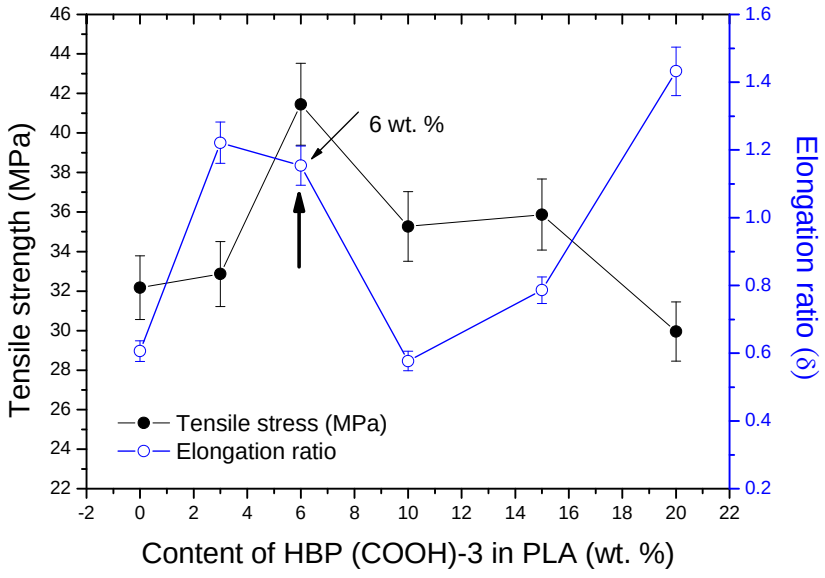

Figure 5.4 Mechanical properties of PLA with various HBP(COOH)-3 concentrations

Stress-strain dependence of HBP(COOH)-4 modified PLA nanocomposites is given in **Figure 5.5**. Their average values of tensile stress and elongation at break are presented in **Figure 5.6**. It can be seen that the weight ratios of 3 wt. %, 6 wt. %, and 10 wt. % exhibit better tensile strength results. Among those samples, 3 wt. % HBP(COOH)-4 gives the maximum tensile strength. However, further increasing filler content to 15~20 wt. % results in a decrease of tensile strength. On the other hand, the sample with 3% of HBP(COOH)-4 presents the best elongation at break, which is increased by 35.0% compared to pure PLA.

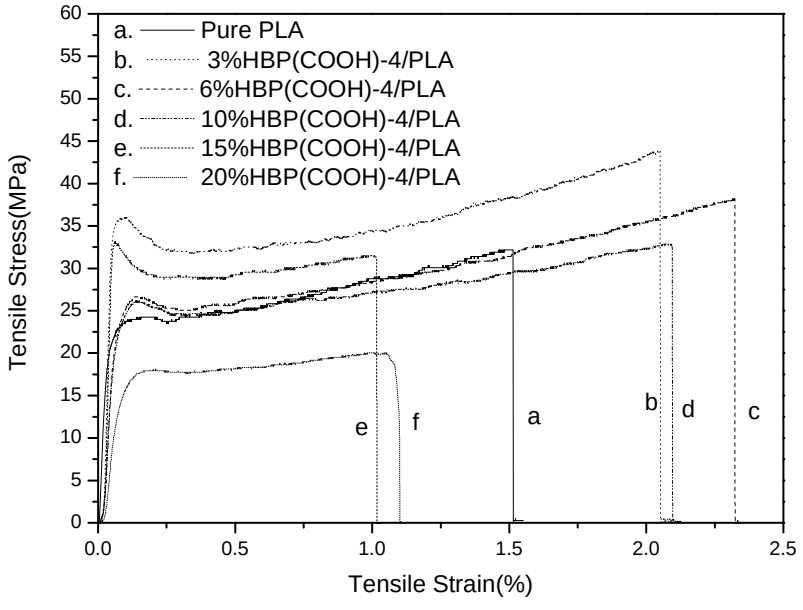

Figure 5.5 Tensile stress-strain curves of the PLA composite with different HBP(COOH)-4 contents

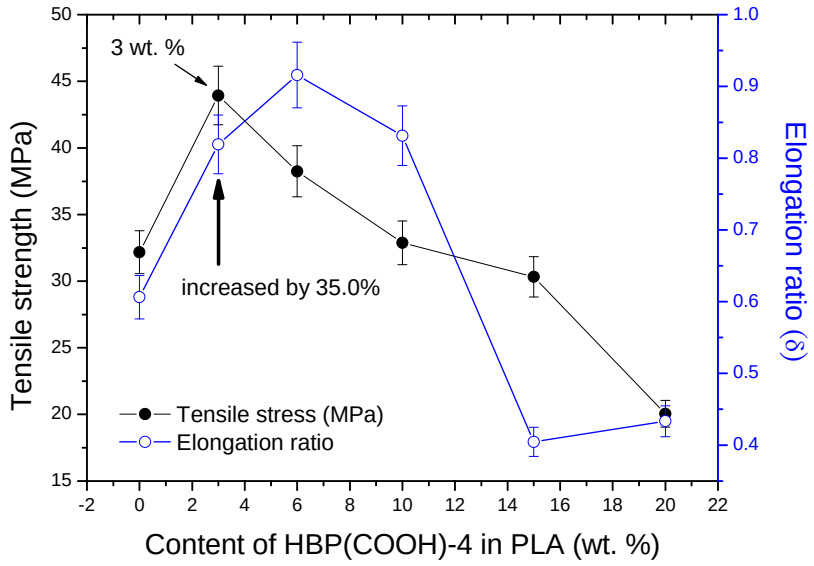

Figure 5.6 Mechanical properties of PLA with various HBP(COOH)-4 concentrations

It seems that the tensile stress-strain behaviour depends on two factors. One is the filler content, and another is the molecular weight of HBP. For samples with low molecular weight HBP(COOH), relatively poor mechanical properties are always resulted. For those with medium molecular weight HBP(COOH) at an optimum level, better properties can be realized. For example, introduction of 6 wt. % HBP(COOH) can improve the mechanical properties of PLA significantly. For the high molecular weight specimens, the best toughness results can be obtained at filler content of ~3 wt. %. High molecular weight HBA(COOH) is also found to be the best toughness modifier in this system among the others.

5.3.2.2 Tensile test of HBP(OH) modified PLA nanocomposites

Stress-strain dependence of HBP(OH)-1-blended PLA nanocomposite specimens is shown in **Figure 5.7**. It can be seen that all the composite samples are weaker than pure PLA.

Stress-strain dependence of HBP(OH)-2-blended PLA nanocomposite specimens is shown in **Figure 5.8**. It can be seen that all the composite samples are weaker than pure PLA.

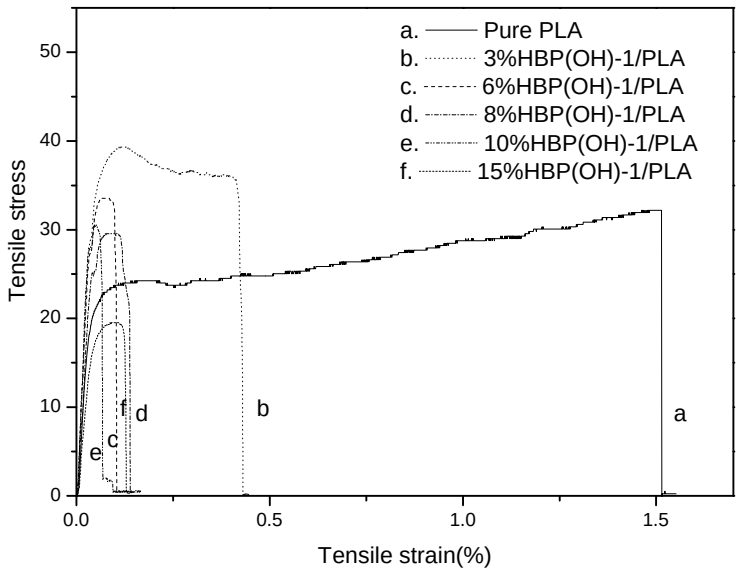

Figure 5.7 Tensile stress-strain curves of the PLA composite with different HBP(OH)-1 contents

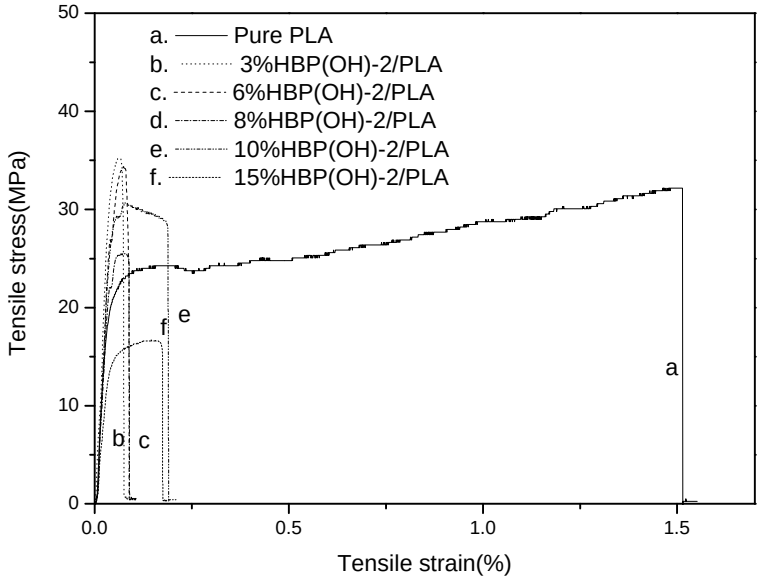

Figure 5.8 Tensile stress-strain curves of the PLA composite with different HBP(OH)-2 contents

5.3.3 Thermal and thermomechanical studies

5.3.3.1 Differential Scanning Calorimetry (DSC)

DSC was used to determine nonisothermal crystallization behavior of the blends. The useful parameters corresponding to their crystallization behaviors can be obtained from the curves as well as using the following formula:

$$X_c(\%) = \frac{\Delta H_m}{\Delta H_{100}} \times 100$$

Where X_c is the degree of crystallinity, ΔH_m is the heat of fusion of the sample, and $\Delta H_{100,m}$ is the heat of fusion for a 100%crystalline PLA, which is taken as 96 J/g.

Figures 5.9 and 5.10 show the DSC cooling curves of the samples. The T_m、ΔH_m、and X_c values of HBP(COOH)/PCL composites are summarized in **tables 13, 14.**

It can be observed from **Table 13** that T_m decreases 3~5 ^oC as the content of HBP(COOH)-3 increases from 3 to 20 wt. %. Compared to pure PLA, the degree of crystallinity of the 3 wt. % HBP(COOH)-3 sample reduces by about 79.5 %. However, the Xc value is enhanced as the content of HBP(COOH)-3 increases. When the weight percentage of HBP(COOH)-3 reaches 20 wt. %, the degree of crystallinity (Xc) was about 78.9% percent of that in pure PLA

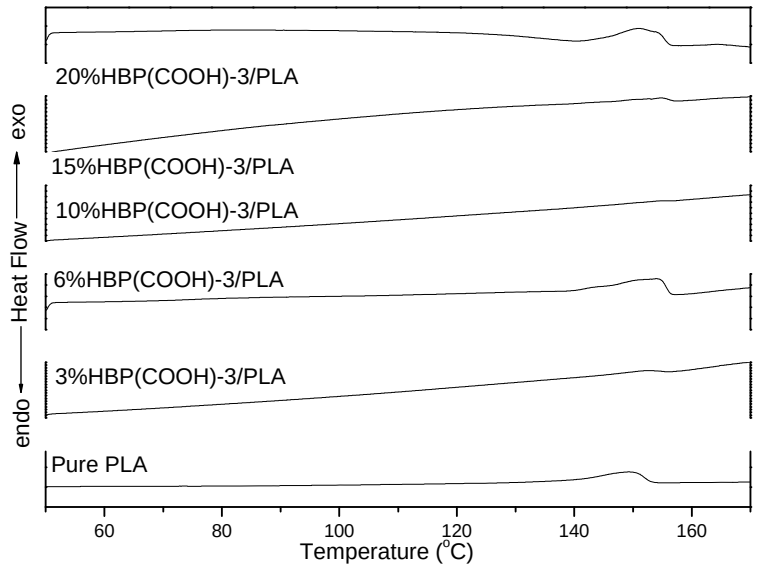

Figure 5.9 DSC thermograms for pure PLA and HBP(COOH)-3 modified composites

Table 13 DSC data of HBP(COOH)-3/PLA blend

HBP(COOH)3/PLA	0%HBP	3%HBP	6%HBP	10%HBP	15%HBP	20%HBP
Tm (^{o}C)	149.18	143.38	145.76	143.62	143.87	146.05
ΔH_m(J/g)	24.9765	5.1224	5.9796	10.0127	10.5154	19.7055
X_c(%)	26.02	5.34	6.23	10.43	10.95	20.53

It can be observed from **Table 14** that T_m decreases 1~3 ^{o}C as the content of HBP(COOH)-4 increases from 3 to 20 wt. %. Compared to pure PLA, the degree of crystallinity of the 3~6 wt. % HBP(COOH)-4 sample reduces by about 61.4 %. However, the Xc value is enhanced as the content of HBP(COOH)-4 increases. When the weight percentage of HBP(COOH)-4 reaches 20 wt. %, the degree of crystallinity (Xc) was about 73.6% percent of that in pure PLA.

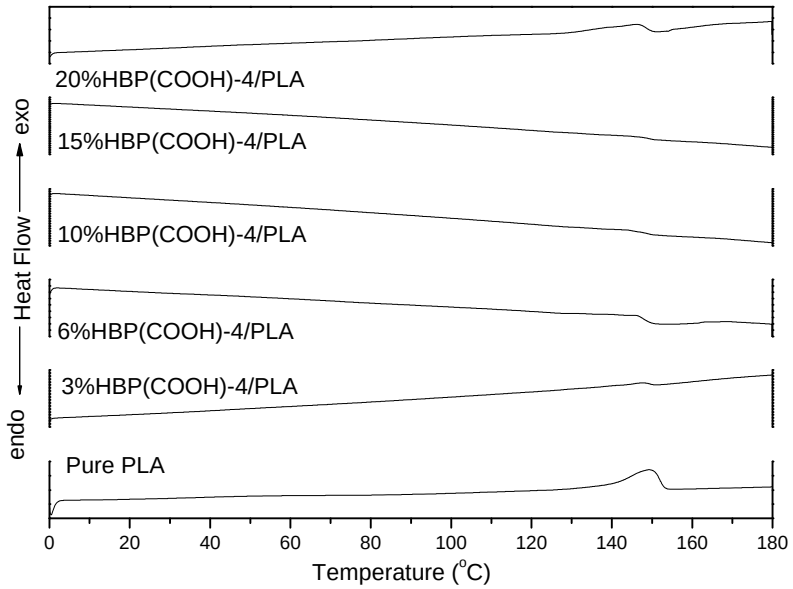

Figure 5.10 DSC thermograms for pure PLA and HBP(COOH)-4 modified composites

Table 14 DSC data of HBP(COOH)-4/PLA blends

HBP(COOH)4/PLA	0%HBP	3%HBP	6%HBP	10%HBP	15%HBP	20%HBP
Tm (^{o}C)	149.18	147.53	147.69	147.06	149.64	143.70
ΔH_m(J/g)	24.9765	10.9759	9.6497	11.875	18.3358	18.3900
X_c(%)	26.02	11.43	10.05	12.37	19.10	19.16

As illustrated from the DSC data, there is no change in crystalline phase when HBP(COOH) is incorporated, however, there is a dramatic change in Xc. When small

amount of HBP(COOH) (3~6 wt. %) is introduced, particularly HBP(COOH)-3 and HBP(COOH)-4, the Xc value was reduced. As the content of HBP(COOH) further increases in the blend, the Xc value likely rebounds back to the original level. It can be seen that only a small percentage of HBP(COOH) is able to interfere with the crystallization behavior, resulting in improvement of brittleness of the blends. However, an excess amount of HBP(COOH) may cause heterogeneous mixing, thus leading to deterioration in mechanical properties.

5.3.3.2 Dynamic Mechanical Analysis (DMA)

DMA for pure PLA and the modified PLA blends were conducted and the influence of temperature on their storage modulus (G') and loss factor (tan δ) were presented in **Figures 5.11** and **5.12**, respectively. As shown in **Figure 5.11**, the peaks in the range of 10 to 60 ^{o}C should be attributed to glass transition temperature (Tg) of PLA, showing a characteristic of semi-crystalline polymers. The peaks at ~0 ^{o}C should be attributed to Tg of HBP(COOH).

Tg of PLA in the blend decreases as the weight percentage of HBP(COOH)-3 increases (minimum Tg achieved is 26.86^{o}C at 20 wt. % HBP(COOH)-3). Tg of HBP(COOH)-3 fluctuates in small amplitude as the weight percentage of

HBP(COOH)-3 increases.

As shown in **Figure 5.12**, G' decreases with increasing temperature for each sample, especially in zone nearly their glass transitions. The G' value of the composite was decrease from 3 wt.% to 20 wt.% weight percentage compared with pure PLA. It is found that G' is at the minimum when the weight percentage of HBP(COOH)-3 reaches 20 wt. %.

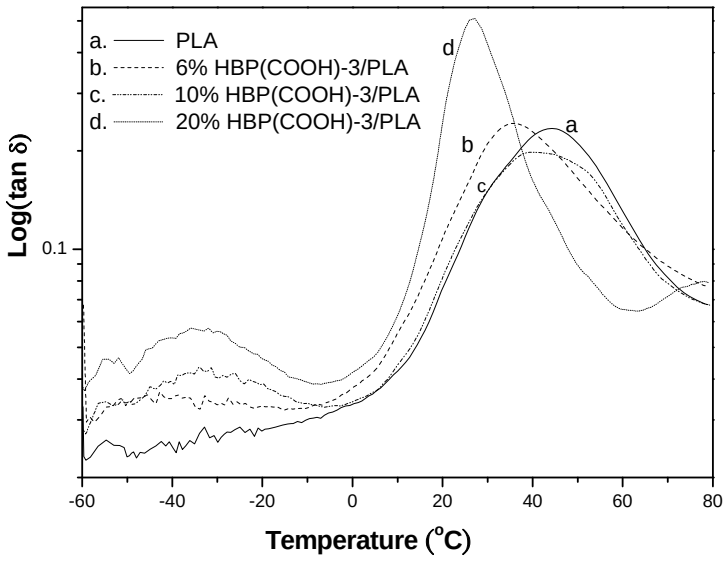

Figure 5.11 Log(tan δ) vs. temperature curves of pure PLA and HBP(COOH)-3 modified PLA composites

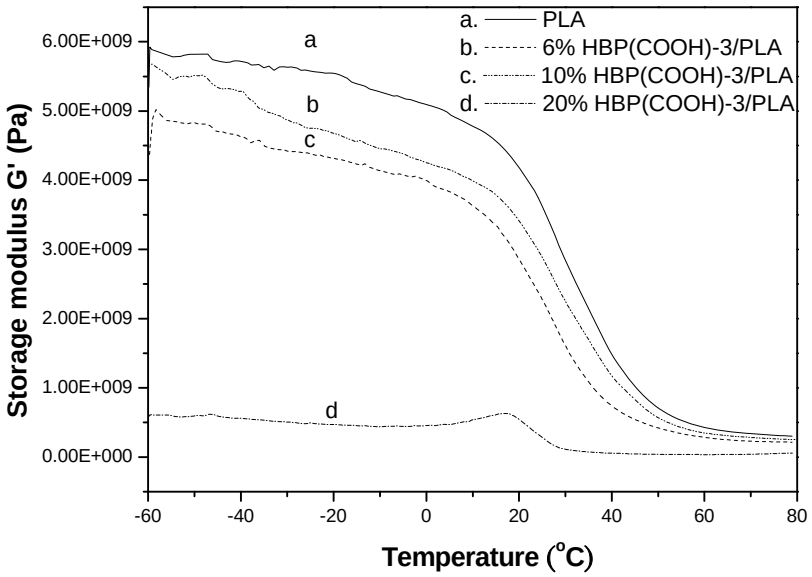

Figure 5.12 Storage modulus G' vs. temperature curves of pure PLA and HBP(COOH)-3 modified PLA composites

Similar study was also conducted for the HBP(COOH)-4/PLA system. As indicated in **Figure 5.13**, Tg of PLA decreases as the weight percentage of HBP(COOH)-4 increases (minimum Tg achieved is 26.89°C at 20 wt. % HBP(CA)-4). Tg of HBP(COOH)-4 fluctuates in small amplitude as the weight percentage of HBP(COOH)-4 increases.

As shown in **Figure 5.14**, G' decreases with increasing temperature for each sample, especially in zone nearly their glass transitions. The G' value of the composite was decrease from 3 wt.% to 20 wt.% weight percentage compared with pure PLA. It is

found that G' is at the minimum when the weight percentage of HBP(COOH)-4 reaches 20 wt. %.

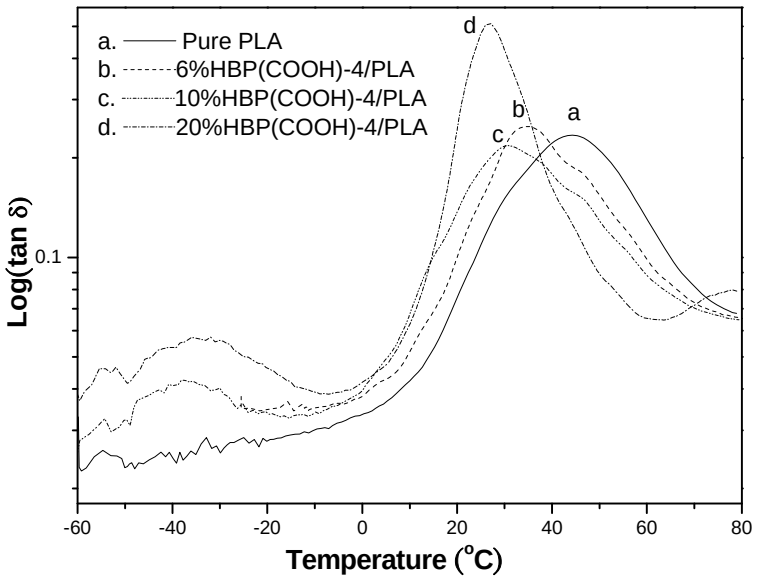

Figure 5.13 Log(tan δ) vs. temperature curves of pure PLA and HBP(COOH)-4 modified PLA composites

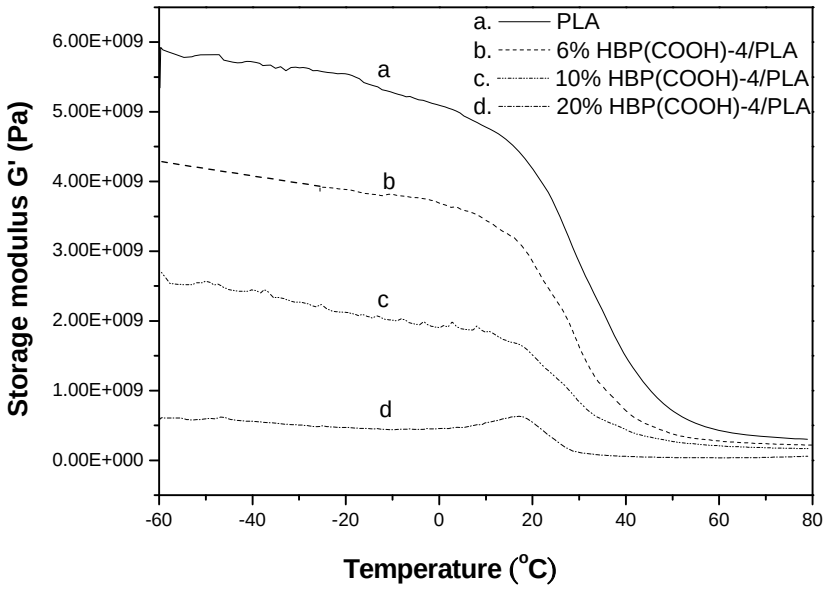

Figure 5.14 Storage modulus G' vs. temperature curves of pure PLA and HBP(COOH)-4 modified PLA composites

There is no significant change in Tg of HBP as HBP(COOH) introduced, but Tg of PLA decreased, thus the difference in Tg between HBP and PLA is getting closer, indicated that the blend system is a miscible. The storage modulus G' of the blend reduced correspondingly with increasing HBP(COOH) content. When HBP(COOH) increased to 20 wt. %, the storage modulus G' of the resulting blend is about 1/6 of the unmodified PLA sample. This is because Tg has been significantly decreased. (At 20 wt. % HBP(COOH), Tg value decreased about 20°C than that in PLA), resulting in less effect in storage modulus G'. Thus the HBP in PLA matrix act as plasticizer in blends processing.

5.3.4 Scanning Electron Microscopy (SEM)

The fractured surface of neat PLA was microscopically flat, indicating the brittle failure of PLA under tensile loading. The tensile fractured surface of 6wt. % HBP(COOH)-3 and 3wt. %HBP(COOH)-4 modified PLA composite exhibited some signatures of ductile tearing and surface roughness. The whole matrix deformation was observed as fibril-like structure. The ductile tearing signature indicated the substantial improvement in toughness corresponding with the results from tension test. Particularly, the increased surface roughness of the fractured surface of the blend suggested that crack propagation absorbed considerable strain energy before tensile failure. The incorporation of small amount of HBP (3~6wt. %) into PLA matrix obviously changed the surface characteristics after tensile induced deformation. As the weight percentage of HBP(COOH)-3 and HBP(COOH)-4 increased to 10wt. %, the fractured surface of the blend showed similar behaviour to that of low HBP(COOH)-3 and HBP(COOH)-4 weight percentage revealed inhomogeniety, formation of fused particles and absence of ductile tearing. This was an indication of phase separation and brittle failure. But At 20 wt. % HBP(COOH)-3 and HBP(COOH)-4 , the fractured surface became less ductile and result in lower strength of the matrix, contributing to lower strain energy release rate.

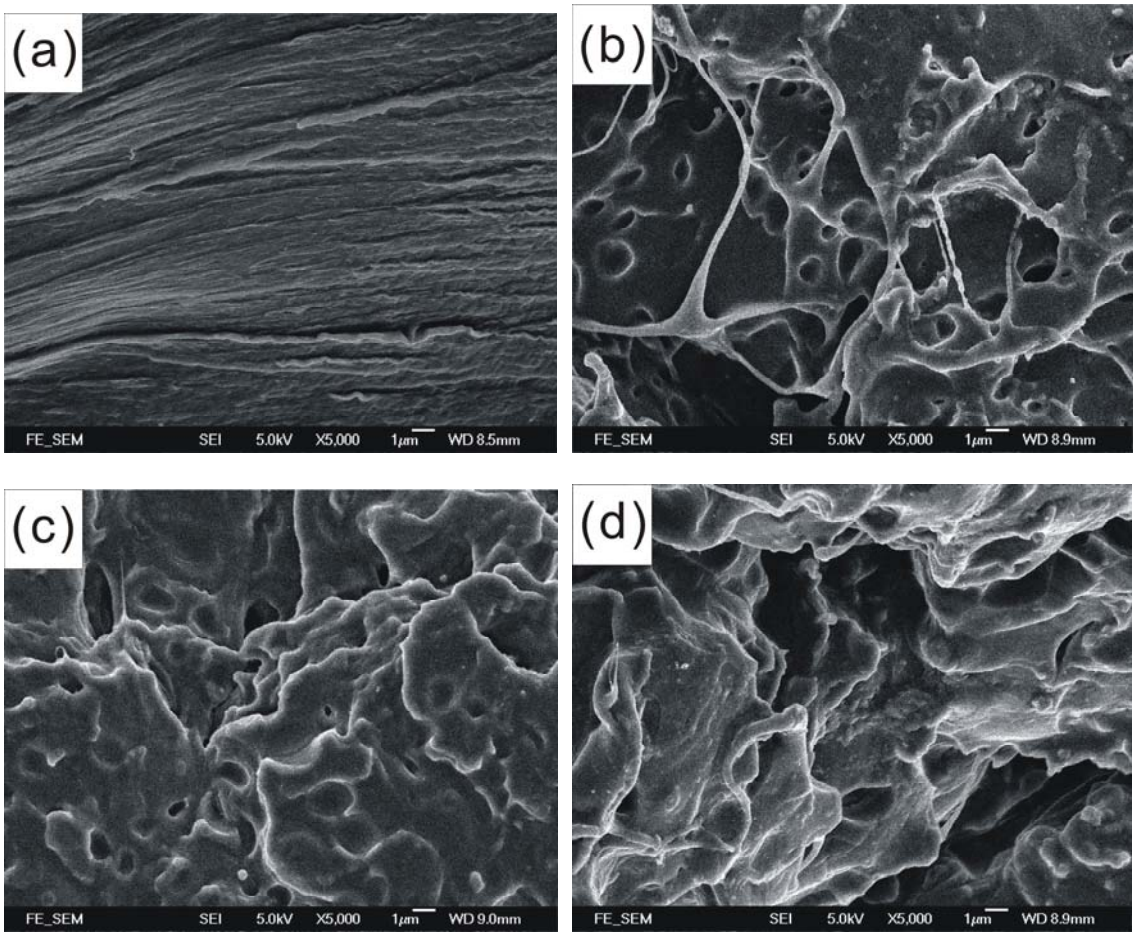

Figure 5.15 FE-SEM images of the fracture surface of PLA composite samples with different weight ratios of HBP(COOH)-3 and PLA: (a) 100/0 ;(b) 94/6 ;(c) 90/10; (d) 80/20 (All magnifications are ×5000)

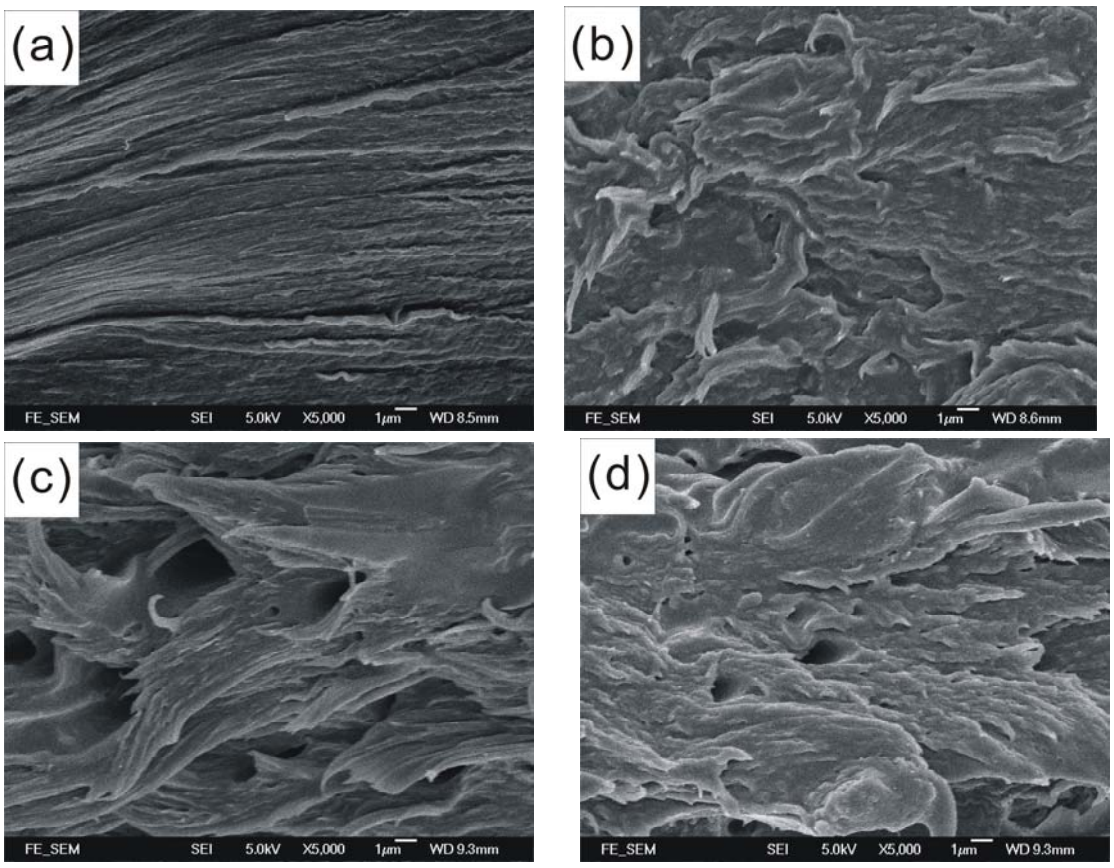

Figure 5.16 FE-SEM images of the fracture surface of PLA composite samples with different weight ratios of HBP(COOH)-4 and PLA: (a) 100/0 ;(b) 94/6 ;(c) 90/10; (d) 80/20; (The magnifications are ×5000)

As illustrated from SEM micrographs we can observe good miscibility between HBP and PLA in 6 wt. % HBP(COOH)-3/PLA and 3 wt. %HBP(COOH)-4/PLA blends, respectively since there is no distinct phase separation. This is an indication of strong interaction between HBP and PLA matrix, leading to better mechanical properties. As the weight percentage of HBP(COOH) increased to 10 to 20 wt. %, the fractured surface became less ductile and result in lower strength of the matrix, contributing to

lower strain energy release rate. (**Figure 5.15 and 5.16**) Thus the interaction between HBP(COOH) and PLA will be reduced and resulted in less toughening effect.

5.3.5 Transmission electron microscopy (TEM)

Transmission electron microscopy (TEM) was carried out to evaluate the morphology and dispersion of cross-linked hyperbranched polymer cluster in the PLA matrix. The ultramicrotoned samples of the HBP(COOH) modified PLA blends was not stained before TEM observation. The TEM micrograph of the blend revealed the nanoscale dimension of HBP clusters and they were well distributed in the PLA matrix. The darker region appeared as discrete agglomerations. This can be attributed to the limit miscibility and inhomogeneous mixing between HBP(COOH) and PLA and the presence of strong intermolecular hydrogen bonding within hyperbranched polymers due to high peripheral hydroxyl functional end group.

Under TEM, the HBP clusters appeared as discrete agglomerations can be distinguished from the dark region due to the specific staining with uranium acetate. As illustrated in **Figure 5.17(a),** HBP(COOH)-3 clusters in diameter between 10 and 20 nm are observed and they exhibit in spherical-like domains in the PLA matrix. Similarly, as illustrated in **Figure 5.17(b)**, HBP(COOH)-4 clusters in diameter between 20 and 50

nm are also obtained and exhibit in spherical-like domains in the PLA matrix.

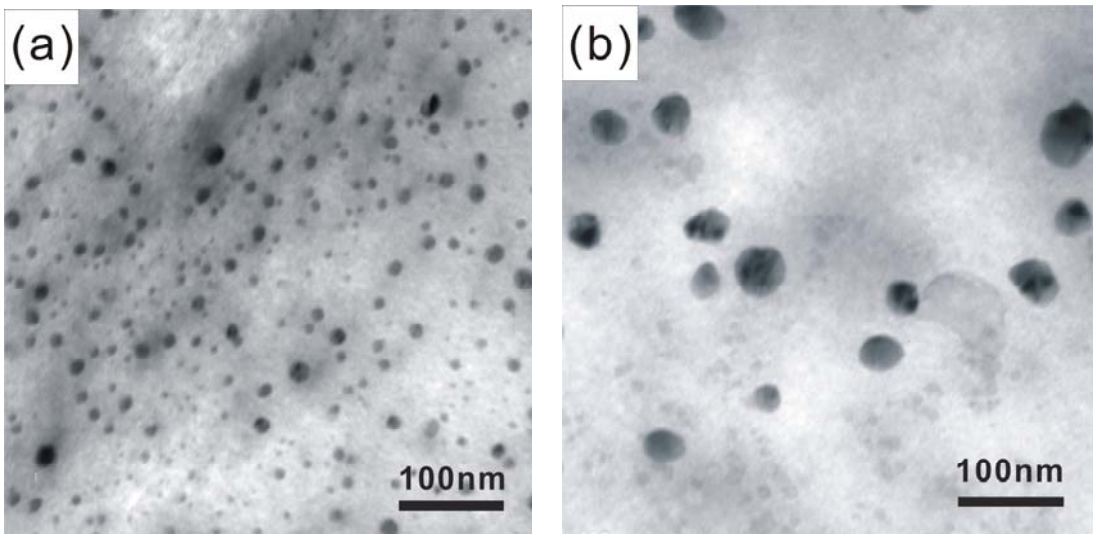

Figure 5.17 TEM micrographs of (a) 6 wt. % HBP(COOH)-3/PLA composite, (b) 3 wt. % HBP(COOH)-4/PLA composite

For both of the blends, the nanosize HBP clusters are well dispersed in the PLA matrix. It is believed that the nanoclusters formed play an important role in the toughening effect.

5.3.6 Degradation study

5.3.6.1 Biodegradability of HBP(COOH)

(Detail procedure refer to **Chapter 4.3.6.1**)

5.3.6.2 Biodegradability of HBP(COOH)/PLA composites

The composite samples before and after the degradation test are shown in **Figure 5.18**. The sample after the treatment still maintains in original shape but exhibits higher opacity and thinner.

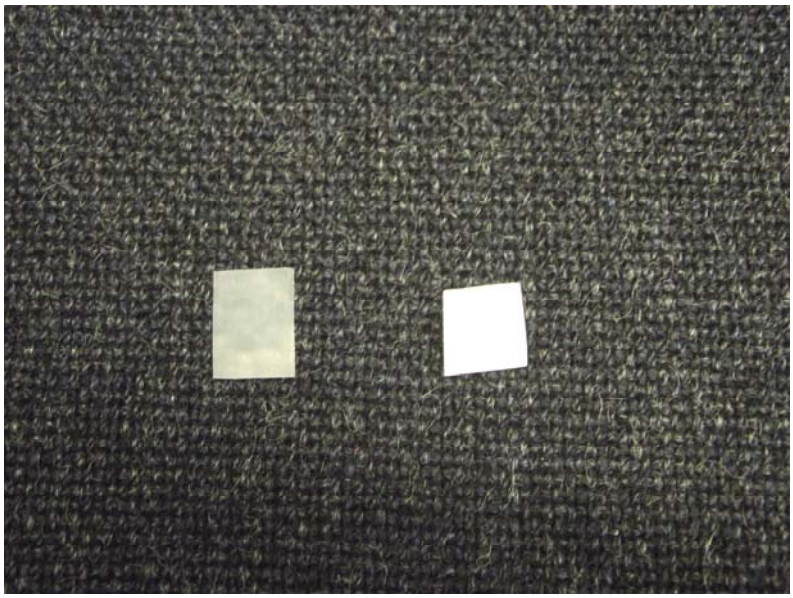

Figure 5.18 Photographs of a HBP/PLA composite sheet (left) before and (right) after the degradation test

The degradation test results of HBP(COOH)-3/PLA specimens in two different media are demonstrated in **Figures 5.19** and **5.20** and **Table 15**. As illustrated from the degradability test in PBS in **Figure 5.19**, the weight percentage of HBP(COOH)-3 increased in PLA with increasing weight loss and the molecular weight of PLA was correspondingly decreased. As illustrated from the degradability test in 0.01M NaOH

solution in **Figure 5.20**, the weight percentage of HBP(COOH)-3 increased in PLA with the weight loss of PLA composites was increased to 60%~65% and becomes stable , and the molecular weight of PLA was increased initially and then decreased during the degradation process. It can be concluded that the degradation process of PLA is the initial degradation of low molecular weight PLA, following by high molecular weight PLA. Therefore, as more HBP(COOH)-3 introduced into PLA, the change in molecular weight starting from increase and subsequently decrease as determined from gel permeation chromatography. Based on the above results indicated that addition of HBP(COOH)-3 into PLA will accelerate the degradation process significantly.

The degradation test on HBP(COOH)-4/PLA in two types of solutions were demonstrated in **Figure 5.21~5.22** and **Table 15**. As illustrated from the degradability test in PBS in **Figure 5.21**, the weight percentage of HBP(COOH)-4 increased in PLA with increasing weight loss and the molecular weight of PLA was increased initially and then decreased significantly during the degradation process. As illustrated from the degradability test in 0.01M NaOH solution in **Figure 5.22**, the weight percentage of HBP(COOH)-4 increased in PLA with the weight loss of PLA composites was increased to 60%~70% and becomes stable. And the molecular weight was increased

initially and then decreased significantly during the degradation process. It can be concluded that the degradation process of PLA is the initial degradation of low molecular weight PLA, following by high molecular weight PLA. Therefore, as more HBP(COOH)-4 introduced into PLA, the change in molecular weight starting from increase and subsequently decrease as determined from gel permeation chromatography. Based on the above results indicated that addition of HBP(COOH)-4 into PLA will accelerate the degradation process significantly.

From the effect of buffer solution pH, the overall degrdation rate of HBP(COOH) modified PLA is higher in 0.01 M NaOH solution than that in PBS buffer.

From the effect of molecular weight at constant solution pH, there is no definite difference in degradation rate for both HBP(COOH)-3/PLA and HBP(COOH)-4/PLA in 0.01 M NaOH solution(pH=12). However, in lower buffer solution pH such as PBS solution (pH=7.4), the degradation of higher molecular weight blend (HBP(COOH)-4/PLA in our experiment) is faster than the degradation rate of HBP(COOH)-3/PLA based on the weight loss measurements.

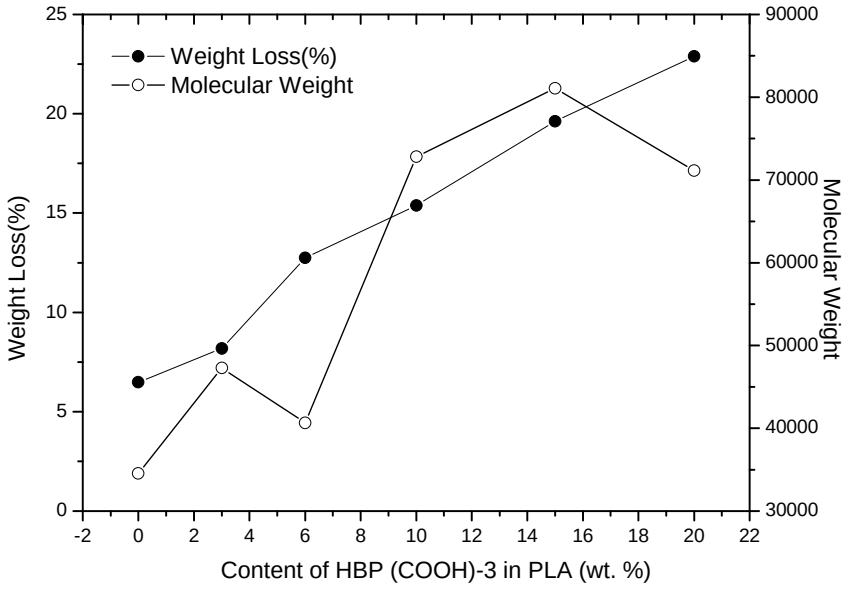

Figure 5.19 Weight loss and molecular weight of the blend vs. wt. % of HBP(COOH)-3 in PLA treated with PBS solution after the test

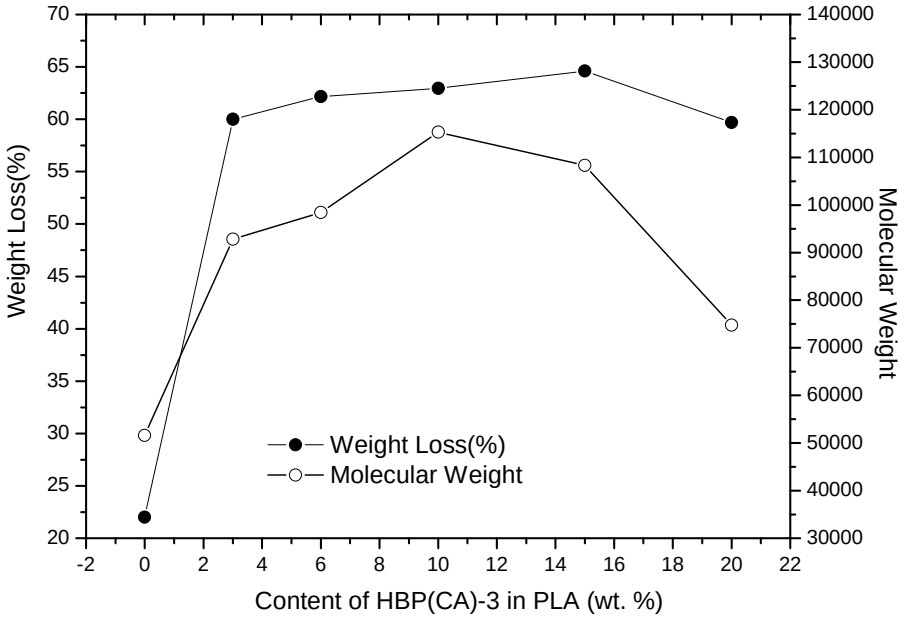

Figure 5.20 Weight loss and molecular weight of the blend vs. wt. % of HBP(COOH)-3 in PLA treated with 0.01M NaOH solution after the test

Table 15 The degradation data of HBP(COOH)-3/PLA and HBP(COOH)-4/PLA composites

Degradation solution		Samples	0%HBP	3%HBP	6%HBP	10%HBP	15%HBP	20%HBP
PBS solution	Weight loss (%)	HBP(COOH)-3/PLA	6.48	8.18	12.75	15.38	19.63	22.90
		HBP(COOH)-4/PLA	6.48	11.11	13.01	15.04	21.25	24.73
	Molecular weight(Mw)	HBP(COOH)-3/PLA	34543	47291	40654	72813	81085	71146
		HBP(COOH)-4/PLA	34543	49419	71234	69358	72911	44381
NaOH solution	Weight loss (%)	HBP(COOH)-3/PLA	22.02	60.0	62.16	62.96	64.6	59.7
		HBP(COOH)-4/PLA	22.02	56.48	64.15	60.53	68.42	57.40
	Molecular weight(Mw)	HBP(COOH)-3/PLA	51593	92833	98423	115307	108285	94713
		HBP(COOH)-4/PLA	51593	85333	86432	76742	78345	74773

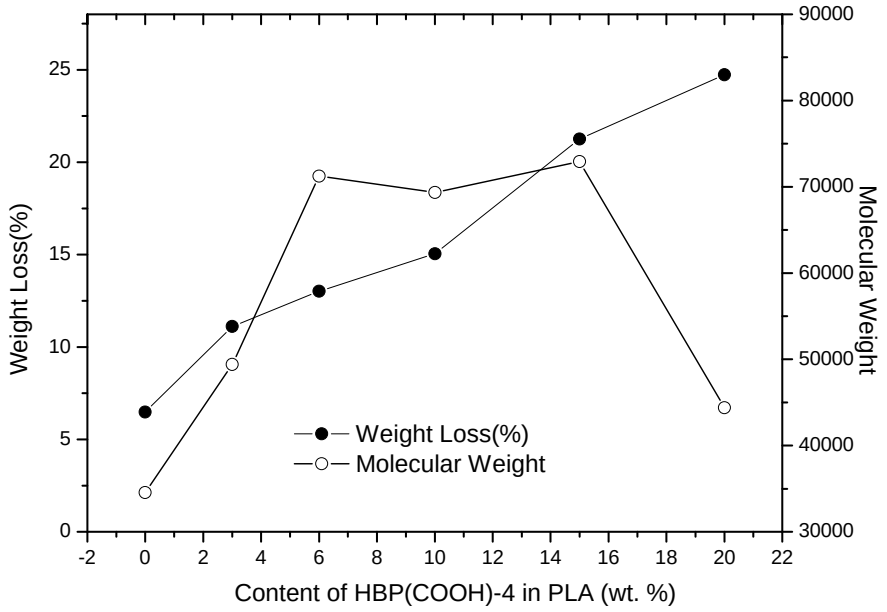

Figure 5.21 Weight loss and molecular weight of the blend vs. wt. % of HBP(COOH)-4 in PLA treated with PBS solution after the test

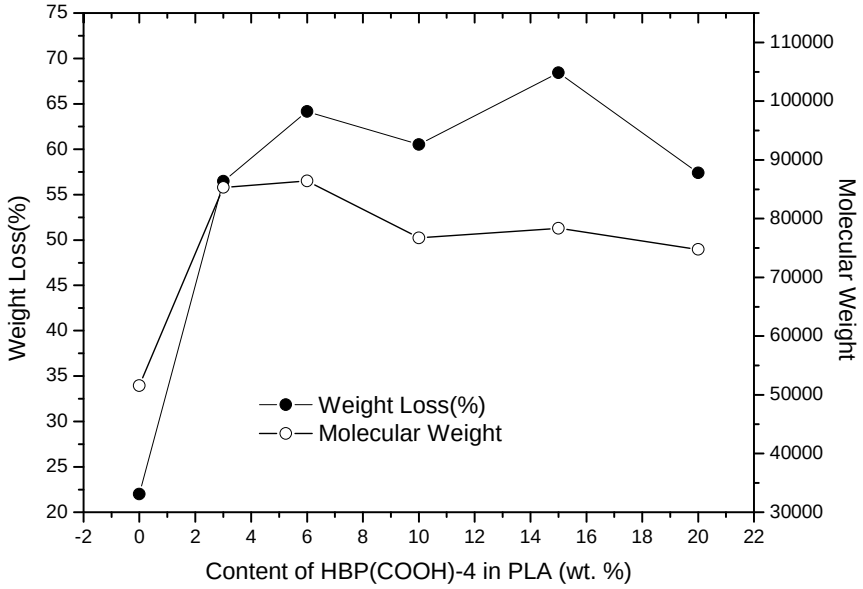

Figure 5.22 Weight loss and molecular weight of the blend vs. wt. % of HBP(COOH)-4 in PLA treated with 0.01M NaOH solution after the test

5.4 Conclusion

Advanced biodegradable composite blends were prepared by solvent casting of PLA with biodegradable HBP(COOH) or HBP(OH). The incorporated modifiers have been comprehensively investigated with respect to their effects on physical, mechanical, thermal, and morphological properties of the end products.

Mechanical properties of PLA can successfully be improved by adding small amounts of HBP(COOH)-3 and HBP(COOH)-4. It is found that the HBPs are able to improve flexibility of the PLA matrix with an increase in toughness of the polymeric blends.

Optimal weight percentages of the fillers (HBP(COOH)-3: 6 wt. %; HBP(COOH)-4: 3 wt. %) can effectively enhance toughness of PCL. SEM micrographs show that the addition of HBPs results in an increase in surface decrease in brittleness and elongated fibrils as well as better interfacial adhesion between PLA and the fillers. A debonding-initiated shear yielding mechanism is probably involved in the toughening of the composite materials. It is found that good miscibility can be realized in the blends when the filler content is lower 10 wt. %. This is an indication of strong interactions between HBP and the polymer matrix, leading to better mechanical properties. When the filler percentage increases to 20 wt. %, the mutual interactions between the HBP molecules become dominate, thus resulting in phase separation in the blends. This phenomenon is no good for toughening.

Well-defined spherical HBP nanosized domains are found in the PLA matrix of the blends, as revealed by TEM investigation. The presence of the clusters in the blends is believed to be beneficial to the polymer modification. The strategy that has been followed should combine the toughening effect of HBP(COOH) in PLA composites from mechanical and thermomechanical analysis[306-308]. DSC and DMA studies reveal the existence of strong molecular interactions in the system. Both Xc and G' are sensitive to the content of the HBPs in the blends.

The incorporation of the organic fillers does affect the bio-stability of PLA, but the degree is subjected to factors such as concentration, type and molecular weight of the fillers, and degradation conditions. In general, higher molecular weight filler or higher filler content would likely induce an increase in biodegradable rate for the end materials. In the GPC and weight loss results for PLA degradation mechanism, PLA with low molecular weight component was degraded first and thus high molecular weight component of PLA degraded at subsequent stage. We have demonstrated that a better hydrophilicity makes the biodegradation to proceed faster. The degradation is faster in an alkaline medium than in a neutral environment. In conclusion, the degradation of HBP(COOH)/PLA blends was buffer solution pH dependent based on the weight loss measurement and the change in weight average molecular weight.

Chapter 6: Conclusion and Future outlook

6.1 Summary of the major achievements

6.1.1 Synthesis of desired HBPs and fabrication of composite materials

We have successfully synthesized desired hyperbranched polymers bearing carboxylic acid and hydroxyl end-groups, respectively, in good yields and further generated the products with different molecular weights. Compared to those reported in the literature, higher molecular weight polymers can be achieved in this study. In terms of composite processing, we have successfully incorporated the hyperbranched products into biodegradable PCL and PLA through a solvent mixing approach. The resulting products obtained were homogeneous films.

6.1.2 Characterization of HBPs

Chemical structures of the synthesized HBPs have been fully characterized by ^{1}H NMR and ^{13}C NMR techniques, respectively. Their molecular weight distribution was determined by GPC, where the experimental data was in good agreement to the theoretical values obtained from NMR analysis. It was also confirmed that the molecular weight of the polymers could be manipulated by controlling the feeding weight ratio of the mixture during the reactions.

6.1.3 Effects of HBPs in PCL and PLA composite materials

The HBPs introduced upon the formation of the nanocomposite architecture have successfully improved the toughening properties of both PCL and PLA. The new composite materials have been further characterized using a wide scope of characterization techniques. In summary, both tensile strength and elongation at break of the materials can be improved. The elongation at break of PCL can be enhanced by 15.5% and 14.9% when 3 wt. % HBP(COOH)-3 (M_W=16354) and 6 wt. % of HBP(COOH)-4 ((M_W=45279) are introduced, respectively. The elongation at break of PLA can be reinforced by 90.3% and 35% when 6 wt. % of HBP(COOH)-3 and 3 wt. % of HBP(COOH)-4 are incorporated, respectively. An optimal weight percentage (6 wt. %) of HBP(OH)-1 also effectively enhances the toughness of PCL, yielding a 21% increase in critical plane-strain fracture toughness. The HBPs are able to form a well dispersion of nano-clusters in the biodegradable polymer matrix, which are believed to be responsible for the properties modification. In addition, DSC and DMA analyses reveal that the hyperbranched fillers affect thermal properties of the bulk polymers, including Tp, Tg, T_m, and crystallinity behavior. It is found that the HBPs in certain weight ratios could effectively increase both T_m and Tg.

6.1.4 Biodegradability study

In vitro degradation behaviors of PLA and PCL and their respective blends with

HBP(COOH) and HBP(OH) were investigated by monitoring their weight loss and change in molecular mass. Their degradation behaviors were obviously changed when HBP(COOH) or HBP(OH) was incorporated. It was found that the HBP(COOH) modified blends experience a surface erosion process at the beginning of degradation. In general, the blends with higher weight percentage of the hyperbranched fillers will degrade faster. The degradation rate was faster in an alkaline medium than in a neutral environment.

6.2 Concluding remarks

Two types of novel HPBs with COOH and OH surface end groups were synthesized, respectively. To the best of our knowledge, this was the first time to successfully synthesize hyperbranched poly(citric acid) and poly(bis-MPA) with molecular weights as high as >750,000 and >50,000, respectively. This capacity allowed us to study widely the molecular weight effect of the HBPs in the bionanocomposite systems. To look into their potential as candidates for bio composite applications, a comprehensive study has been conducted on their formed materials with PCL and PLA.

Incorporation of the HBPs under the control of proportion in the blends gives rise to improved brittleness of the biodegradable polymers. This is due to the fact that their

highly branched structure and densely populated surface groups allow for enhanced interaction with the bulk material, which in turn strengthen the matrix and could aid in improving various properties such as the mechanical and thermal properties. The end group chemistry can get used to keep decrease in brittleness properties without causing significant loss in Tg and crystallinity.

Besides, adequate toughening could be guaranteed if the fibrillar structure at fracture surface is adapted in the blends. The presence of spherical HBP nanosized clusters in the polymer matrix is believed to be beneficial to the polymer modifications. A debonding-initiated shear yielding mechanism is probably involved in the toughening of the composite materials.

The incorporation of the organic fillers does affect the bio-stability of PCL and PLA, but the degree is subjected to factors such as concentration, type and molecular weight of the fillers, and degradation conditions. In general, higher molecular weight filler or higher filler content would likely induce an increase in biodegradable rate for the end materials. The degradation is faster in an alkaline medium than in a neutral environment.

In sum, the new approach has several distinct advantages: 1) a wide range of

functionalization on HBP structure for better control of end material properties; 2) simple processing steps; 3) a commercially viable route for making novel green nanocomposites.

6.3 Future outlook

6.3.1 Applications of HBP(COOH) and HBP(OH) to other polymeric systems

In this work, we employ HBP(COOH) or HBP(OH) to modify PCL and PLA through solvent mixing technique. Under the control of certain parameters of the HBPs, properties improvement for the bulk polymers can be realized. Similarly, it is expected the same principle can be applied for other nonbiodegradable systems like PE, PC, and PET to achieve the same effects. It is also expected that the non-biodegradable nature of the polymers can be improved upon the incorporation of the biodegradable compounds.

6.3.2 Novel hyperbranched polymers with other types of end groups

In this study, focus is made on two types of HBPs containing COOH and OH end groups, respectively, and got basic understanding on their effects. Actually, there are many different types of HBPs available, which contain different types of end groups such as NH_2, Ph, etc., and they are all promising for the same application. It is expected more

relevant studies about the new candidates will be available in the near future.

6.3.3 Further study on biodegradability of the nanocomposites

In this study, chemical degradation of the composite materials has been investigated. Apart from the chemical way, biological degradation is also important in the degradation process. The study on the degradation process by enzymes and other microbial species can provide further information for their complicated degradation mechanisms.

References

[1] Mezzenga, R.; Boogh, L.; Manson, J. A. E., *Compos. Sci. Technol*. **2001**; *61*, 787.

[2] Rogunova, M.; Lynch, T. Y. S.; Pretzer, W.; Kulzick, M.; Hiltner, A.; Baer, E. *J. Appl. Polym. Sci.* **2000**, *77*, 1207.

[3] Newkome G R, Moore®eld C N, Vo$ gtle F, In: *Dendritic Molecules: Concepts*, *Syntheses*, *Perspecti.es*. VCH, NewYork, **1996**

[4] P. J. *Principles of Polymer Chemistry*, Cornell University Press, Ithaca, New York, **1953**.

[5] Kim Y H, Webster O W, Hyperbranched polyphenylenes.*Macromolecules,* **1992,** 25, 5561.

[6]. Fréchet, J.M.J. *Science* **1994**, *263*, 1710.

[7] Kim, Y. H.; *J. Polym. Sci. A: Polym. Chem*. **1998**, *36*, 1685.

[8] Sunder, A.; Hanselmann, R., Frey, H.; Mühlhaupt, R. *Macromolecules* **1999**, *32*, 4240.

[9] Fréchet, J. M. J.; Henmi, M.; Gitsov, S. Aoshima, S.; Leduc, M. R.; Grubbs, R. B. *Science* **1995**, *269*, 1080.

[10] Voit, B. *J. Polym. Sci. A: Polym. Chem.* **2000**, *38*, 2505.

[11] Voit, B. *J. Polym. Sci. A: Polym. Chem.* **2005**, *43*, 2679.

[12] Hult, A.; Johansson, M.; Malmström, E. *Adv. Polym. Sci.* **1999**, *143*, 1.

[13] Sunder, A.; Heinemann, J.; Frey, H. *Chem. Eur. J.* **2000**, *6*, 2499.

[14] Jikei, M.; Kakimoto, M. *Prog. Polym. Sci.* **2001**, *26*, 1233

.

[15] Gao, C.;Yan, D. *Prog. Polym. Sci.* **2004**, *29*, 183.

[16] Yates, C. R.; Hayes, W. *Eur. Polym. J.* **2004**, *40*, 1257.

[17] Inoue, K. *Prog. Polym. Sci.* **2000**, *25*, 453.

[18] Hawker, C. J. *Adv. Polym. Sci.* **1999**, *147*, 113.

[19] Hölter, D.; Burgath, A.; Frey, H. Acta Polym. **1997**, *48*, 30.

[20] Fried, J. R. *Polymer Science and Technology*, Prentice-Hall, Englewood Cliffs, NJ, **1995**.

[21] Wooley, K.L.; Hawker, J.M.; Pochan, J.M.; Frechet, J.M.J. *Macromolecules*, **1993**, *26*, 1514.

[22] Schmaljohann, D.; Häußler, L.; Pötschke, P.; Loontjens, T.J.A.; Voit, B. *Macromol. Chem. Phys*., **2000**, *201*, 49.

[23] Wooley, K.L.; Hawker, C. J.; Pochan, J.M.; Frechet, J.M.J. *Macromolecules*, **1993**, *26*, 1514.

[24] Sunder, A. Albert-Ludwigs-Universit¨at Freiburg, **2000**.

[25] Hult, A.; Johansson, M.; Malmström, E. *Adv. Polym. Sci*. **1999**, *143*, 1.

[26] Rogunova, M.; Lynch, T.Y.S.; Pretzer, W.; Kulzick, M.; Hiltner, A.; Baer, E. *J. Appl. Polym. Sci.* **2000**, *77*,1207.

[27] Berry, G.C.; Fox, T.G. *Fortschritte der Hochpolymeren-Forschung* **1968**, *5*, 262.

[28] Kraus, G.; Gruver, J. *J. Polym. Sci. B: Polym. Phys.*, **1970**, *8*, 305.

[29] Fujimoto, T.; Narukawa, H.; Nagasawa, M. *Macromolecules*, **1970**, *3*, 57.

[30] Mendelson, R.A.; Bowles, W.A.; Finger, F.L. *J. Polym. Sci.* **1970,** *A-28*, 105.

[31] Masuda, T.; Ohta, Y.; Onogi, S. *Macromolecules* **1971**, *4*, 763.

[32] Graessley, W.W.; Masuda, T.; Roovers, J.E.L.; Hadjichristdis, N. *Macromolecules* **1976**, *1*, 127.

[33] Mourey, T. H.; Turner; S. R.; Rubinstein, M.; Frechet, J.M.J.; Hawker, C.J.; Wooley, K.L. *Macromolecules* **1992**, *25*, 2401.

[34] Burchard, W. *Adv. Polym. Sci.* **1999**, *143*, 113.

[35] De Luca, E.; Richards, R.W. *J. Polym. Sci. B: Polym. Phys.* **2003**, *41*, 1339.

[36] Hawker, C.J.; Frechet, J.M.J. *Comparison of linear, hyperbranched and dendritic macromolecules*, in: J.L. Hedrick, J.W. Labadie (Eds.), *Step-Growth Polymers for High-Performance Materials*, Oxford Press, Oxford, **1996**.

[37] Scherrenberg, R.; Coussens, B.; Van Vliet, P.; Edouard, G.; Brackman, J.; De Brabander, E.; Mortensen, K. *Macromolecules* **1998**, *31*, 456.

[38] Mackay, M.E.; Carmezini, G. *Chem. Mater.* **2002**, *14*, 819.

[39] Xu, M.; Yan, X.; Cheng, R.; Yu, X. *Polym. Int.* **2001**, *50*, 1338.

[40] Ishizu, K.; Mori, A. *Polym. Int.* **2001**, *51*, 50.

[41] Ishizu, K.; Takashimizu, C.; Shibuya, T.; Uchida, S. *Polym. Int*. **2003**, *52*,1010.

[42] Kharchenko, S.B.; Kannan, R.M.; Cernohous, J.J.; Venkataramani, S. *Macromolecules* **2003**, *36* , 399.

[43] Striolo, A.; Prausnitz, J.M.; Bertucco, A.; Kee, R.A.; Gauthier, M. *Polymer* **2001**,

42, 2579.

[44] Lue, L. *Macromolecules* **2000**, *33*, 2266.

[45] V.M. Garamus, T. Maksimova, W. Richtering, C. Aymonier, R. Thomann, L. Antonietti, S. Mecking, *Macromolecules*, **2004**, *37*, 7893–7900.

[46] T. Satoh, T. Imai, H. Ishihara, T. Maeda, Y. Kitajyo, Y. Sakai, H. Kaga, N. Kaneko, F. Ishii, T. Kakuchi, *Macromolecules*, **2005**, *38*, 4202–4210.

[47] Mulder, T.; Lyulin, A.V.; van der Schoot, P.; Michels, M.A.J. *Macromolecules* **2005**, *38*, 96.

[48] Wooley, K.L.; Hawker, C.J.; Lee, R.; Frĕchet, J.M.J. *Polym J*. **1994**,*26*,187.

[49]Wan, Q.; Schricker, S.R.; Culbertson, B.M. *J Macromol Sci, Pure Appl Chem* **2000**; *A37(11)*:1301.

[50] Peez, R.F.; Dermody, D.L.; Franchina, J.G.; Jones, S.J.; Bruening, M.L.; Bergbreiter, D.E.;.Crooks, R.M. *Langmuir* **1998**;1*4*,4232.

[51] Weimer, M.W.; Fréchet, J.M.J.; Gitsov, I. *J Polym Sci, Part A: Polym Chem*, **1998**, *36*,955.

[52] Kuo, P.L.; Ghosh, S.K.; Liang, W.J.; Hsieh, Y.T. *J Polym Sci, Part A: Polym Chem* **2001**,*39*, 3018.

[53] Lach, C.; Hanselmann, R.H.; Frey, H.; Mülhaupt, R. *Macromol Rapid Commun*, **1998**;*19*,461.

[54] Al-Muallem, H.A.; Knauss, D.M.; *J Polym Sci, Part A: Polym Chem*, **2001**,*39*, 3547.

[55] Johansson, M.; Malmström, E.; Jansson, A.; Hult, A. *J. Coat Technol* **2000**;*72*, 49.

[56] Benthem, R.A.T.M.. *Prog Org Coat.* **2000**,*40*,203.

[57] Mancyzk, K.; Szewczyk, P. *Prog Org Coat,* **2002**,*44*,99.

[58] Zhu, S.W.; Shi, W.F. *Polym Degrad Stab*, **2002**,*75*, 543.

[59] Lange, J.; Stenroos, E.; Johansson, M.; Malmström, E. *Polymer* **2001**,*42*, 7403.

[60] Wan, Q.; Schricker, S.R.; Culbertson, B.M. *J Macromol Sci, Pure Appl Chem* , **2000**, *A37(11)*,1301.

[61] Wan,Q.; Schricker, S.R.; Culbertson, B.M. *J Macromol Sci, Pure Appl Chem* , **2000**;*A37(11)*,1317.

[62] Johansson, M.; Glauser, T.; Rospo, G.; Hult, A. *J Appl Polym Sci*. **2000**, *75*,612.

[63] Claesson, H.; Malmström, E.; Johansson, M.; Hult, A.; Doyle, M.; Månson,

J.A.E. *Prog Org Coat*. **2002**;*44*,63.

[64] Staring, E.; Dias, A.A.; van Benthem, R.A.T.M. *Prog Org Coat.***2002**,*45*,101.

[65] Wei, H.; Lu, Y.; Shi, W.; Yuan, H.; Chen, Y. *J Appl Polym Sci*, **2001**,*80*,51.

[66] Mezzenga, R.; Boogh, L.; Månson, J.A.E. *Compos Sci Technol.* **2001**,*61*,787.

[67] Mezzenga, R.; Plummer, C.J.G.; Boogh, L.; Månson, J.AE. *Polymer***2001**,*42*,305.

[68] Xu, J.; Wu, H.; Mills, O.P.; Heiden, P.A. *J. Appl Polym Sci*. **1999**,*72*,1065.

[69] Gopala, A.; Wu, H.; Xu, J.; Heiden, P. *J. Appl Polym Sci*. **1999**,*71*,1809.

[70] Wu, H.; Xu, J.; Heiden, P. *J Appl Polym Sci*. **1999**, *72*,151.

[71]Mezzenga, R.; Boogh, L.; Pettersson, B.; Månson, J.A.E. *Macromol Symp*. **2000**,*149*,17.

[72] Boogh, L.; Pettersson, B.; Månson, J.A.E. *Polymer* **1999**,*40*, 2249.

[73] Gryshchuk, O.; Jost, N.; Karger-Kocsis, J. *Polymer* **2002**,*43*, 4763.

[74] Gryshchuk, O.; Jost, N.; Karger-Kocsis, J. *J. Appl Polym Sci.* **2002**,*84*,672.

[75] Oh, J.H.; Tang, J.; Lee, S.H. *Polymer* **2001**,*42*,8339.

[76]Emrick, T.; Chang, H.T.; Fréchet, J.M.J.; Woods, J.; Baccei, L. *Polym Bull*. **2000**,*45*,1.

[77] Liu, H.; Wilén, C-E.; Skrifvars, M.; *J. Polym Sci, Part A: Polym Chem*. **2000**,*38*, 4457.

[78] Burkinshaw, S.M.; Froehling, P.E.; Mignanelli, M. *Dyes Pigments* **2002**,*53*,229.

[79] Schmaljohann, D.; Pötschke, P.; Hässler, R.; Voit, B.I.; Froehling, P.E.; Mostert, B.; Loontjens, J.A. *Macromolecules* **1999**,*32*,6333.

[80] Jannerfeldt, G.; Boogh, L.; Månson, J.A.E. *J. Polym Sci, Part A: Polym Chem*. **1999**,*37*,2069.

[81] Star, A.; Stoddart, J. F. *Macromolecules* **2002**,*35*,7516.

[82] Hong, Y.; Cooper-White, J. J.; Mackay, M.E.; Hawker, C.J.; Malmström, E.; Rehnberg, N. *J. Rheol* **1999;***43*, 781.

[83] Hong, Y.; Coombs, S.J.; Cooper-White, J.J.; Mackay, M.E.; Hawker, C. J.; Malmström, E.; Rehnberg, N. *Polymer* **2000**;*41*,7705.

[84] Mulkern, T. J.; Tan, N.C.B. *Polymer* **2000**,*41*,3193.

[85] Jang, J.; Oh, J.H.; Moon, S.I. *Macromolecules* **2000,***33*,1864.

[86] Ratna, D.; Simon, G.P. *Polymer* **2001**,*42*,8833.

[87] Tang, L.M.; Qiu, T.; Tuo, X.L.; Zhang, X.L.; Liu,D.S. *Polym J*. **2002**,*34*,112.

[88] Baek, J.B.; Qin, H.; Mather, P.T.; Tan, L. S. *Macromolecules* **2002,***35*,4951.

[89] Hawker, C.J.; Chu, F.; Pomery, P. J.; Hill, D.J.T. *Macromolecules* **1996**,*29*,3831.

[90] Tanaka, S.; Takeuchi, K.; Asai, M.; Iso, T.; Ueda, M. *Synthetic Metals* **2001**,*119*,139.

[91] Fang, J.; Kita, H.; Okamoto, K. *Macromolecules* **2000,***33(13)*, 4639.

[92] Chen, H.; Yin, J.; *J Polym Sci, Part A: Polym Chem*, **2002,***40*, 3804.

[93] Nguyen, C.; Hawker, C.J.; Miller, R.D.; Huang, E.; Hedrick, J.L. *Macromolecules* , **2000**;*33,*4281.

[94] Lebib, A.; Natali, M.; Li, S.P.; Cambril, E.; Manin, L.; Chen, Y.; Janssen, H.M.; Sijbesma, R. P. *Microelectron Engng,* **2001**,*57/58*,411.

[95] Lebib, A.; Chen, Y.; Cambril, E.; Youinou, P.; Studer, V.; Natali, M.; Pépin, A.; Janssen, H.M.; Sijbesma, R.P. *Microelectron Engng,* **2002**,*61/62*,371.

[96] Frey, H.; Haag, R. *Rev. Mol Biotechnol.* **2002,** *90*, 257.

[97] Crooks, R.M. *Chem Phys Chem* **2001**, *2*, 644.

[98] Lackowski, W.M.; Ghosh, P; Crooks, R.M. *J Am Chem Soc.* **1999**,*121*,1419.

[99] Ghosh, P.; Crooks, R.M. *J Am Chem Soc*. **1999**,*121*,8395.

[100] Ghosh, P.; Amirpour, M.L.; Lackowski, W.M.; Pishko, M.V.; Crooks, R.M. *Angew Chem Int Ed*. **1999,***38*,1592.

[101] Ghosh, P.; Lackowski, W.M.; Crooks, R.M. *Macromolecules* **2001**, *34,*1230.

[102] Rowan, B.; Wheeler, M.A.; Crooks, R.M. *Langmuir* **2002,***18,*9914.

[112] Yim, S. H.; Huh, J.; Ahn, C. H.; Park, T. G.. *Macromolecules* **2007**, *40,* 205.

[113] Albertsson, A. N. in *Biodegradation of Polymers, Handbook of Polymer Degradation*, Hamid, S. M.; Arnin, M. B.; Maadhah, A. G., Eds., Marcel Dekker. New York, **1992**, p. 345.

[114] Coury, A. J. in *Biomaterials Science*, Academic Press, **1996,** Chap. 6

[115] Anderson, J. M. in *Biomedical applications of Synthetic Biodegradable Polymers*, J. O. Hollinger, Ed., **1995**. Chap. 10.

[116] Ray, S. S.; Okamoto, M. *Macromol. Rapid Commun.* **2003,** *24*, 815.

[117] Borda, J.; Bodnar, I.; Kekl, S.; Sipos, S.; Zsuga, M. *J. Polym. Sci. A: Polym. Chem.* **2000**, *28*, 2925.

[118] Gupta, A. P.; Kumar, V. *Eur Polym. J.* **2007**, *43*, 4053.

[119] Jahno, D. V.; Ligabue, R.; Einloft, S. *J. Biomed. Mater. Res.* **2007**, *83*, 209.

[120] Holma, V. K.; Mortensenb, G.; Vishart, M. *Int. Dairy J.* **2006**, *16*, 931**.**

[121] Aminabhavi, T.M.; Balundgi, R.H.; Cassidy, P.E. *Polymer Plastics Technology and Engineering.* **1990**, *29(3)*, 235.

[122] Mayer, J.; Kaplan, D. *Trends in Polymer Science* **1994**,*2(7)*, 227.

[123] Andreopoulos, A.G. *Journal of Elastomers and Plastics.* **1994**,*24(4)*,308.

[124] *ASTM Standards,* Vol. 08.01. 1998. D883-96: Standard Terminology Relating To Plastics.New York, NY.: ASTM

[125] Blanco, A. *Plastics Engineering.* **2002**,*58(10)*, 6

[126]Leaversuch, R. Biodegradable polyesters; Packaging goes green. *Plastics Technology.* **2002**,*48(9)*, 66-73.

[127] Bastioli, C. 1998. Bak 1095 and Bak 2195: Completely biodegradable synthetic Thermoplastics. 59(1-3): 263-272.

[128] Fomin, V.A. 2001. *Progress In Rubber and Plastics Technology.* **2001**,*17(3)*,186.

[129] Blanco, A. *Plastics Engineering.* **2002**, *58(10)*, 6

[130] Guan, J.; Hanna, M.A. **2002**. Modification of macrostructure of starch acetate extruded with natural fibers. ASAE Paper No. 026148. Chicago, Illinois. ASAE.

[131] Li, F. M.; Guo, A.H.; Wei, H. *Field Crops Research.* **1999**, *63*,79.

[132] Huang, J. C.; Shetty, A. S.; Wang, M. S. Biodegradable plastics: A review. *Advances in Polymer Technology.* **1990**,*10(1)*, 23.

[133] Kokubo, T.; Kim, H.; Kawashita, M. *Biomaterials* **2003**, *24*, 2161.

[134]Sakiyama-Elbert, S.; Hubbell, J. *Annual Review of Materials Research.* **2001**,*31*,183.

[135] Lammers, P.; Kromer, K. **2002**. Competitive Natural Fiber Used in Composite Materials for Automotive Parts. ASAE Paper No. 026167. Chicago, Illinois. ASAE.

[136] Fomin, V.A. *Progress In Rubber and Plastics Technology.* **2001**,*17(3)*,186.

[137] Pitt, C. G.; Chasalow, F. I.; Hibionada, Y. M.; Klimas, D .M.; Schindler, A. *Journal of AppliedPolymer Science* **1981**, *26 (11)*, 3779.

[138] Ratner, B. D.; Hoffman, A. S.; Schoen, F. J.; Lemons, J.E. *Biomaterials science*. AcademicPress; **2004**.

[139] Pitt, C. G.; Jeffcat, A. R.; Zweidinger, R. A.; Schindler, A. *Journal of Biomedical Materials Research* **1979**, *13 (3)*, 497.

[140] Woodward, S. C.; Brewer, P. S.; Moatamed, F.; Schindler, A.; Pitt, C. G. *Journal of Biomedical Materials Research* **1985**; *19 (4)*, 437.

[141] Tjong, S. C.; Xu, Y.; Meng, Y. Z. *Polymer* **1999**, *40*, 3703.

[142] Lijian, L.; Suming, L.; Gareau, H.; Vert, M. *Biomacromolecules* **2000**, *1*, 350.

[143] Wang, L.; Ma, W.; Gross, R. A., McCarthy, S. P. *Polym. Degrad. Stab.* **1998**, *59*, 161.

[144] Martin, O.; Avérous, L. *Polymer* **2001**, *42*, 6209.

[145] Cruz, C. A.; Paul, D. R.; Barlow, J. W. *J. Appl. Polym. Sci.* **1979**, *23*, 589.

[146] Fernands, A. C.; Barlow, J. W.; Paul, D. R. *J. Appl. Polym. Sci.* **1984**, *29*, 1971.

[147] Brode, G. L.; Koleske, J. V. *J. Macromol. Sci. Chem Ed.* **1972**, *6*, 1109.

[148] Don, T. M.; Bell, J. P. *Polym. Engng Sci*. **1996**, *36*, 2601.

[149] Clark, J. N.; Daly, J. H.; Garton, A. *J. Appl. Polym. Sci.* **1984**, *29*, 3381.

[150] Zhong, Z.; Guo, Q. *Polymer* **1997**, *38*, 279.

[151] Coleman, M. M.; Moskala, E. J. *Polymer* **1983**, *24*, 251.

[152] Eldsäter, C.; Relandsson, B.; Renstad, R.; Albertsson, A. C.; Karlsson, S. *Polymer* **2000**, *41*, 1297.

[153] Tokiwa, Y.; Suzuki, T. *Nature* **1977**, *270*, 76.

[154] Chong, E.; Phan, T.; Lim, I.; Zhang, Y.; Bay B.; Ramakrishna, S. *Acta Biomaterialia* **2007**, *3 (3)*, 321.

[155] Jabbari, E.; Wang, S.; Lu, L.; Gruetzmacher, J. A.; Ameenuddin, S.; Hefferan, T. E.*Biomacromolecules* **2005**; *6 (5)*, 2503.

[156] Araujo, J.; Martins, A.; Leonor, I.; Pinho, E.; Reis, R.; Neves, N. *Journal of Biomaterials Science, Polymer Edition* **2008**; *19*, 1261.

[157] Mavis, B.; Demirtaş, T. T.; Gümüşderelioğlu, M.; Gündüz, G.; Çolak, Ü.." *Acta*

Biomaterialia **2009**, *5 (8)***,** 3098.

[158] Garlotta, D. *J. Polym. Environ.* **2002**, *9(2)*, 63.

[159] Hartmann, H. High molecular weight polylactic acid polymers , in *Biopolymers from Renewable Resources,* Ed.: Kaplan D.L. , 1st ed., Springer-Verlag , Berlin , **1998** , pp. 367 – 411 .

[160] Auras, R.; Harte, B.; Selke, S. *Macromol. Biosci.* **2004**, *4*, 835.

[161] Mehta, R.; Kumar, V.; Bhunia, H.; Upahyay, S. N. *J . Macromol. Sci., Polym. Rev.* **2005**, *45*, 325.

[162] Sodergard, A.; Stolt, M. *Prog. Polym. Sci.* **2002**, *27*,1123.

[163] Drumright, R. E.; Gruber, P. R.; Henton, D. E. *Adv. Mater.* **2000**, *12,* 1841.

[164] Mohanty, A.; Misra, M.; Hinrichsen, G. *Macromol. Mater. Eng.* **2000**, *276/277*, 1.

[165] Labrecque, L. V.; Dave, V.; Gross, R. A.; McCarthy, S. P. *J. Appl. Polym. Sci.* **1997**, *66*, 1507.

[166] Andreopoulos, A. G. *Clin. Mater.* **1994**, *15*, 89.

[167] Sheth, M.; Kumar, A.; Dave, V.; Gross, R. A.; McCarthy, S. P. *J. Appl. Polym. Sci.* **1997**, *66*, 1495.

[168] Jacobsen, S.; Fritz, H. G. *Polym. Eng. Sci.* **1999**, *39*,1303.

[169] Auras, R.; Harte, B.; Selke, S. *Macromol. Biosci.* 2004, *4*, 835.

[170] Sodergard, A.; Stolt, M. *Prog. Polym. Sci.* **2002**, *27*,1123.

[171] Amass, W.; Amass, A.; Tighe, B. *Polym. Int.* **1998**, *47,* 89.

[172] Li, S. M.; Garreau, H.; Vert, M. *J . Mater. Sci. Mater. Med.* **1990**, *1*, 123.

[173] Zhang, J. F.; Sun X. "Poly(lactic acid)based bioplastics" in *Biodegradable polymers for industrial applications,* Ed.: Smith R. ,CRC, 2005, Woodhead Publishing Limited , Cambridge -England , **2005** , pp. 251 – 288.

[174] Ramakrishna, S.; Mayer, J.; Wintermantel, E.; Leong, K.W. *Compos. Sci. Technol.* **2001**, *61*,1189.

[175] Hakkarainen, M.; Karlsson, S.; Albertsson, A. C. *Polymer* **2000** , *41,* 2331.

[176] Hartmann, H. , High molecular weight polylactic acid polymers , in *Biopolymers from Renewable Resources,* Ed.: Kaplan D.L. ,1st edition , Springer-Verlag , Berlin , **1998** , pp. 367 – 411.

[177] Gattin, R.; Copinet, A.; Bertrand, C.; Couturier, Y. *J . Appl. Polym. Sci.* **2003**, *88* , 825.

[178] Sinha Ray, S.; Kazunobu, Y.; Okamoto, M.; Ueda, K. *Macromol. Mater. Eng.* **2003,** 288(3), 203.

[179] Doi, Y.; Steinbüchel, A. *Biopolymers, Applications and Commercial Products – Polyesters III* , Wiley-VCH , Weiheim – Germany , **2002** , p. 410.

[180] Tormala P. , Vasenius J. , Vainionpaa S. , Laiho J. , Pohjonen T. , Rokkanen P. , Ultra-high-strength absorbable self-reinforced polyglycolide (SR-PGA) composite rods for internal fi xation of bone fractures: *I n vitro* and *i n vivo* study , *J . Biomed. Mater.Res.* , **25** , 1991 , 1 – 22 .

[181] Albertsson, A. C.; Varma, I. K. *Biomacromolecules* **2003**, *4* , 1466.

[182] http://www.natureworksllc.com .

[183] http://www.european-bioplastics.org/ .

[184] Utracki, L.A. **1990** Polymer Alloys and Blends - Thermodynamics and Rheology ,Hanser Publishers, Munich.

[185] Seidenstucker, T; Fritz, H. *Polymer Degradation and Stability* **1998,** *59*, 279.

[186] Bastioli, C. *Polymer Degradation and Stability* **1998**, *59*, 263.

[187] St-Pierre, N. et al. *Polymer* **1997**, *38*, 647.

[188] Bhattacharya, M. *The Journal of AppliedManufacturing Systems* 1997 vol. Winter, pp. 25-30.

[189] Koenig, M. F.; Huang, S. J. *Polymer* **1995**, *36*, 1877.

[190] Jacobsen, S.; Fritz, H.G. *Polymer Engineering and Science* 1996, 36(22), 2799.

[191] Ratto, J. and Stenhouse, P. 1995 'Investigation of Biodegradable Thermoplastic Polyester/Starch Blends', Annual Technical Conference - ANTEC '95 , Society Plastics Engineers, Boston, vol. 2, pp. 1824-1828.

[192] Davies, M. C.; Shakesheff, K. M.; Shard, A. G.; Domb, A.; Roberts, C. J.; Tendler, S. J. B.; Williams, P. M. *Macromolecules* **1996**, *29*, 2205.

[193] Domb, A. J. *J. Polym. Sci., Part A: Polym. Chem.* **1993**, *31*, 1973.

[194] Shakesheff, K. M.; Chen, X. Y.; Davies, M. C.; Domb, A.; Roberts, C. J.; Tendler, S. J. B.; Williams, P. M. *Langmuir* **1995**, *11*, 3921.

[195] Chandra, R.; Rustgi, R. *Prog. Polym. Sci.* **1998**, *23*, 1273.

[196] Pouton, C.; Saghir, A. *Adv. Drug Delivery Rev.* **1996**,*18*,133.

[197] Janvinoga, I.; Lacik, I.; Chodak, I. *Polym. Degrad. Stab.* **2002**, *77*, 35.

[198] Gassner, F.; Owen, A. J. *Polymer* **1994**,*35*, 2233.

[199] Knowles, J. C. *J. Med. Eng. Technol.* **1993**, *17*, 129.

[200] Kumagai, Y.; Doi, Y. *Polym. Degrad. Stab.* **1992**, *36*, 241.

[201] Chee, M. J. K.; Ismail, J.; Kummerlowe, C.; Kammer, H.W. *Polymer* **2002,** *43*,1235

[202] Kotliar, A. M.; *J. Polym. Sci., Macromol.Rev.* **1981,** *16***,** 367

[203] Kunioka, M.; Doi, Y. *Macromolecules* **1990**, *23*, 1933.

[204] Quental, A. C.; Felisberti, M. I. e-Polymer, Conference Papers, Macro 2004, Section 4.3.5 (2004).

[205] Cruz, D.M.G.; Ribelles, J.L.G.; Sanchez, M.S. *J Biomed Mater Res* B *Appl Biomater* **2008**, *85B*, 303.

[206] Honma, T.; Senda, T.; Inoue, Y. *Polym Int* **2003**, *52*,1839.

[207] Honma, T.; Zhao, L.; Asakawa, N.; Inoue, Y. *Macromol Biosci* **2006**, *6*, 241.

[208] Olabarrieta, I.; Forsstrom, D.; Gedde, U.W.; Hedenqvist, M. S. *Polymer* **2001**, *42*, 4401.

[209] Sarasam, A.; Madihally, S.V. *Biomaterials* **2005**, *26*, 5500.

[210] Sarasam, A.R.; Krishnaswamy, R. K.; Madihally, S.V. *Biomacromolecules* **2006**,*7*,1131.

[211] Sarasam, A.R.; Samli, A. I.; Hess, L.; Ihnat, M.A.; Madihally, S. V. *Macromol Biosci* **2007**, *7*,1160.

[212] She, H. D.; Xiao, X. F.; Liu, R. F. *J Mater Sci* **2007**, *42*, 8113.

[213] Senda, T.; He, Y.; Inoue, Y. *Polym Int* **2002**, *51*, 33.

[214] Garcia Cruz Dunia, M.; Coutinho, D.,F.; Martinez, E. C.; Mano, J.F.; Gomez Ribelles Jose Luis; Sanchez, M.S. *J Biomed Mater Res B Appl Biomater* **2008**, *87B*, 544.

[215] Koening, M. F.; Huang, S. J. *Polymer* **1995**, *36*, 1877.

[216] Pranamuda, H; Tokiwa, J; Tanaka, H. *J.Environ.Polym,Degrad*. **1996,** *4*, 1

[217] Koenig, M. F.; Huang, S. J. *Polymer* **1995**, *36*, 1877.

[218] Bastioli, C.; Cerutti, A.; Guanella, I.; Romano, G. C.; Tosin, M. *J. Environ. Polym. Degrad*. **1995**, *3*, 81.

[219] Bastioli, C. *Polym. Degrad. Stab*. **1998**, *59*, 263.

[220] Vikman, M.; Hulleman, S. H. D.; van der Zee, M.; Myllarinen, P.; Feil, H. *J. Appl. Polym. Sci.* **1999**, *74*, 2594.

[221] Averous, L.; Moro, L.; Dole, P.; Fringant, C. *Polymer* **2000**, *41*, 4157.

[222] Yavuz, H.; Baba, C. *J. Polym. Environ*. **2003**, *11*, 107.

[223] Singh, R. P.; Pandey, J. K.; Rutot, D.; Degee, P.; Dubois, P. *Carbohydr. Res.* **2003**, *338*, 1759.

[224] Azevedo, H. S.; Gama, F. M.; Reis, R. L. *Biomacromolecules* **2003**, *4*, 1703.

[225] Mano, J. F.; Koniarova, D.; Reis, R. L. *J. Mater. Sci.: Mater. Med.* **2003**, *14*, 127.

[226] Kweon, D.-K.; Kawasaki, N.; Nakayama, A.; Aiba1, S. *J. Appl. Polym. Sci.* **2004**, *92*, 1716.

[227] Mano, J. F.; Sousa, R. A.; Boesel, L. F.; Neves, N. M.; Reis, R. L. *Compos. Sci. Technol.* **2004**, *64*, 789.

[228] Gomes, M. E.; Sikavitsas, V. I. ; Behravesh, E.; Reis, R. L.; Mikos, A. G. *J. Biomed. Mater. Res.* **2003**, *67A*, 87.

[229] Oliveira, A. L.; Reis, R. L. *J. Mater. Sci.: Mater. Med.* **2004**, *15*, 533.

[230] Costa, S. A.; Reis, R. L. *J. Mater. Sci.: Mater. Med.* **2004**, *15*, 335.

[231] Alves, C. M.; Reis, R. L.; Hunt, J. A. *J. Mater. Sci.: Mater. Med.* **2003**, *14*, 157.

[232] Marques, A. P.; Reis, R. L.; Hunt, J. A. *J. Mater. Sci.: Mater. Med.* **2003**, *14*, 167.

[233] Narayan, R.; Krishnan, M.; Snook, J. B.; Gupta, A.; DuBois, P. U.S. Patent 5,969,089 (**1999**).

[234] Buchanan, C. M.; Gedon, S. C.; White, A. W.; Wood, M. D. *Macromolecules*

1992, *25*, 7373.

[235] Scandola, M.; Ceccorulli, G.; Pizzoli, M. *Macromolecules* **1992**, *25*, 6441.

[236] Buchanan, C. M.; Gardner, R. M.; Komarek, R. J. *J. Appl. Polym. Sci.* **1993b**, *47*, 1709.

[237] Komarek, R. J.; Gardner, R. M.; Buchanan, C. M.; Gedon, S. *J. Appl. Poly. Sci.* **1993**, *50*, 1739.

[238] Glasser, W. G.; McCartney, B. K.; Samaranayake, G. *Biotechnol. Progr*. **1994**, *10*, 214–219.

[239] Narayan, R. Structural requirements for designing biodegradable cellulosic materials. *Preprints of Kyoto Conference on Cellulosics*, October 31 – November 1, **1994** Kyoto, p. 55.

[240] Yoshioka, M.; Shiraishi, N. Biodegradable polymers from cellulose derivatives. *Preprints of Kyoto Conference on Cellulosics*, October 31–November 1, **1994** Kyoto, p. 52.

[241] Brode, G. L.; Koleske, J. V. Lactone polymerization and polymer properties. *J. Macromol. Sci. Chem.* **1972,** *A6*, 1109.

[242] Koleske, J. V. Blends containing poly(ε-caprolactone) and related polymers. In *Polymer Blends, Vol. 2* (D. R. Paul and S. Newman, eds). New York: Academic

Press, **1978** pp. 369–389.

[243] Hubbell, D. S.; Cooper, S. L. *J. Appl. Polym. Sci*. **1977**, *21*, 3035.

[244] Krikorian, V.; Pochan, D. J. *Macromolecules* **2004**, *37*, 6480.

[245] German Patent DE 100279 A1, Kjeschke, K.;.Timmermann, R.; Voight, M. assigned to Bayer AG, 12/13/2001.

[246] European Patent 776927 A1, Ikado, S.; Kobayashi, N.; Kurokit, T.; Saruwatarim, M.;Suzuki, K; Wanibe, H.assigned to Mitsui Toatsui Chem, Inc., 6/04/1997.

[247] Auras R. , Harte B. , Selke S. *Macromol. Biosci.* **2004** ,*4* , 835 – 864 .

[248] Zhang J.F. , Sun X. , Poly(lactic acid)based bioplastics , i n *Biodegradable polymers for industrial applications,* Ed.: Smith R. , CRC, 2005, Woodhead Publishing Limited , Cambridge -England , 2005 , pp. 251 – 288 , Chapter 10.

[249] Doi Y. , Steinbüchel A. , *Biopolymers, Applications and Commercial Products – Polyesters III* , Wiley-VCH , Weiheim –Germany , 2002 , p. 410 .

[250] Martin, O. , Avérous, L. , *Polymer* **2001**, *42* (14) , 6237.

[251] Zhang, J. F.; Sun, X. *Polymer International* **2004**, *53*, 716.

[252] Graaf, R.A.D.; Janssen, L.P.B.M. *Polym. Eng. Sci.* 2001,*41*(3), 584..

[253]Carlson, D.; Nie, L.; Narayan, R.; Dubois, P. *J. Appl. Polym. Sci.* , **1999**, *72* , 477.

[254] Zhang, J. F.; Sun, X. *Biomacromolecules* **2004**, *5*, 1446.

[255] Ke, T.; Sun, X. S. *Journal of Polymers and the Environment* **2003**, *11*, 7-14.

[256] Park, J. W.; Lee, D. J.; Yoo, E. S.; Im, S. S.; Kim, S. H.; Kim, Y. H. *Korean Polymer Journal*, **1999**, *7*, 93.

[257] Ke, T.; Sun, X. S.; Seib, P. *Journal of Applied Polymer Science* **2003**, *89(13)*, 3639.

[258] European Patent Application, 0 533 314 314 A2, J. Lunt, J. Kwok, J. M. Makuc, and M. Castrlotta, assigned to Novacor Chemicals, 3/24/1993.

[259] World Patent WO 200463282 A1 assigned to NEC Corp, K. Inoue, M. Iji and S. Serizawa, 7/29/2004.

[260] Japanese Patent JP 2003313417 A, assigned to Toyota, 11/06/2003.

[261] Oksman, K. et al. *Composite Science and Technology* **2003**, *63*, 1317.

[262] Japanese patent application JP 2005035134 A2, assigned to Toray Industries, Inc., 2/10/2005.

[263] Martin, O.; Averous, L. *Polymer* **2001**, *42*, 6209.

[264] Hu, Y.; Hu, Y. S.; Topolkaraev, V.; Hiltner, A.; Baer, E. *Polymer* **2003**, *44*, 5681.

[265] Hu, Y.; Hu, Y. S.; Topolkaraev, V.; Hiltner, A.; Baer, E. *Polymer* **2003**, *44*, 5701.

[266] Hu, Y.; Hu, Y. S.; Topolkaraev, V.; Hiltner, A.; Baer, E. *Polymer* **2003**, *44*, 5711.

[267] Sheth, M.; Kumar, A.; Dave´, V.; Gross, R. A.; McCarthy, S. P. *J. Appl. Polym.Sci.* **1997**, *66*, 1495.

[268] Blümm, E.; Owen, A. J. *Polymer* **1995**, *36*, 4077.

[269] Ferreira, B. M. P.; Zavaglia, C. A. C.; Duek, E. A. R. *J. Appl. Polym. Sci.* **2002**, *86*, 2898.

[270] Focarete, M. L.; Scandola, M.; Dobrzynski, P.; Kowalczuk, M. *Macromolecules* **2002**, *35*, 8472.

[271] Iannace, S.; Ambrosio, L.; Huang, S. J.; Nicolais, L. *J. Appl. Polym. Sci.* **1994**,

54, 1525.

[272] Koyama, N.; Doi, Y. *Can. J. Microbiol.* **1995**, *41*, 316.

[273] Koyama, N.; Doi, Y. *Macromolecules* **1996**, *29*, 5843.

[274] Koyama, N.; Doi, Y. *Polymer* **1997**, *38*, 1589.

[275] Zhang, L. L.; Xiong, C. D.; Deng, X. M. *Polymer* **1996**, *37*, 235.

[276] Zhang, L. L.; Deng, X. M.; Zhao, S. J.; Huang, Z. T. *J. Appl. Polym. Sci.* **1997**, *65*, 1849.

[277] Focarete, M. L.; Scandola, M.; Dobrzynski, P; Kowalczuk, M.; *Macromolecules* , **2002**, *35*, 8472.

[278] Maglio, G.; Migliozzi, A.; Palumbo, R. *Polymer* **2003**, *44*, 369.

[279] Aslan, S.; Calandrelli, L.; Laurienzo, P.; Malinconico, M.; Migliaresi, C. *J. Mater. Sci.* **2000**, *35*, 1615.

[280] Cha, Y.; Pitt, C. G. *Biomaterials* **1990**, *11*, 108.

[281] Choi, N. S.; Kim, C. H.; Cho, K. Y.; Park, J. K. *J. Appl. Polym. Sci.* **2002**, *86*, 1892.

[282] Dubois, P.; Jacobs, C.; Jerome, R.; Teyssie, P. *Macromolecules* **1991**, *24*, 2266.

[283] Lostocco, M. R.; Borzacchiello, A.; Huang, S. J. *Macromol. Symp.* **1998**, *130*, 151.

[284] Siparsky, G. L.; Voorhees, K. J.; Dorgan, J. R.; Shilling, K. *J. Environ. Polym. Degr.* **1997**, *5*, 125.

[285] Yang, J. M.; Chen, H. L.; You, J. W.; Hwang, J. C. *Polym. J.* **1997**, *29*, 657.

[286] Wang, L.; Ma, W.; Gross, R. A.; McCarthy, S. P. *Polym. Degrad. Stabil.* **1998**, *59*, 161.

[287] Diao J.Z.; Yang, H. F.; Zhang, J. M.; Song, X.H. *Iran Polym J* **2007**, *16*, 97-104.

[288] Bhardwaj, R.; Mohanty, A. K. *Biomacromolecules*, **2008**, *9*, 758-758.

[289] Zhang, J. F.; Sun X. Z. *Polym Int*. **2004**, *53*, 716-722.

[290] Wong S.; Shanks A.R.; Hodzic A. *Macromol Mater Eng*. **2004**, *289*, 447-456.

[291] Bahari, K.; Mitomo, H.; Enjoji, T.; Hasegawa, S.; Yoshii, F.; Makuuchi K. *Angew Makromol Chem*, **1997**, *250*, 31-44.

[292]Mansfield, M. L. *Macromolecules*, **1993**, 26, 3811

[293] Brigitte, I. Voit., *Hyperbrached polymers: a chance and challenge.* C R Chimie, **2003**, 6, 821

[294] Jinna, L., Xingrong, Z., Youjun, H., Hongju, S., *Polymer-Plastics Technology and Engineering*, **2008**, 1(47), 237

[295] Zhang J. Hu C. P., *European polymer Journal*, **2008**, 11(11), 3708

[296] Jena, K. K., Mishra, A. K., Raju K. V. S., *Journal of Applied Polymer Science*, **2008**, 12(110), 4022

[297] Akbari S, Kish M. H. , Entezami A. A. , *Polymer International*,**2008**,54, 846-853

[298] Helene Magnusson, Eva Malmstrom, Anders Hult, *Macromolecules*, **2000**, *33,* 3099

[299] Hartmut Komber, Antje Ziemer, Brigitte Voit, *Macromolecule,* **2002**, *35,* 3514

[300] Malmstro¨m, E.; Hult, A. *Macromolecules* **1996**, *29*, 1222.

[301] Malmstro¨m, E.; Johansson, M.; Hult, A. *Macromolecules* **1995**, *28*, 1698.

[302] Ihre, H.; Hult, A.; So¨derlind, E. *J. Am. Chem. Soc.* **1996**, *118*, 27, 6388.

[303] Malmstro¨m, E.; Hawker, C. J.; Johansson, M.; Hult, A. Manuscript in preparation.

[304] Guarino, V.; Causa, F.; Taddei, P.; di Foggia, M.; Ciapetti, G.; Martini, D.; Fagnano, C.; Baldinid, N.; Ambrosio, L. *Biomaterials* **2008**, *29*, 3662.

[305] Wnek, G.;Bowlin, G. Encyclopaedia of biomaterials & biomedical engineering. (**2008**) In forma Health Care, UK (1st ed.).

[306] Rahul Bhardwaj, Amar K. Mohanty, *Biomacromolecules*, **2007**, *8,* 2476-2484

[307] Ying Lin, Kun-Yu Zhang, Zhong-Min Dong, Li-Song Dong, Yue-Sheng Li, *Macromolecules*, **2007**, 6257-6267

[308] Jian-Feng Zhang, Xiuzhi Sun, *Polymer Internationa*l, **2004**, *53:*716-722

[309] Seiler,M. Dendritic Polymers-Interdisciplinary Research and Emerging Applications from Unique Structural Properties. *Chem. Eng. Technol.* **2002,** *25* (3), 237.

[310] Janerfeldt, G.; Boogh, L.; Manson, J. A. E. Tailored interfacial properties for immiscible polymers by hyperbranched polymers. *Polymer* **2000**, *41*, 7627.

[311] Kil, S. B.; Aygros, Y.; Leterrier, Y.; Manson, J. A. E. Rheological Properties of Hyperbranched Polymer/Poly(ethylene Terephthalate) Reactive Blends. *Polym. Eng. Sci.* **2003**, *43* (2), 329.

[312] Malmostrom, E.; Hult, A. *Rev. Macromol. Chem. Phys.* **1997**, *37*, 555.

[313] Mohanty, A.; Misra, M.; Hinrichsen, G. *Macromol. Mater. Eng.* **2000**, *276/277*, 1.